SPbGASU
1832

ARCHITECTURE & ENGINEERING

Volume 8
Issue 1
March, 2023

By Architects. For Architects.
By Engineers. For Engineers.

Architecture
Civil and Structural Engineering
Mechanics of Materials
Building and Construction
Urban Planning and Development
Transportation Issues in Construction
Geotechnical Engineering and Engineering Geology
Designing, Operation and Service
of Construction Site Engines

eISSN: 2500-0055
http://aej.spbgasu.ru/

Architecture and Engineering

Volume 8 Issue 1 (2023)

ISSN: 2500–0055

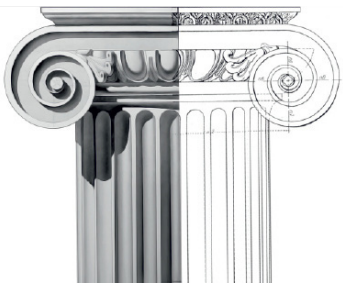

CONTENTS

Architecture and Engineering
peer-reviewed scientific journal
Start date: 2016/03
4 issues per year

Founder, Publisher:
Saint Petersburg State University of Architecture and Civil Engineering

Indexing:
Scopus, Russian Science Citation Index, Directory of Open Access Journals (DOAJ), Google Scholar, Index Copernicus, Ulrich's Periodicals Directory, WorldCat, Bielefeld Academic Search Engine (BASE), Library of University of Cambridge and CyberLeninka

Corresponding address:
4 Vtoraya Krasnoarmejskaja Str.,
St. Petersburg, 190005, Russia

Website: http://aej.spbgasu.ru/
Phone: +7(812)316–48–49
Email: aejeditorialoffice@gmail.com

Date of issue: 31.03.2023

The Journal was re-registered by the Federal Service for Supervision of Communications, Information Technologies and Mass Communications (Roskomnadzor) on May 31, 2017;
registration certificate of media organization El No. FS77–70026

DOI: 10.23968/2500-0055-2023-8-1-3-12

THE DEPICTION OF STRUCTURAL AND CIVIL ENGINEERING IN VITRUVIUS'S TEN BOOKS ON ARCHITECTURE — A STATE-OF-THE-ART REVIEW

Christopher Fapohunda

Federal University Oye-Are Road
Oye-Ekiti, Nigeria

*Corresponding author's e-mail: christopher.fapohunda@fuoye.edu.ng

Abstract
Introduction: Ten Books on Architecture (De Architectura) is a treatise by Vitruvius that describes construction work, as taught and practiced in the 1st century. In it, the functions and duties performed in the built environment by architects, construction workers, civil engineers, surveyors, sculptors, decorators, etc., are all lumped together into either architecture or civil engineering. However, for civil engineers, who operate both in built and unbuilt environments, the scope and depth of subjects covered by this work could serve as useful resources as they develop their competences in core practical aspects of civil engineering. **Materials and Methods:** This paper explores Ten Books on Architecture in relation to civil engineering in the 21st century. The materials used for this work were obtained from internet sources, university libraries, textbooks, write-ups and commentaries that were purchased from open markets and bookshops. **Results:** The review shows that: (i) the profession of the architect, used in the times of Vitruvius interchangeably with the civil engineer and town planner, as well as the very concept of architecture or civil engineering, in terms of social standing, differs significantly from the present times; (ii) most of the projects discussed in the book form the core of what is classified in the 21st century as civil engineering; (iii) civil engineers ought to be versatile in the art solving of problems that may arise during the course of construction, both in the built and unbuilt environments; and (iv) the buildability issues of civil engineering make knowledge of how to assemble simple construction equipment a necessity. **Conclusion:** Though not recommended in the curriculum, a working knowledge of either Latin or Greek will help to make the book an indispensable companion for structural and civil engineering practitioners and also enhance their performance capacity.

Keywords: architecture, built environment, civil engineering, structural materials.

Introduction

The title that Vitruvius gave his treatise, Ten Books on Architecture (Vitruvius, 1914) may be misleading on the surface, as one can easily conclude that its subject is the modern-day concept of architecture. But a closer look at the book's table of contents will reveal a curious discovery. Apart from the fact that Vitruvius's perception of construction as such is very broad in scope and includes all major projects classified today as civil engineering, other topics covered are medicine, astrology, philosophy, and construction of military machines. Putting these together, one may conclude that Vitruvius's interpretation of architecture, representing how architecture was seen during his time, was quite different from the architecture of today. His concept of architecture and civil engineering reflects the work of many different 21st century professionals in the modern built environment, specifically civil engineers, structural materials engineers, surveyors, mechanical engineers, etc. But one may ask: who was Vitruvius as an individual? According to biographical overviews given in De Architectura (Wikipedia, 2011) and Cigola and Ceccarelli (2014), Marcus Vitruvius was a Roman military engineer and architect under both Julius Caesar and his son Augustus Caesar between 46 B. C. and 14 A. D. This is further confirmed in the preface to this book by Vitruvius himself, as he dedicates his work to Augustus Caesar as follows:

> "...for in the first place, it was this subject which made me to be known to your father to whom I was devoted on account of his great qualities. After the council of Heaven gave him a place in the dwellings of immortal life and transferred your father's power to your hand, my devotion continues unchanged as I remember him, inclined me to support you..."

He can thus be described as the architect and engineer of Caesar's Roman Empire, responsible not only for building utilitarian public infrastructure, but also for supplying and maintaining military structures like those he referred to as ballistae, scorpions and artillery. Given that in the times of Julius and Augustus Caesar, multiple wars were fought on land and sea, covering extensive territories

over the course of many years, it is understandable that Vitruvius's brand of architecture was shaped by its military undertones and subjects. Furthermore, the book was based on the average Roman's world-view at the time, hence the inclusion of subjects like astronomy and philosophy, as well as the choice of certain building and construction models, adopted exclusively to please the divine being. According to Barrow (1955), Romans of the time believed that there was a power, in form of divine beings that ruled the world, that was superior to humans and had to be submitted to in order to ensure human wellbeing. This submission to divine beings was also what allowed the ruler to dominate over the human race. Thus, Ten Books on Architecture also contains copious amounts of religious notions and thinking habits of the first-century Romans. Next, environmental and health issues cannot be divorced from construction activities, since construction workers must be healthy and able to overcome the environmental challenges at their place of work in order to proceed. This may justify the inclusion of climate and medicine concerns.

Thus, the book seems to rest on the following underlying substructures: Vitruvius's imperial military background, subjection to divinity, and environmental and health issues. It also must be noted that, in the language of that period, architects and civil engineers were considered to be the same thing as city planners and builders, and the word for them was derived from the word for kings and emperors (Barrow, 1955). No one could pursue any of those professions without previously having being a successful farmer and soldier, for a typical Roman was essentially both a farmer and military man (Barrow, 1955). According to Barrow (1955),

> "The Roman mind is the mind of the farmer and soldier, not farmer, not soldier, but farmer-soldier. Unremitting work is the lot of the farmer, for the seasons wait for no Man. Yet his own work by itself will achieve nothing, he may plan and prepare, till and sow, in patience he must await the aid of forces which he cannot understand, still less control. If he can make them favourable, he will, but more often, he can only cooperate and he places himself in line with them that they may take him as their instrument and so he may achieve his end. Accidents of weather and pest may frustrate him, he must be patient. Routine is the order of his life; seed-time, growth and harvest follow in appointed times. The life of the field is his life. If as citizen he is moved to political action at last, it will be for the defence of his land or markets or the labour of his sons. To him the knowledge born of experience is worth more than speculative theory. His virtues are honesty and thrift, forethought and patience, work, endurance and courage, self-reliance, simplicity, and humility in the face of what is greater than himself. Such are the virtues of a soldier. He too will know the value of routine, which is part of discipline, for he must respond as by instinct to a sudden call. He must be self-reliant. The strength and endurance of the farmer serve the soldier; his practical skill help him to become what Roman soldier must be, *a builder and digger of ditches, and maker of roads and ramparts. He lays out a camp or a fortification as well as he lays out a plot or a system of drains"*

The above statement is echoed in De Architectura (Wikipedia, 2011). This work notes that Roman architects were skilled in engineering, art, and craftsmanship combined. The present-day understanding of architecture, especially in the developing world, which is linked to houses, had no place in architectural practice during the times of Vitruvius, as we will see later in Table 4. The Romans' understanding of the word architecture, as per the classical studies of the time, can be described through Eq. 1:

$$\text{architecture} = \text{arche (prince/state/government)} + \text{teknon (to build)} \quad (1)$$

"To build" had the implication of "to construct" or "to assemble together" (Seward, 2007), i.e., form a resilient whole, a concept derived from the militaristic Roman mindset of the time. That is why Roman architecture encompassed not only houses, but also bridges, waterways, roads, urban drainage systems, machines, ships, and more. That Vitruvius was first and foremost a military engineer who tried to put the knowledge acquired in military campaigns to peacetime use, becomes evident in the preface to Book 1 of the Ten Books of Architecture.

In the preface, he mentions enjoying the patronage of Julius Caesar as he built war machines and engines for his military operations. This continued under Augustus Caesar, both in his wars and in the reconstruction work that followed his victory, ushering in a reign of peace. Vitruvius covers a wide variety of subjects he saw as relevant to first-century architecture or civil engineering. This includes many aspects that may seem irrelevant to modern eyes, ranging from mathematics to astronomy, meteorology, and medicine. In the Roman mindset, architecture or civil engineering needed to take into account everything touching on the physical and intellectual life of man and his surroundings. Thus, the Ten Books on Architecture treatise was the work of a Roman man with the characteristic farmer-soldier outlook.

This work has been reviewed by multiple authors and researchers. For example, Cartwright (2015) reviewed the book by summarizing each chapter and bringing out salient points. In a review by Erismis and Gezerman (2013), an attempt was made to critique the treatise, by asking questions such as: how can the time of Vitruvius be interpreted? How did Vitruvius conceptualize architecture? What did Vitruvius emphasize the most in his study? Are there any surviving buildings from the time of Vitruvius, and if there are, how exactly do they fit Vitruvius's explanations? What insights can this study offer our peers? Did Vitruvius, in fact, ever live and is there really a book called *De Architectura*? Their conclusions were that neither such a book nor the author ever existed. These conclusions were apparently drawn without knowledge of the Roman

mind, the Roman society and the political system of the time when Ten Books on Architecture was written. Some authors focused on specific aspects of the book: for example, Thiemann et al. (2010) and Small (2019) examined its plaster and painting aspects, Bosman (2015) looked at architectural theory and practice, as applied to proportions and building materials. Others like Ghazvini et al. (2020), Grúňová and Holešová (2018), Heath (1989), Newman and Vassigh (2014), Patterson (2004), Schulzová and Bošová (2019), and Wozniak-Szpakiewicz and Zhao (2018), treated the book exclusively within a present-day architectural framework. The book's examination by civil engineers, either in practice or in academia, is very scarce. Apparently, the title of the book gives the first impression that it is dedicated only to present-day architectural practices. That is, the book is perceived to contain nothing of interest to civil engineering training and practice. This paper intends to change this mindset by attempting to give insight into the civil engineering aspect of the book, which is very deep and wide in scope. This will demonstrate that civil engineers can avail themselves of the plentiful resources contained in the book for robust professional practice and academic research, especially the principles governing the design of civil works and selection of construction materials.

Thus, the aim of this study is to review the Ten Books of Architecture treatise by Vitruvius (1914), by adapting the training and practices from what was called architecture or civil engineering in the 1st century into 21st century civil engineering. The paper will focus on bringing out insights that can provide useful resources for civil engineering training and practice. This review focuses on civil engineer training, buildings, construction economy, and construction materials.

Methodology

The method employed in this review was to search the archives for materials covering the time when the Ten Books on Architecture treatise was written. These materials were obtained from internet sources and university libraries, as well as from textbooks, write-ups and commentaries that were purchased from open markets and bookshops. They were studied in an attempt to understand the society and the practices at the time when Vitruvius wrote his book.

Review

As stated in the Introduction, the concepts of architect, engineer, and town planner were used interchangeably in the times of Vitruvius because of similar professional training (Wikipedia, 2011). It is, however, obvious that in the present times, the education paths for each of these professions are different, though they do occasionally intersect, and may finally converge into a single genius architect or civil engineer as described by Vitruvius, through continuous training and practice. Bearing this in mind, the authors, being civil engineers, have decided to give insight into the book within the context of civil engineering, and have tried to situate 1st century architecture, or civil engineering, exclusively in the 21st century civil engineering framework.

Education and Training in Civil Engineering

There is no doubt that Vitruvius drew up his curriculum with his own prior education in mind. He expected civil engineers to be well-versed in many varied fields, putting all the work done by others to test through his professional judgement. Table 1 provides a summary of Vitruvius's civil engineer's curriculum.

Vitruvius's curriculum requires instruction in 9 (nine) branches of learning, which, during his time, served as the foundation for nurturing and training a potential architect, civil engineer, or urban planner. He also provided reasons for the branches' relevance, which are briefly summarized in the table. Tables 2 and 3 outline a typical curriculum of BSc. (or BEng.) degree in civil engineering, as approved by the Accrediting Agency of Nigerian Universities (NUC, 2022). The comparison between this curriculum and the contents of Table 1 reveals an inherent weakness in training a person to become Vitruvius's idea of a civil engineer.

Some elements of Vitruvius's curriculum are particularly strange to the present-day civil engineering students and professionals, but in the long run, they prove necessary for robust practices. For instance, his inclusion of political history as part of the curriculum was informed by the reasoning that a building or any form of civil infrastructure, either in part or as a whole, likely has some historical events associated with it.

He cited some structures from his time, pointing to features were meant to serve as a reminder of certain historical, cultural, and political events that had shaped the life of the nation. This is shown in Fig. 1 (Vitruvius, 1914).

Similar examples of modern-day structures conveying a political message include the Statue of Liberty and the Empire State Building, both located in the United States of America. These are shown in Fig. 2 (Maguth et al., 2013).

Analysis of Borucińska-Bieńkowska (2020) showed that cultural factors and past historical events not only influence civil infrastructure, but also provide inspiration for new art directions. Vitruvius includes philosophical knowledge in the training of civil engineers to help develop their moral character and professional ethics. He lists concepts like honesty, courtesy, righteousness, and incorruptibility. Vitruvius believes that a civil engineer cannot function without being honest and resisting corruption. According to him, these qualities can

Table 1. **Breakdown of Vitruvius's civil engineer curriculum (Vitruvius, 1914)**

	Knowledge required	Relevance to the profession
1	Pencil drawing skill	a) Required for sketching the proposed design
2	Knowledge of geometry	a) Knowing to use a ruler and a compass is required for planning buildings on the ground b) Teaches the right application of the square, the level and the plummet c) The optical aspect of geometry shows how natural light enters the building d) The arithmetical aspect of geometry allows for calculating construction costs and computing measurements e) Geometrical theories and methods help to solve symmetrical issues
3	Knowledge of (political) history	a) Allows the civil engineer to explain the underlying ideas and stories behind the ornamental elements (see Figure 1 for illustrations)
4	Knowledge of philosophy	a) Teaches the civil engineer to be not self-assuming and avaricious, but courteous, just, and honest b) Honesty and incorruptibility are essential qualities for the civil engineer c) The fundamentals of physics, which were also taught under philosophy at the time, allow for handling numerous construction tasks
5	Knowledge of music	a) Provides knowledge of canonical and mathematical theory b) Allows for properly attuning ballistae, catapults and scorpions c) Allows for building water organs and objects resembling them
6	Knowledge of medicine	a) Required for addressing issues with climate, air, healthiness and other site properties, and using different water sources to ensure that the dwelling is healthy to live in
7	Knowledge of the law	a) Required for safeguarding the interests of both the employer and the contractor while drawing up contracts b) The civil engineer must understand laws applicable to specific building elements, for example, drains, windows, water supply, etc.
8	Knowledge of astronomy	a) Required for locating the cardinal directions: East, West, South, and North
9	Theory of Heavens	a) Theory of Heavens includes knowledge of the equinox, solstice, and course of the stars b) The civil engineer must be able to comprehend the Theory of Heavens

only be obtained through philosophical studies. In the present day, when corruption is rampant in the construction industry, taking the form of extortion, contract inflation, working for officials who steal public money, abandoning professional integrity for pecuniary gains, bribery, nepotism, and so on (Chan and Owusu, 2017; Locatelli et al., 2016), this curriculum recommendation is most apt. Vitruvius's

Table 2. **Breakdown of a typical curriculum for BSc/BEng. Degree in Civil Engineering**

Level	General Studies	Basic Sciences	Basic Engineering	Core Courses	Electives	SIWES	Total
100	10	30	4	0	0	0	44
200	6	0	34	2	0	0	42
300	0	0	6	38	0	0	44
400	0	0	2	21	0	6	29
500	0	0	3	28	6	6	43
TOTAL	16	30	49	89	6	12	202
Percent of Total	7.92%	14.85%	24.26%	44.06%	2.97%%	5.94	100%

Table 3. **Divisions in the Curriculum for BSc/BEng. Degree in Civil Engineering**

Curriculum	Contents
General Studies	English Language, History
Basic Sciences	Mathematics, Physics, Chemistry, Computer Skills, Drawing
Basic Engineering	Computer Skills, Introduction to Computer Programming. Drawing, Mechanics, Strength of Materials, Engineering Materials, Surveying
Core Courses	Highways, Transportation, Geotechnics, Structures, Water Resources, Hydraulics, Environmental Engineering
Electives	At the student's discretion. Usually departmental electives
SIWES	Students Industrial Work Experience Scheme

a) Single column b) Double column

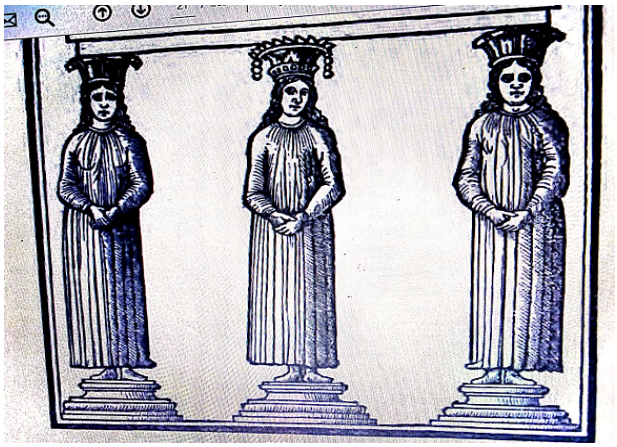

c) Triple column

Fig. 1. Columns with decorations depicting historical events (Vitruvius, 1914)

a) Statue of Liberty b) Empire State Building

Fig. 2. Statue of Liberty and American Empire State Building (Maguth et al., 2013)

recommendation to include medicine on the civil engineering curriculum will not come as a surprise to a civil engineer involved in road construction or civil projects in unbuilt areas. In fact, most civil engineering construction is performed in the open field under harsh environmental conditions. It is thus necessary that civil engineers approach the issues of health and environmental resilience as pivotal to their professional excellence. In addition, there is a growing concern regarding the environmental impact of construction and the concomitant sustainability issues. The recent COVID-19 pandemic has underscored the importance of some medical training and knowledge, not because a civil engineer might want to become a medical doctor, but because they need to take the necessary precautions for preventing health hazards and fatalities in an environment where there are no medical facilities. Thus, training and acquisition of knowledge on how to adapt to different climate conditions and air quality, improve unhealthy site properties, and treat unpotable water becomes a necessity. Vitruvius appears to imply that it takes being a sound and rational person, not necessarily academic brilliance, to practice civil engineering.

The practice of civil engineering involves two or more parties, either as individuals, or as institutions and even governments; therefore, knowledge of legal principles and opinions of lawyers is necessary. Thus, Vitruvius included legal training as part of his curriculum in civil engineering. However, by law and lawyers, Vitruvius meant the civil law and lawyers from Rome, which he saw as a force that had established peace over the known world, and which his client, Emperor Augustus Caesar, personified at the time of writing his book. This was briefly stated in the Introduction. It should also be noted here that, in the Roman mindset of the time, peace meant "settled order and security of life and property" (Barrow, 1955). This is the environment that gave birth to civil engineering (Merdinger, 1949; Watson, 2020). Thus, without peace, there can be no civil engineering. Furthermore, it is through the Roman law that the established peace was administered. According to Justinian (The Ames Foundation, 2020), the precepts of Roman law are to live honestly, injure none, and give every man his due. This applies to persons, actions, and objects. Thus, in drawing up civil engineering contracts at the time, the interests of both the customer and the contractor were safeguarded under the prevailing Roman peace and law.

In our modern times, we will do well to learn the prevailing law of peaceful corporate existence, as established by the constituted authority, while practicing the civil engineer's profession. This will be a continuous process, because human society is dynamic, and law changes with the government. Nonetheless, the civil engineer's intent is to remain (The Ames Foundation, 2020), regardless of whether the government was overthrown, established where it is non-existent, or continues to operate; and that intent is: to conduct oneself honestly, injure none

(either individuals or society as a whole) and give everyone their due while practicing one's profession, at all times. According to Bonenberg (2015), basing construction planning documents on peace-driven and civilization-driven principles facilitates subsequent modernization, especially for complex metropolitan projects.

The knowledge of music, astronomy and "Theory of Heavens" may not seem relevant to many of us in the present day. This is because only few people now have the same background and experience as Vitruvius, which warranted his recommendations for the curriculum. The experience of military service and having a reigning Emperor as client is not particularly relevant to many of us. No doubt, Vitruvius's exposure to challenges in a nation of wayfaring men from a law-based republic seemed to be the bedrock of professional competence that broadened his horizons. It must be said at this point that Vitruvius's treatment of astrology and Theory of Heavens (i.e., a discussion of such things as the universe, the power of nature, etc.), though outside the scope of this paper, does not contradict the definition of civil engineering according to the Institution of Civil Engineers (ICE, 2018) of the United Kingdom. In the charter granted to the Institution of Civil Engineers (ICE, 2018) in 1828, to incorporate the profession into the body politic and corporate, civil engineering was defined as:

> "... the art of directing the great sources of power in Nature for the use and convenience of man, as the means of production and of traffic in states both for external and internal trade, as applied in the construction of roads, bridges, aqueducts, canals, river navigation and docks, for internal intercourse and exchange, and in the construction of ports, harbours, moles, breakwaters and lighthouses, and in the art of navigation by artificial power for the purposes of commerce, and in the construction and adaptation of machinery, and in the drainage of cities and towns..."

Similarly, the phrase "forces of nature" is also included in the definition of civil engineering by the American Society of Civil Engineers (ASCE, 2008). In order words, in order to fit the ICE (2018) and ASCE (2008) definition of civil engineering, a person must complete the curriculum designed by Vitruvius. All things considered, it becomes clear that continuous learning is "desiderata" to reach the peak of being recognized as authority in the profession. It is not possible to acquire all the skills recommended for a civil engineer by Vitruvius at any Civil Engineering Department in any University at any level, from undergraduate to PhD. Thus, as their duty demands, a civil engineer will have to seek further tutelage in other areas and at other departments that are not part of present-day curriculum offered by conventional civil engineering departments at universities worldwide. It is obvious that Vitruvius was an erudite scholar and voracious reader.

Practice of Civil Engineering

Knowing the nature of civil engineering in the 1st century and understanding its scope is necessary if one is to situate it within the 21st century practice. First, Vitruvius divides the civil engineering of his era into three sections, namely (i) the practice of building, (ii) construction of time pieces, and (iii) fabrication and construction of machinery. The breakdown of the building practice is presented in Table 4. Although items 1 and 2 in Table 4 were originally grouped together into one, it has been broken down into two parts for the purpose of this work.

Most of the construction projects described in Table 4 are civil engineering projects in nature from the standpoint of the 21st century practice, though some would have to be completed in collaboration with other professionals like 21st century architects. Thus, we should not lose sight of the immense overall civil engineering aspects of Table 4. Considering item 1, for example, the execution of such a project will involve nearly all the 21st century branches of civil engineering, like survey, soil and foundation engineering, structural engineering, construction materials, and provision of water and sanitation. Correspondingly, in Book 2 of De Architectura, Vitruvius deals with construction materials, while in Book 8, he sets out principles to be employed when searching for potable water in different locations, for use in homes, towns and cities. All other aspects are also addressed in different chapters of the book. Building defensive structures is purely civil engineering work. While we may not be considering military attacks in this case, structural loads on buildings can be modeled in a similar manner to resist other threats, such as erosion, winds, hurricanes, seismic effects, etc., which also bring about destruction from the civilian perspective. Such

Table 4. **Types of built structures according to Vitruvius**

	Type	Description	Example
1	Fortified towns	Fortified towns	Site planning for towns and cities
2	Public works	Defensive	Walls, towers, gates, devices against hostile attacks
		Religious	Shrines and temples to the gods
		Utilitarian	Harbors, markets, colonnades, baths, forums, circuses, emporiums, theaters, promenades, aqueducts, etc.
3	Dwellings of private individuals	Dwellings of high-status Roman citizens	Houses for different classes of people, farm houses, houses in cities and towns.

situations call for suitable, robust, strong and stable construction in form of retaining walls, shear walls, etc. Vitruvius's work gives us insight into how to create these. Religious buildings in Vitruvius's time were similar in nature to the churches, mosques and synagogues of the 21st century. But unlike the 21st century, the construction of religious edifices in the 1st century was the duty and function of the state, which was personified by the Emperor, hence Vitruvius grouping such buildings together with public projects. All these contained a substantial civil engineering element. In the same vein, the examples of construction projects Vitruvius grouped under utilities are relevant to civil engineering. The same is true for building houses for private individuals with different status and means. These are described in the respective chapters of the book. A brief analysis of Table 4 demonstrates that the projects that Vitruvius described as construction in his 1st century language, in fact, either are civil engineering projects, or contain substantial civil engineering elements. The execution of these projects requires training in the legal, philosophical and psychological aspects of human behaviors, as recommended by Vitruvius. First of all, contracts will have to be drafted for different clients, suppliers, and labor. Furthermore, daily peaceful administrative control over workers is important for maintaining an undisturbed construction process. Lastly, harmonious interactions between the construction work force and the environment where the construction is taking place cannot be neglected either, if disturbances are to be prevented. According to Arya (2009), a civil engineer should, by training amongst others, become capable of: (i) carrying out, both in concept and execution, the entire planning process for a new building structure (as seen in Table 4), (ii) studying project feasibility through mathematical calculations and drawings, and (iii) preparing the bills of quantities, specifications and contracts that will form the necessary legal and organizational framework. Civil engineering professionals should thus turn to Vitruvius's book to enrich their practices.

The second branch of civil engineering, according to Vitruvius, was the making of time pieces. What are time pieces? According to Dictionary (2020) and Merriam-Webster.com (2022), a time piece is an instrument such as a clock or watch, intended for measuring or showing progress of time. For the civil engineering practice in the 21st century, the relevance of making time piece may not make sense, since we have grown up with wrist watches and lately mobile handsets, which show time in any place and in any weather. But the 1st century Romans did not have the luxury of being able to determine the time of day regardless of location or weather conditions. Hence time piece creation, described by Vitruvius in Book 9, formed part of the civil engineering practice. Although 21st century civil engineering may not involve the construction of time pieces, there is an underlying principle to be kept in mind. Namely, that civil engineering training in any century must include elements that will allow civil engineers to be versatile in the art of solving any problems that may arise, both in the built and unbuilt environments.

Finally, the third type of civil engineering in Vitruvius's work is the construction of machinery, that is, machines and engines. In the 21st century, it is normal to expect this function from mechanical engineering, but this was not the case in the 1st century. It is to be noted, however, that general knowledge of mechanical science and engineering does form an integral part of civil engineering practice, even in the 21st century. This is because the sentence leading to the definition of civil engineering by the Institution of Civil Engineers (ICE, 2018), contains the following wording:

> "...advancement of mechanical science...".

Thus, we can deduce that this requirement is still expected in civil engineering practice in the 21st century, just as it was in the 1st century. According to Vitruvius, machines and engines are, in principle, practical necessities in civil engineering. Many constructs that fall under these terms are discussed by Vitruvius in Book 10. The machines covered in Book 10, in terms of operation principles and structures, range from military to non-military equipment. The non-military machines described by Vitruvius and relevant to this paper include, but are not limited to: (i) climbing machine — for the construction workers to view the construction site, (ii) hoisting machines of various types — for lifting materials and workers, (iii) water raising engines like water wheels on rivers, water screws, water mills, and water pumps, (iv) odometers — for measuring mileage on roads and sea, (v) balances — for testing weight, (vi) utilities like ladders, cranes, and so on. The civil engineer is expected to be conscious of the equipment requirements and include them in their designs, especially at the conception and development stage. The civil engineer either procures the necessary equipment or has the ability to construct it, or at least, was expected to do that in the 1st century practices. This is also important in the 21st century practice. Availability of construction equipment relates to the 21st century concept of buildability in civil engineering. This cannot be overemphasized (Arya, 2009). In developing countries, where resources for equipment procurement are scarce, it is imperative for civil engineers to be familiar with the principles of constructing simple essential tools like cranes, balances, etc., as described by Vitruvius, to keep their work going.

Economical Civil Engineering

One of the fundamental principles of civil engineering design projects is that the structure must

be economical in cost and maintenance (ASCE, 2008; Fapohunda, 2019).

That said, a substantial percentage of construction costs, over 40%, accounts for materials alone (Adedeji, 2012; Deepa et al., 2019). As a way to make civil construction more economical, Vitruvius noted that, firstly, the civil engineer should not recommend materials or items that cannot be obtained or assembled without great expense. Additionally, it ought to be noted that, apart from procuring the materials themselves, their transportation to the site also increases the materials cost component of the total construction costs (Ahmadian et al., 2014; Shakantu et al., 2003). Here, we ought to explore the importance of using any unconventional construction materials available in the site's vicinity, as a way to make the process more economical (Fapohunda and Daramola, 2019). To be able to do this, the civil engineer must be able to not only experiment, but also assemble, if required, the equipment and machines for such experiments. Engineering practice founded on a curriculum is as diverse, broad and deep as what was recommended by Vitruvius is essential for accomplishing this.

Construction Materials in Civil Engineering

The materials that were used for civil engineering in the 1st century should also interest the 21st century civil engineering practitioners. While these materials did not include steel and aluminum, what they did include was brick, sand, lime, stone, timber, and pozzolans. Vitruvius describes them from what can be considered a 21st century structural engineering perspective, with emphasis on strength and durability. For each of them, he extensively covers issues like material types and sources, time spent on making the material, how long it ought to be left to dry before use, how best to apply the material, simple tests to determine suitability, possible combinations with other materials, how and when the material is to be applied, and more. In this discussion, he highlights the natural, "primordial" state of each of the materials, which he considers to be a fundamental part of learning more about their nature and application. According to Vitruvius, all materials, including civil engineering construction materials, are composed of four fundamental elements, namely, heat, water, earth, and air. He believed that all things consisted of these elements or were produced by the elements coming together, resulting in infinite combinations. Thus, his book does not discuss concrete, which is a product of combining other materials, though it does mention it. Today, the world is gradually becoming aware of the negative environmental impact of using non-renewable resources, perceiving it as a portent of danger to future generations (Kau, 2007; RILEM, 2019). The construction industry is also facing some challenges due to the materials used. Concrete in particular is associated with such issues as CO_2 emissions, depletion of natural resources, and landfills, which are becoming major concerns (Savija, 2020). The fear that the construction industry will be unable to sustain the current use of materials, especially structural concrete, is driving innovation and academic research, aimed at finding alternative sources of construction materials. Researchers are looking into obtaining structural materials from industrial and agricultural wastes, as well as non-traditional materials. Familiarity with, or even in-depth knowledge of, Vitruvius's principles of the four primordial elements, which he believed all materials consisted of, would help researchers in no small measure, either to innovate new materials, or enhance suitability of previously unsuitable materials.

Final Comments About Vitruvius's Ten Books on Architecture

This exploration of Vitruvius's Ten Books on Architecture from the civil engineering perspective is not meant to be exhaustive, and neither was it a detailed discussion of every matter relevant to civil engineering that was contained in the book. The paper's main intent is to encourage civil engineers to look past the title of the book and study its contents. It appears that the word "architecture" as used in the 1st century was different from the usage in the 21st century. Architecture, as in Eq. 1, is a combination of two Greek words: "arche", meaning the state or its ruler, such as an emperor or prince, and "tekton", meaning to build or to construct. When these two words are combined to form the term "architecture", it can be understood in two ways. The first meaning it conveyed in the times of Vitruvius was a reference to a person who built an Empire, or a State. This could be Emperors, Kings, Princes, etc. The second meaning referred to a person who built for the Emperor, the King, or the State. That is, such a person had a King, an Emperor, a Prince, etc. as their client. Throughout the book, Vitruvius uses the word "architect" in the second sense, that is, a builder for the ruling Emperor, King, or Prince. This was because Vitruvius himself was the builder for two Emperors, Julius Caesar and Augustus Caesar, the two men who personified the state in their time. In addition, his work mentions others in this profession who built for rulers, namely: Dinocrates, who built the city of Alexandria for Emperor Alexander, along with Myron, Polycleitus, Phidias, and Lysippus. Furthermore, Vitruvius speaks of builders who constructed machines and engines in Book 10, for instance Diognetus (Rhodes architect), Callias (Aradus architect), Epimachus (Athenian architect under King Demetrius) and Trypho (Alexandrine architect), which clearly demonstrates a scope that no professional group in the 21st century construction industry can capture in its training. At the same time, if we place the word "architecture" within the context

of its 1st century use, we will discover that the projects discussed in Vitruvius's book actually form the core of 21st century civil engineering. Thus, the book is relevant to civil engineering training and practice. It can also serve as a guideline for the modern civil engineer in the process of skill building and in the pursuit of continuous professional training.

Conclusions

From the exposition above, it can be concluded that (i) most of the activities classified by Vitruvius as construction are, in fact, civil engineering activities in nature, if we look at them from the 21st century perspective, thus the content of his treatise ought to appeal to civil engineering professionals; (ii) civil engineers need to be versatile in the art of solving problems that may arise during the course of construction, both in the built and unbuilt environments; and (iii) the buildability issues associated with civil engineering make the knowledge of construction equipment a necessity. It should also be noted that in the 1st century, the language of communication was Latin and Greek, which everyone understood; and thus, it was not part of the curriculum designed by Vitruvius. His treatise uses copious amounts of Latin and Greek terminology, which may make the book unreadable for 21st century civil engineers. Though it is not required for the curriculum, a working knowledge of either Latin or Greek will help make the book an indispensable companion for the civil engineering practitioner.

References

Adedeji, Y. M. D. (2012). Sustainable housing provision: preference for the use of interlocking masonry in housing delivery in Nigeria. *Architecture Research*, Vol. 2, No. 5, pp. 81–86. DOI: 10.5923/j.arch.20120205.03.

Ahmadian, A. F. F., Akbarnezhad, A., Rashidi, T. H., and Waller, S. T. (2014). Importance of planning for the transport stage in procurement of construction materials. In: *2014 Proceedings of the 31st ISARC, Sydney, Australia*, pp. 466–473. DOI: 10.22260/ISARC2014/0062.

Arya, C. (2009). *Design of structural elements: concrete, steelwork, masonry, and timber designs to British standards and Eurocodes, 3rd edition*. London: Spon Press, 528 p.

ASCE (2008). *Civil engineering body of knowledge for the 21st century – preparing the civil engineer for the future*. [online] Available at: https://ascelibrary.org/doi/book/10.1061/9780784409657 [Date accessed October 12, 2021].

Barrow, R. H. (1955). *The Romans*. London: Penguin Books, 224 p.

Bonenberg, W. (2015). Planning documents as an element of modernizing the urban structure of the Poznań metropolitan area. *Civil and Environmental Engineering Reports*, Vol. 17, No. 2, pp. 25–32.

Borucińska-Bieńkowska, H. (2020). The influence of cultural-historical determinants on functional-spatial development of rural areas. *Civil and Environmental Engineering Reports*, Vol. 30, No. 4, pp. 48–55.

Bosman, L. (2015). Proportion and building material, or theory versus practice in the determination of the module. *Architectural Histories*, Vol. 3, Issue 1, 10. DOI: 10.5334/ah.cm.

Cartwright, M. (2015). *Vitruvius*. [online] Available at: https://www.ancient.eu/Vitruvius/ [Date accessed April 21, 2020].

Chan, A. P. C. and Owusu, E. K. (2017). Corruption forms in the construction industry: literature review. *Journal of Construction Engineering Management*, Vol. 143, Issue 8, 04017057. DOI: 10.1061/(ASCE)CO.1943-7862.0001353.

Cigola, M. and Ceccarelli, M. (2014). Marcus Vituvius polio (Second half of the 1st Century B. C.). In Ceccarelli, M. (eds.) Distinguished Figures in Mechanism and Machine Science. Springer. History of Mechanism and Machine Science, Vol. 26. https://doi.org/10.1007/978-94-017-8947-9_15 [Date accessed March 13, 2023]

Deepa, V., Eldhose, S., and Anu, V. V. (2019). Analysis of material cost in road construction through lot sizing techniques. *Journal of Civil and Construction Engineering*, Vol. 5, Issue 1, pp. 38–45.

Dictionary (2020). *Timepiece*. [online] Available at: https://www.dictionary.com/browse/timepiece [Date accessed April 21, 2020].

Erismis, M. C. and Gezerman, A. O. (2013). A critical look at Vitruvius. *Elixir International Journal*, Vol. 55A, pp. 13324–13328.

Fapohunda, C. A. (2019). *Limit state design of reinforced concrete structural elements*. [online] Available at: http://repository.fuoye.edu.ng/bitstream/123456789/1463/3/Limit%20State%20Design%20of%20Reinforced%20Concrete%20Structural%20Elements%20by%20C.%20A.%20Fapohunda.pdf [Date accessed January 11, 2011].

Fapohunda, C. A. and Daramola, D. D. (2019). Experimental study of some structural properties of concrete with fine aggregates replaced partially by pulverized termite mound (PTM). *Journal of King Saud University - Engineering Sciences*, Vol. 32, Issue 8, pp. 484–490. DOI: 10.1016/j.jksues.2019.05.005.https://doi.org/10.1016/j.jksues.2019.05.005

NUC (2022).Core Curriculum and Minimum Academic Standards for the Nigerian University System (CCMAS). https://www.nuc.edu.ng [Date assessed march 13, 2022]

Ghazvini, K., Zandieh, M., and M. Vafamehr (2020). Exploring KPIS utilization effects on decision making for the architectural design process in industrial buildings. *Civil and Environmental Engineering*, Vol. 16, Issue 1, pp. 198–209. DOI: 10.2478/cee-2020-0019.

Grúňová, Z. and Holešová, M. (2018). Columnar entasis In Vignola's and other renaissance works. *Civil and Environmental Engineering*, Vol. 14, Issue 2, pp. 132–137. DOI: 10.2478/cee-2018-0017.

Heath, T. (1989). Lessons from Vitruvius. *Design Studies*, Vol. 10, Issue 4, pp. 246–253. DOI: 10.1016/0142-694X(89)90008-2.

ICE (2018). *Royal Charter, By-Laws, Regulations and Rules*. London: Institution of Civil Engineers, pp. 1 – 29.

Kau, K. W. (2007). Incorporation of sustainability concepts into a civil engineering curriculum. *Journal of Professional Issues in Engineering Education and Practice*, Vol. 133, Issue 3, pp. 188–191. DOI: 10.1061/(ASCE)1052-3928(2007)133:3(188).

Locatelli, G., Mariani, G., Sainati, T., and Greco, M. (2016). Corruption in public projects and megaprojects: there is an elephant in the room! *International Journal of Project Management*, Vol. 35, Issue 3, pp. 252–268. DOI: 10.1016/j.ijproman.2016.09.010.

Maguth, B. M., Dustman, J., and Kerr, M. (2013). Re-examining the Statue of Liberty: different perspectives on history and the promise of America. *Social Studies and the Young Learner*, Vol. 25, No. 4, pp. 9–14.

Merdinger, C. J. (1949). *A history of civil engineering. PhD Thesis*. [online] Available at: https://ora.ox.ac.uk/objects/uuid:76bd9626-ba71-4339-840e-92c39c64ac77 [Date accessed April 1, 2021].

Merriam-Webster.com (2022). *Timepiece*. [online] Available at: https://www.merriam-webster.com/dictionary/timepiece. [Date accessed May 19, 2022].

Newman, W. E. and Vassigh, S. (2014). What would Vitruvius do? Re-thinking architecture education for the 21st century university. In: Rockwood, D. and Sarvimäki, M. (ed.). *Proceedings of the ARCC/EAAE 2014 International Conference on Architectural Research Beyond Architecture: New Intersections & Connections*. Honolulu, HI: University of Hawaii at Manoa, pp. 67–74.

Patterson, R. (2004). Interpretations of Vitruvius critical misunderstanding. Classical rhetoric. *Architectural Research Quarterly*, Vol. 8, Issue 2, pp. 101–102. DOI: 10.1017/S1359135504210120.

RILEM (2019). A global call for sustainable developments of the built environment. In: *International Union of Laboratories and Experts in Construction Materials, Systems and Structures. 2019–2020. Technical Report*, pp. 15–16.

Savija, B. (2020). Use of 3D printing to create multifunctional cementitious composites: review, challenges and opportunities. *RILEM Technical Letters*, Vol. 5, pp. 16–25. DOI: 10.21809/rilemtechlett.2020.113.

Schulzová, K. and Bošová, D. (2019). The quality of daylight in various types of

residential buildings. In: *Proceedings of International Conference, ENVIBUILD – Buildings and Environment, November 7, 2019, Bratislava, Slovakia*, pp. 159–164. DOI: 10.2478/9788395669699-026.

Seward, D. (2007). *Understanding structures: analysis, materials, design. 2nd edition*. London: MacMillan Press Ltd, 320 p.

Shakantu, W., Tookey. J. E., and Bowen, P. A. (2003). The hidden cost of transportation of construction materials: an overview. *Journal of Engineering Design and Technology*, Vol. 1, Issue 1, pp. 103–118. DOI: 10.1108/eb060892.

Small, J. P. (2019). Circling round Vitruvius, linear perspective, and the design of Roman wall painting. *Arts*, Vol. 8, Issue 3, 118. DOI: 10.3390/arts8030118.

The Ames Foundation (2020). *Justinian, Institutes*. [online] Available at: https://amesfoundation.law.harvard.edu/digital/CJCiv/JInst.pdf [Date accessed April 21, 2020].

Thiemann, L., Gerzer, S., and Kilian, R. (2010). Vitruvius and antique techniques of

plaster work and painting. In: *2nd Historic Mortars Conference HMC2010 and RILEM TC 203-RHM Final Workshop, September 22–24, 2010, Prague, Czech Republic*.

Vitruvius, M. P. (1914). *The Ten Books of Architecture*. Cambridge: Harvard University Press, 331 p.

Watson, J. G. (2020). *Civil engineering*. [online] Available at: https://www.britannica.com/technology/civil-engineering [Date accessed April 21, 2021].

Wikipedia (2011). *De Architectura*. [online] Available at: https://en.wikipedia.org/wiki/De_architectura# [Date accessed October 21, 2021].

Wozniak-Szpakiewicz, E. and Zhao, S. (2018). Modular construction industry growth and its impact on the built environment. *Technical Transactions*, Vol. 115, Issue 12, pp. 43–52. DOI: 10.4467/2353737XCT.18.178.9666.

DOI: 10.23968/2500-0055-2023-8-1-13-24

COMPUTATIONAL DESIGN FOR FUTURISTIC ENVIRONMENTALLY ADAPTIVE BUILDING FORMS AND STRUCTURES

Aref Maksoud*, Hayder Basel Al-Beer, Aseel Ali Hussien, Samir Dirar,
Emad Mushtaha, Moohammed Wasim Yahia

United Arab Emirates University of Sharjah
Sharjah, United Arab Emirates

*Corresponding author's e-mail: amaksoud@sharjah.ac.ae

Abstract

Introduction: With the rapid development in computational design, both architectural design and representation processes have witnessed a revolutionary change from the analog to the digital medium, opening new doors for adaptability in the architectural design process by leveraging nature concepts in design. The computational design approach starts with the mathematical model definition based on numerical relations and equations, thus, replacing the standard visual representation. **Purpose of the study:** We aimed to integrate computational design technologies to create self-learning buildings that could adapt to environmental challenges and adjust accordingly by collecting data from the surrounding environment via the implementation of sensors. **Methods:** We started with extensive research on state-of-the-art computational design in architecture, followed by the design implementation and the implementation of the architectural design of a building. The design followed a parametric approach to design and strategies. An algorithm was developed with Grasshopper Scripting to generate documents that mimic the growth process of cellular bone structures and adapt that form to a selected project site. To ensure that the generated form is adaptable, we performed multiple analyses, such as sunlight, radiation, and shadow analysis, before selecting the form and finishing its development. The results show that an environmentally responsive form that extends from the surrounding environment is characterized by high levels of adaptability. **Results:** In the course of the study, the effectiveness of computational design technologies in architecture was established.

Keywords: computational design; Grasshopper; parametric design; architecture; adaptive design.

Introduction

Integrating computational design (CD) via parametric architecture has been done with machines mimicking the human mind. The ability to mimic such skills as critical thinking, problem-solving, and decision-making refers to the desired attribute of CD intelligence and its ability to think and make decisions to achieve a specific goal (Choi et al., 2010).

The advancement of technology increases the evolvement of CD to benefit a wide variety of industries (Dimitropoulos et al., 2021). Nowadays, various tools are being developed in the AEC industry that leverage CD to automate tasks and decrease the time of their performing from days to minutes.

This big jump in technology is setting a new standard for the way architecture is practiced. It is taking architectural practices in a direction where it will no longer be optional to upgrade to new design methods (Emaminejad and Akhavian, 2022). Caetano et al. (2020) identified the positive impact of CD on architecture and established that it enables architects to enhance the design process by expanding its conceptual boundaries. Nisztuk and Myszkowski (2017) demonstrated that recent studies still focus on finding accurate and effective computational approaches for the generation of floor plans with less focus on the effectiveness of a particular algorithm or IT solution.

Caetano and Leitão (2020) focused on three aspects: analyzing CD, discussing advancements in CD tools, and presenting architectural projects and events that explored CD. The results showed that technological developments continue to shape architectural theory and practice and, simultaneously, are guided by their needs and aspirations.

In this study, we explore the potential of integrating Artificial Intelligence in architecture to create self-learning buildings that can adapt to future challenges and enhance their performance, and improve the architectural design process using computational design technologies. This paper focuses on two aspects. First, we dive into the subject of CD and how it would serve architecture in a hypothetical scenario.

The second part shows the architectural design process in implementing a building using computational design. By looking at the factors that influenced architecture throughout history, it can be noticed that a new historical event happens every few decades, such as a natural disaster, war, or pandemic, which inspires architects, engineers, and designers to address new design challenges (Hendy, 2020).

This study aims to create a building that uses a system providing innovative solutions for any potential challenge facing the building. Such a system would take advantage of the latest machine-learning technologies. It would merge sensors and bio-digital materials, which work perfectly together to deal with any challenge (Estévez and Navarro, 2017). An example of this would be the challenges that occurred during the COVID-19 era. In this case, the building would adapt by activating social distancing from within the building, which could be done through the communication between the CD cloud system of the building and the robots, which are inside the building. This means the CD would take the necessary actions to adapt and achieve the goal of social distancing (Ahmed, 2021).

Another way to deal with COVID-19 challenges could be by placing an innovative skin on the buildings' interior walls, which does not pick up germs. This can ensure that the spaces are sanitized at all times (Assaf, 2021).

The goal of this study is to create a self-learning building. It would be a building that can adapt and learn from all sorts of aspects of its environment (Cortiços, 2019). For example, if a project is implemented in a particular place, the intelligent building system would be able to study and collect information internally about the culture of that place and adapt itself to that culture. It would use sensors to know the number of people in the building, the time they spend together, the clothes they are wearing, and the actions they are taking.

After some time, it would see patterns and learn from them to predict what will happen in the future (Hutson, 2017). Another example of what the building can learn is the environmental conditions of its site, which can be sensed externally. This means the building would be able to collect and store data about the environmental conditions and energy use of the building.

Based on the data collected, it would decide on the actions needed to reduce the energy use of the building, such as changing the tint of the windows to reduce the amount of heat in the building (Mehra and Sharma, 2019).

1. *Use of technology to enhance building performance*

When it comes to the performance of buildings, new automation systems can be used to control security, comfort, and energy efficiency (Birangal et al., 2015). AI enables buildings to become places driven by real-time data and feedback, communicating with itself like a living organism (Cotrufo et al., 2020).

It creates a system where buildings, smartphones, cars, and public places share to improve living conditions, limit waste and traffic, and increase safety. This would allow the building's AI to predict any challenges that might come up (Alexander, 2020). AI also opens the doors to creating smart homes, living spaces that are complex real-time data-driven living organisms (Pala and Özkan, 2020).

For architects, the challenge is how to use AI to fit it into the design language of the home to improve the lives of the residents (Chua, 2013). With AI, we would be able to tailor the building performance according to the people's needs and have buildings learn, adapt, and respond to the data that they receive from the users (Zhao et al., 2019).

AI in buildings takes complete care of residents' comfort and safety and helps with energy and financial savings (Joshi, 2019). AI-based energy management platforms can track usage patterns to create proper conditions for tenants, conserving energy and saving money (Chen et al., 2021). Fig. 1 shows a Nest Thermostat, an excellent example of a system that can adapt and keep the building at a safe and optimal temperature. It can also alert users if the temperature increases to reach a dangerous range. AI devices can analyze data from sensors to monitor leaks or malfunctions. This makes it easier than ever to track the building's performance and efficiency (Oberste-Ufer, 2019).

In addition, building managers can maximize operational efficiency, properly utilize assets, and improve the comfort level of occupants (Rocha et al., 2021).

2. *Use of AI in the architectural design process*

As architects, we start our projects by spending many hours on research to understand the design philosophy of that project and analyze previous similar projects. However, this process takes much time, and here AI comes in (Al-Azzawi and Al-Majidi, 2021). AI can collect and combine limitless amounts of data in little time, make decisions, and give recommendations that ease the architect's research process (Kurtoglu et al., 2009).

The architect can test many ideas and conceptual designs simultaneously without needing a pen and paper, and, as a result, better understand the design philosophy using a faster strategy. We are living in the world where AI has become a tool to leverage the design process. However, it is not convenient

Fig. 1. AI Nest Thermostat device keeping the building at an optimal temperature (Wollerton, 2018)

to automate the entire design process and solely depend on AI as there are always possible errors.

The real advantage of using AI comes from a collaboration between human intelligence and Artificial Intelligence (Wang, 2011). Today, there are many AI engines, such as DeepArt, MidJourney, and DALL-E, which open doors to a wide variety of possibilities that can affect the architectural design process. These engines can visualize anything the user desires. The user (provided that they have some prior knowledge in coding) just needs to type a prompt.

This means that the concept stage in the design process will no longer need to involve sketching the ideas. It can simply be visualized with high quality in seconds (Jaruga-Rozdolska, 2022). Fig. 2 shows images of buildings generated by the AI engine MidJourney in a matter of minutes. These images were obtained by typing a prompt to generate a building in a nature-inspired style. The engine creates four images and allows the user to select the best ones to further create more images and make enhancements. Traditionally, it might take days to manually design and render, but with AI, it can be reduced to minutes.

3. *Computational design in the architectural design process*

Parametric/Computational Design is a significant field where technology and architecture work together harmoniously and where programming tools have quite an impact on architecture. CD allows us to create a parameter-based system that can generate the desired output, such as forms, structures, and systems, with the ability to control high levels of complexity.

The CD approach to architectural design gives the designer many advantages, such as creating complex structures and having complete control over them, automating redundant tasks, which take a lot of time in the design process, and easily modifying the design at the late stages (Oxman, 2017). Intelligent software like Grasshopper Scripting gives the architect the opportunity to use geometric component-based programming with complex algorithms to generate design variations that follow a specific design vocabulary and offer numerous design options. One of the advantages of using Grasshopper is its ability to control and produce high-quality complex organic geometries (Cubukcuoglu et al., 2019).

Another advantage is that it is supported by a variety of plugins, providing access to external libraries such as Ladybug, thus giving you the opportunity to perform a real-time environmental analysis of your project, which will be demonstrated in Section 2.2.2 below (Roudsari et al., 2013). Another popular CD software is Dynamo. It is a visual programming software created by Autodesk, which can be used with Revit, a BIM software. As

Fig. 2. An example of images of buildings generated by MidJourney (source: the authors)

opposed to Grasshopper, Dynamo's advantage is not in creating geometries but rather in ensuring data management for the project, which makes it an excellent choice for BIM. Dynamo is a very important tool in the automation of a lot of BIM processes, which increases the efficiency of the design process (Shishina and Sergeev, 2019).

It works on a node-based system. Each node carries a piece of code inside, but instead of writing the code, a node can be dropped easily with a ready-to-use code. These nodes can be connected with wires to be merged into one piece of code that performs a specific function. A full algorithm would usually look similar to the one shown in Fig. 3, where groups of nodes connected perform one or more specific actions. These CD strategies are almost like an architect's own programming language. They can be made even more vital when paired with Virtual Reality (VR) and Augmented Reality (AR) devices, where you would be able to use devices like the Magic Leap to observe your design as if it is built in front of you and make adjustments from a different perspective (Philips, 2020).

Methods

The approach followed in this paper to show the architectural design process for the implementation of the building is divided into three phases. The first phase is the form generation process. In this phase, a concept for an adaptable organism is selected to inspire the form generation strategy. After that, an algorithm is designed using Grasshopper Scripting to generate various adaptive forms. The second phase is the form selection process. In this phase, the forms generated in the previous phase get filtered according to many different analyses, such as structure, radiation, and shadow analysis. The filtration process will help in selecting the most

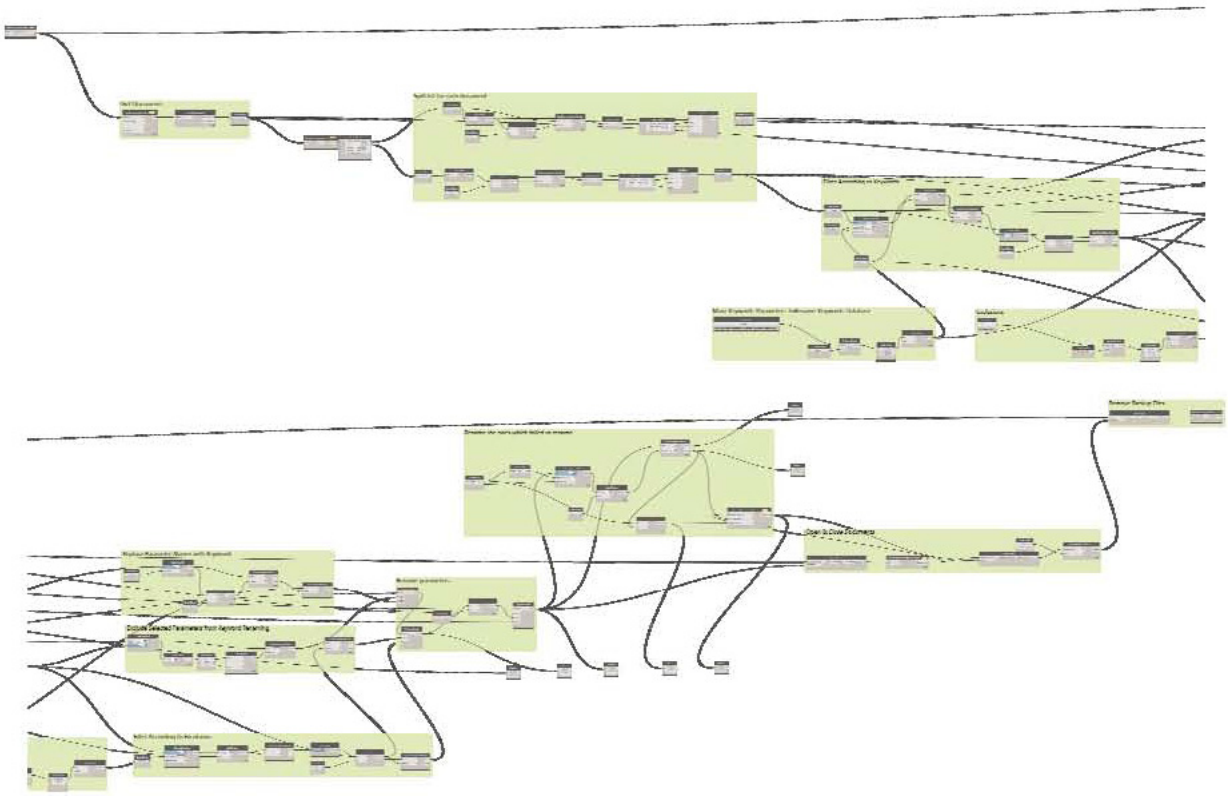

Fig. 3 shows an example of an algorithm design in Dynamo. As seen from Fig. as well as Fig. 5, which is a Grasshopper algorithm, the way these tools work is similar to coding but more convenient

environmentally responsive form. In the third phase, the final selected generation is developed further to finalize the design and ensure a more ecologically responsible approach.

1. *Phase 1: Form generation process*

1.1. Concept development

The basis of this project was adaptation. The research interests lie in form finding, form optimization, architectural facades, skin, and other geometrical explorations using computational tools such as Rhino and Grasshopper. When we look at nature, we can see a lot of naturally adaptive forms and processes. This makes nature the mother of inspiration for adaptive designs. We followed the natural process of adaptation, combining parametric modeling and CD modeling to explore avant garde bio-inspired concepts. We also aimed to take a concept from idea to form and visually present it in a convincing rendering. It was planned to use growth as a generative tool to create unexpected forms that resemble those found in nature and organisms.

In the course of the study, we used Rhinoceros paired with Grasshopper + plugins to obtain biomorphic designs. We tried to use computational tools and strategies to create complex forms morphing and mimicking the growth of bone cellular structures, which are shown in Fig. 4. The goal was to bio-mimic the process of growth in these organisms that causes them to evolve into an adaptive structure. These organisms grow in a way that produces voids of different sizes in structures.

In architecture, such voids could help create different-sized patios that would allow sunlight to go into the building to reach the internal spaces and wind to flow and naturally ventilate the building, thus making an environmentally responsive form. These

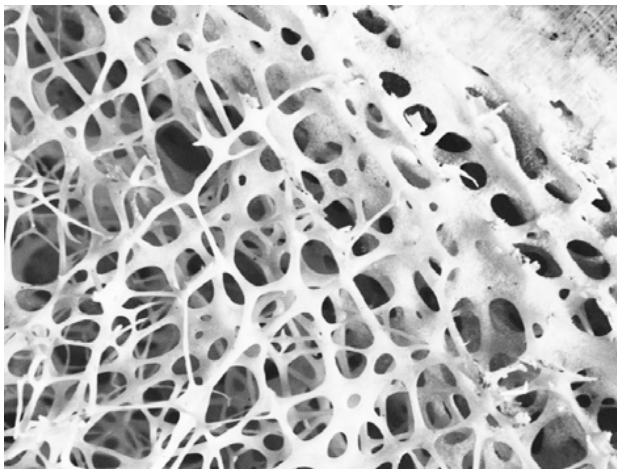

Fig. 4. Cellular structures' growth pattern (Naboni and Kunic, 2017)

structures also could melt into each other forming bridges between the different cells. The formed bridges would connect functions on different levels (Chen et al., 2015).

1.2. Grasshopper script design

To generate architectural forms that mimic the growth of bone cellular structures, intelligent CD technology and component-based programming tools such as Grasshopper were used in the design process. This design technology allowed for developing an algorithm creating a system that can generate complex forms based on logic.

The CD tools and principles were used to design a Grasshopper definition that can generate adaptive forms bio-mimicking the natural process. The Cocoon plugin was applied in the process since it helps generate organic forms that connect masses by melting them into each other. As shown in Fig. 5, the main component is called the Cocoon, which is the script's core. The Cocoon generates the form based on the inputs, which are shown on the left side and called Charges.

These charges include three input parameters.

The first parameter is the site-surrounding blocks shown in Fig. 6. Using the site surroundings as a parameter guarantees a form specifically tailored to the selected site. The second parameter is the connection lines including the connection to the surrounding blocks, the entrances to the site, and the overall circulation pattern. Using those as a parameter helps in defining the mobility and circulation path of the building. To generate a final form, the volume of the function was used as the third input.

It was used as an input parameter instead of the area of each function to generate 3D forms, not 2D patterns. Finally, the last component on the right is the Smooth component which is used to smoothen the connection between the masses.

2. *Phase 2: Form selection process*

2.1. Experimental studies

The approach followed to generate an adaptive, environmentally responsive form was subject to experimental studies. In this phase, tens of experimental studies are generated and filtered by analyzing and selecting the most adaptive form. To achieve this, the Grasshopper definition was developed further by using the Millipede plugin. This plugin gives an opportunity to analyze the structure of each generated form and provides essential values such as maximum deflection, weight, yield, bending moment, and more.

The generation process for all the experimental studies was implemented using the Grasshopper Galapagos tool. It is an Artificial Intelligence tool in Grasshopper that changes the selected parameters to find the best solution which maximizes or minimizes a selected value. In this case, the value that was selected to be minimized is the maximum deflection of each form, which was calculated with the Millipede components.

The parameters that were altered to change the form were the radius and the position of each Cocoon charge assigned to the site-surrounding blocks and connections. Fig. 7 shows the best 24 generated results of experimental studies with the Galapagos tool.

2.2. Selection analysis.

At this stage, we analyzed the results of experimental studies generated at the previous stage. Fig. 8 shows all the structural analyses for the generated forms. The colors show the distribution of deflection around the form; the red color shows the high-deflection areas, and the blue color shows lower amounts of deflection distribution.

The filtration process will depend on the forms with the lowest maximum deflection, deflection distribution

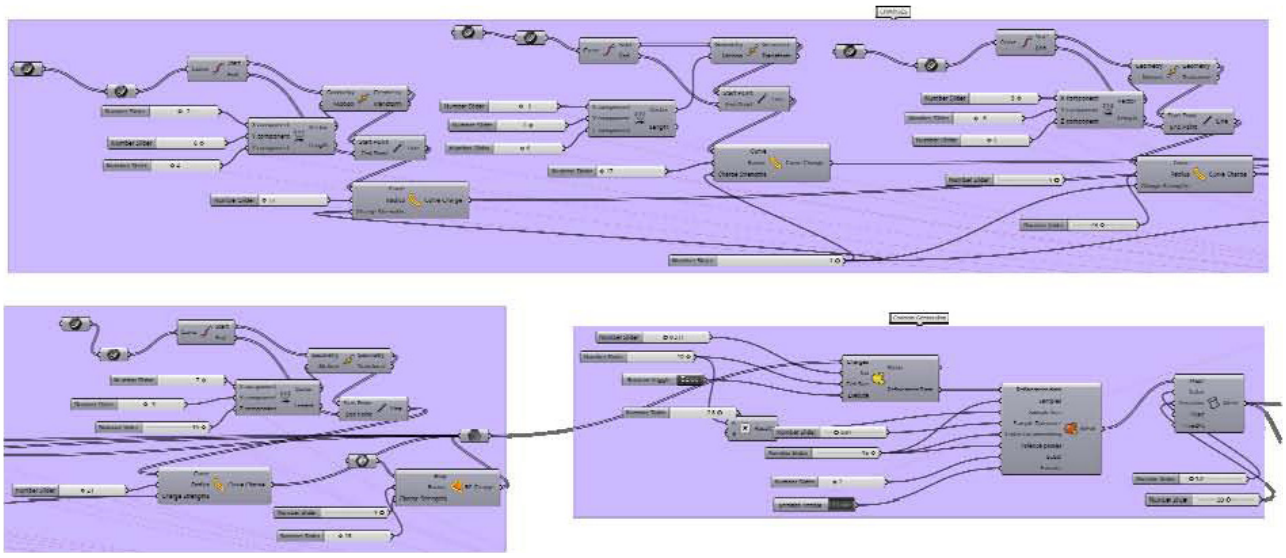

Fig. 5. Grasshopper algorithm designed to generate building forms

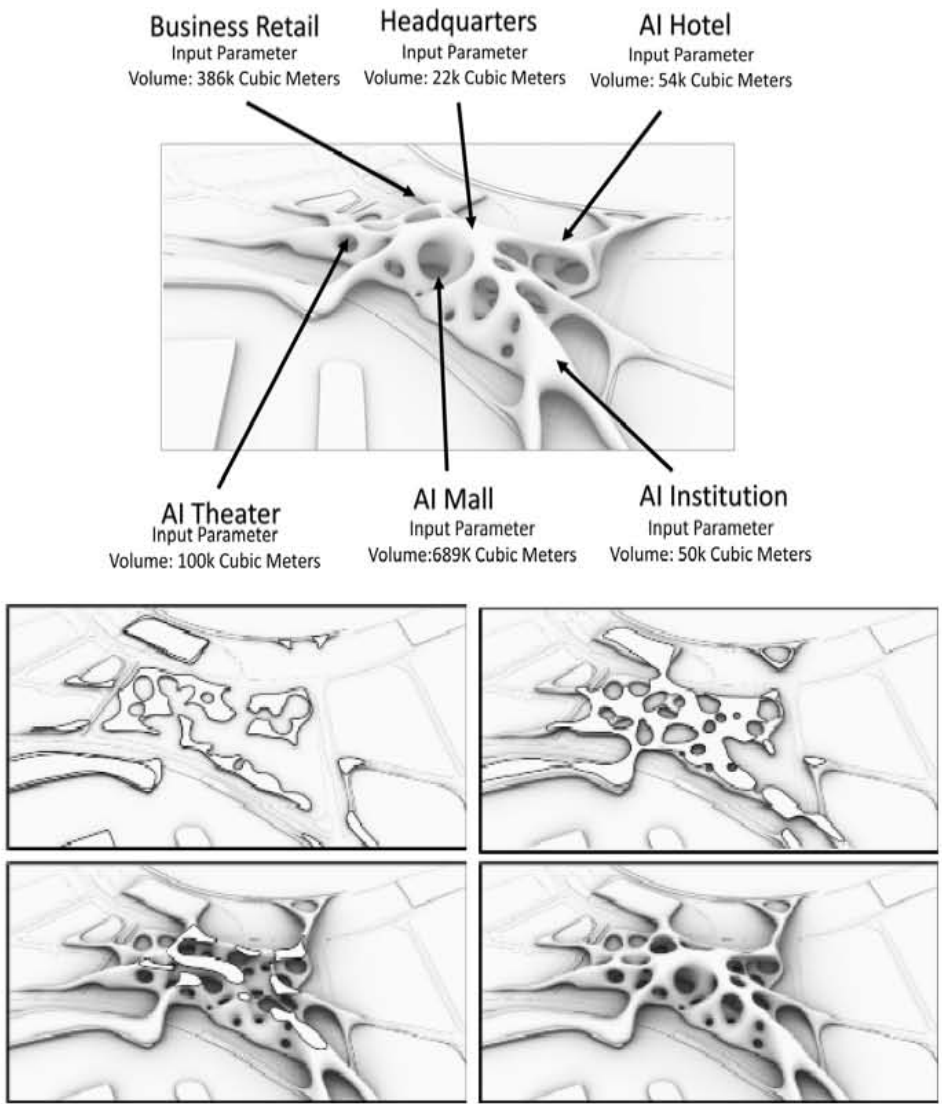

Fig. 6. Site surroundings and volume of each function as the parameters defining how the building will look like

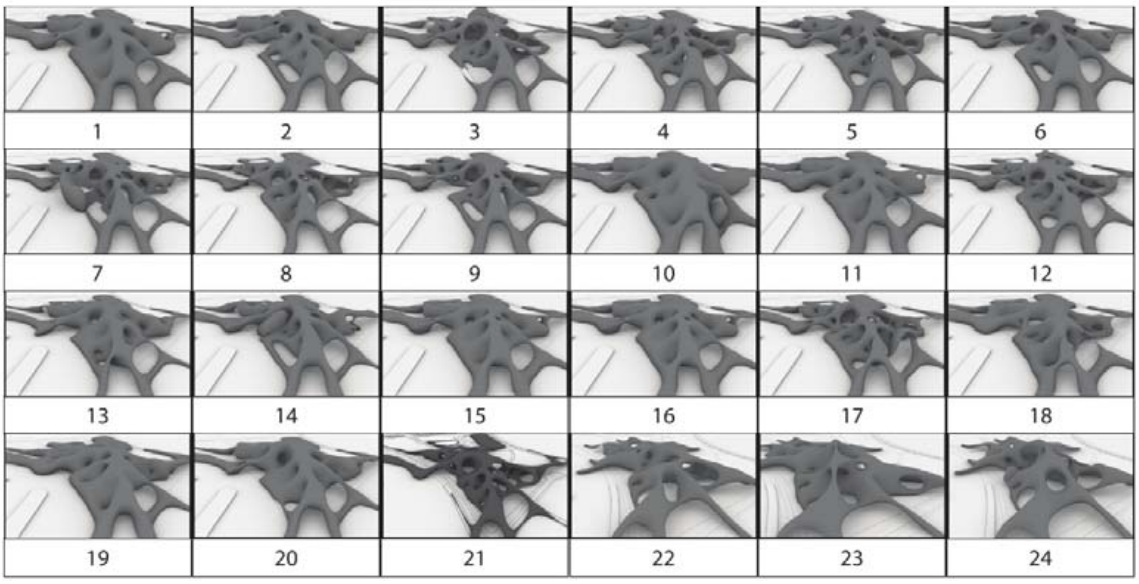

Fig. 7. Experimental studies performed in the process of generating the best form

pattern, density of the structure, and availability of errors in the form. According to these criteria, the best four forms are generations 21, 22, 24, and 24, with the minor deflection in all the experiments.

In addition, as seen from the colors, their deflection distribution pattern is acceptable. It can be noticed that all four of these generations are very similar, which makes sense since they have similar performances. These four forms then went through shadow and radiation analysis to select the most adaptive final form. Fig. 9 shows the shadow analysis for the four selected forms. It can be seen from Fig. 9 that the best selection would be generation 21.

Since this selection has more considerable curvature, it provides a more extensive surface area towards the side of the Sun's movement. It casts shadows for a longer time of the day, with only one hour of direct sunlight hitting the internal part of the building. Fig. 9 also shows the radiation analysis for the same four generations (Maksoud et al., 2022). Similarly, the same selection performed the best in terms of radiation on the internal part of the building with a value below 467.98 kWh/m^2, which makes sense since this form will have the least amount of direct sun exposure. The performed analysis helped in selecting the most environmentally responsive form.

3. *Phase 3: Form development process*

3.1. Skin and structure development

After selecting the most adaptive form, we developed it into a finalized form. At this stage, another Grasshopper definition was designed to generate the skin and the structure of the building. As you can see in Fig. 10, this definition uses the Weaverbirds plugin, which helps in generating triangle-shaped panels forming the geometry of the form.

It also helps in generating the structural members that are supporting these panels. The skin that is used for the building is smart skin. It can sense the Sun's heat using CD and change the tint of the glass when the heat increases and decreases. The panels that are facing the Sun moving from the south will be filled with solar PV panels to generate energy for the building. As for the rest of the panels that are facing the other sides, they will be filled with smart glass, which helps bring diffused light into the building. (Abdalla, S.B et al., 2022)

Results and discussion

1. *Adaptive expansion system using CD*

The final form of the building was produced after finishing the form development, shown in Fig. 11. As seen from the Figure, the strategy of using CD in the design process helped in creating an elegant

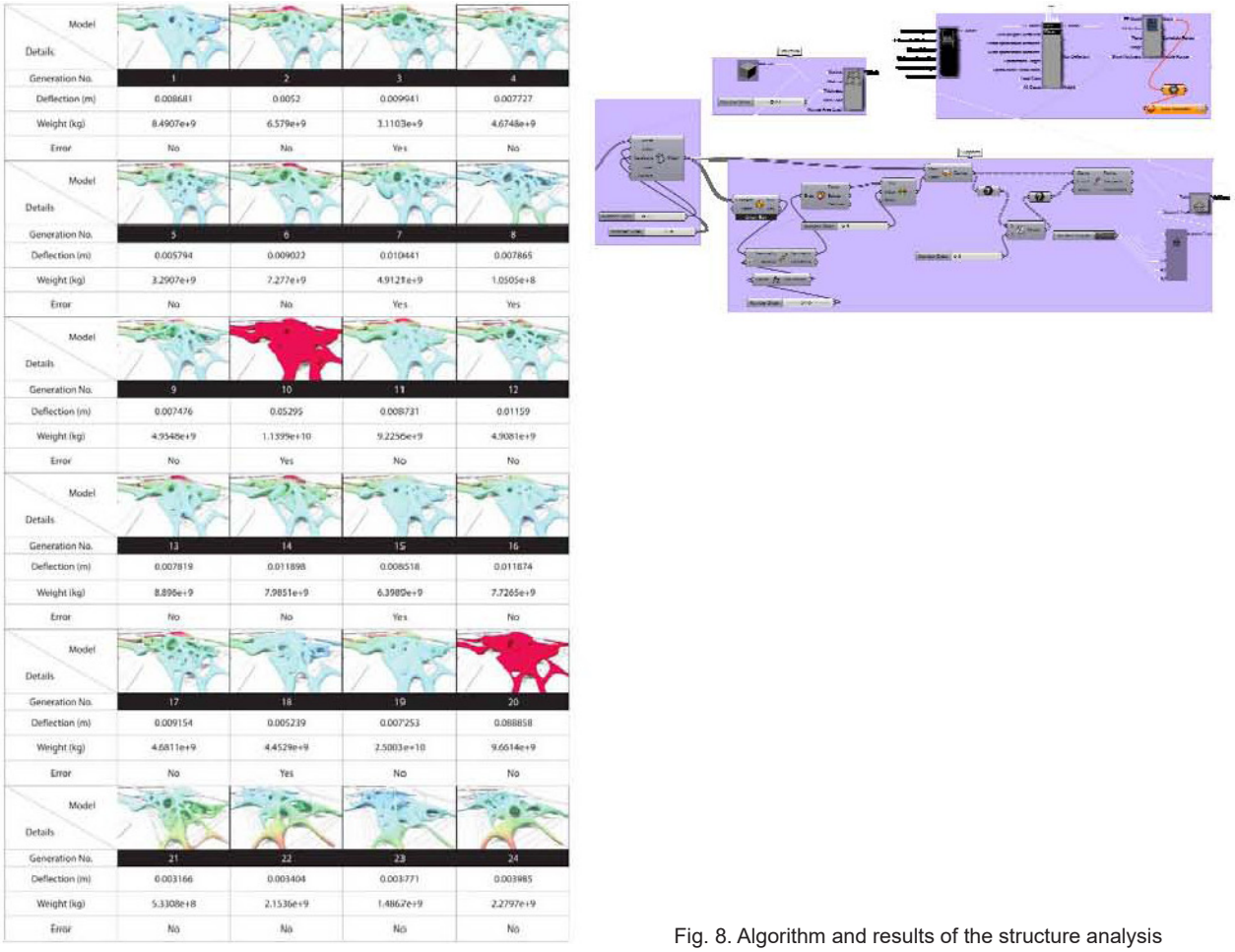

Fig. 8. Algorithm and results of the structure analysis

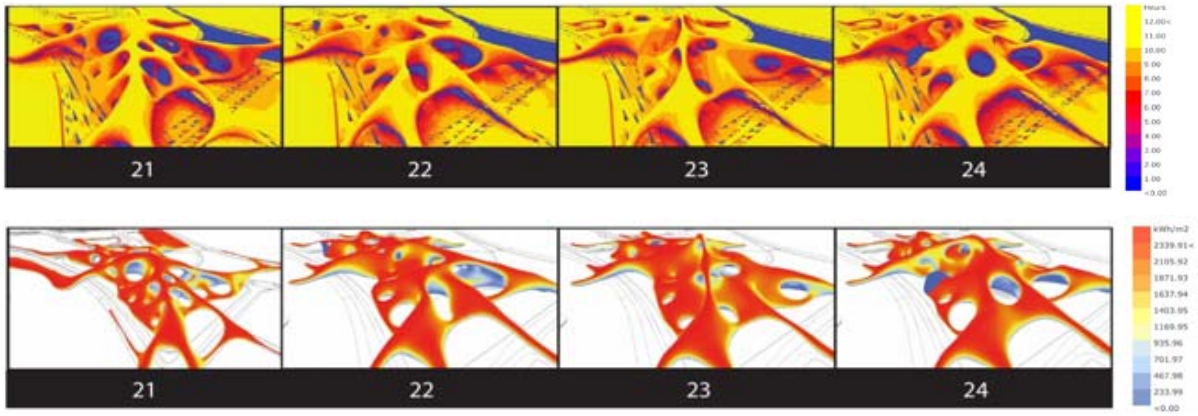

Fig. 9. Shadow and radiation analysis for the best four generations

originally looking building adapted to the site. The obtained final design looks futuristic, and some might argue that it's not buildable. However, CD tools provide more strategies for us in the digital fabrication of such designs.

For example, each of those panels that make the skin of the building can be easily tracked with Grasshopper to produce a report with all the pieces required to build this using manufacturing and assembly data.

The story does not end here because a new analysis must be made to test the performance of the final building after its development and check if the building is environmentally responsive.

To analyze the performance, a new Grasshopper algorithm was developed using the Ladybug plugin, which is shown in Fig. 12.

The table in Fig. 12 shows the results of the analysis that was generated from the algorithm. As seen from the Table, the total radiation per year is 161.36 kWh/m^2. To know if that is a good result, it can be compared to the Emirates GBC BEA Project from the Emirates GBC 2020 Green Building Market Brief, which is shown in Fig. 13.

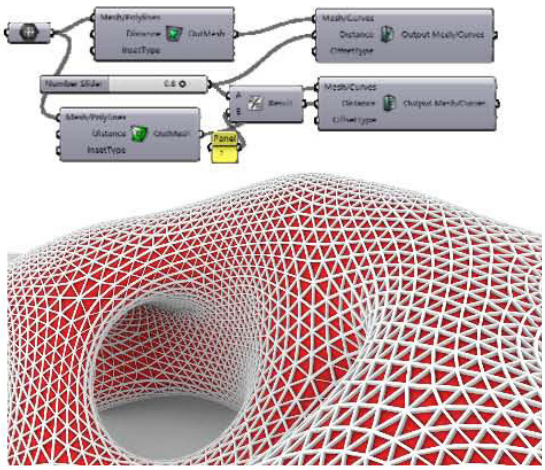

Fig. 10. Skin and structure of the building

Fig. 13 shows that the best performers in terms of radiation are the buildings that have less than 171 kWh/m^2 for hotels, 193 kWh/m^2 for resorts, 92 kWh/m^2 for schools, and 378 kWh/m^2 for malls (Emiratesgbc.org, 2020). Fig. 14 shows that a significant part of this building is a CD Mall, and there are some parts of the building that act as a CD Hotel and CD Institute. (Mushtaha, Emad et al., 2022)

When comparing our results to those of the BEA project, it can be concluded that the building is considered a best performer when it comes to the mall and hotel and a median performer when it comes to the institute. These results prove that the building generated by CD is, in fact, environmentally responsive.

In addition, it can be noticed from Fig. 12 that the PV panels placed on the south façade provide 368,070.02 kWh per year, which is 12% of the building's energy.

2. *Adaptive expansion system using CD*

CD has many potentials in design. At this stage, a CD engine called Deepart.io was used to predict the future expansion of the building on the project's site and in the city of Dubai. This is a global CD engine that has been used by international universities like MIT & organizations like AA in London. It can alter a picture based on a given style, which acts as a parameter controlling the output. So, a picture of the site was uploaded as an input with another picture of one of the experimental studies, as shown in Fig. 14.

The CD engine was able to study the style of the building and produce an output showing how the entire site would look when filled with this form. In architectural terms, this CD engine could predict future expansion of the building based on its information as a parameter. This makes architecture no longer about one building; it is rather about an adaptive system that can be applied in any location. By changing the picture of the site to a picture of a different site, the CD engine will adapt the form to the new site and produce a different result.

Conclusion

CD technologies not only enhance the efficiency of the design process but also help create adaptive

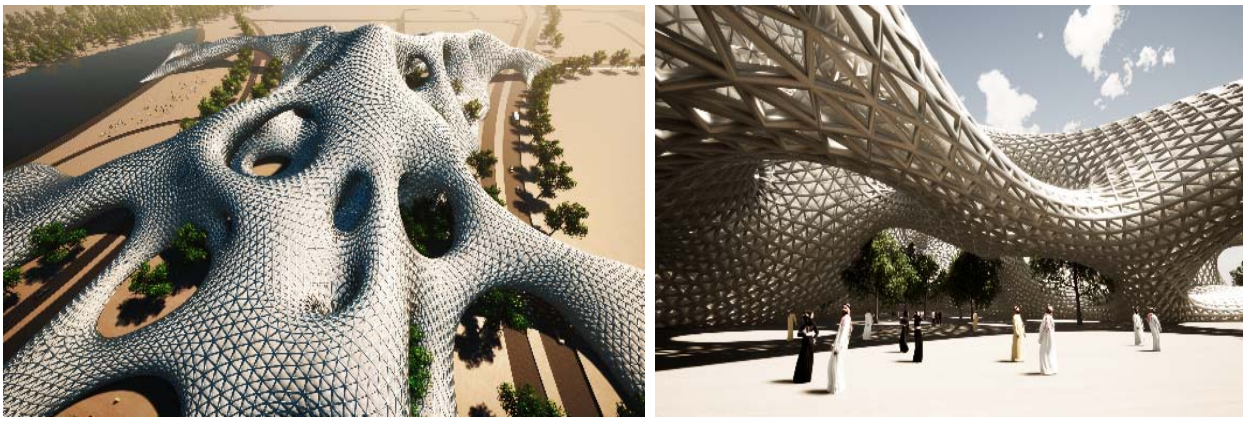

Fig. 11. Final form of the building after the development stage

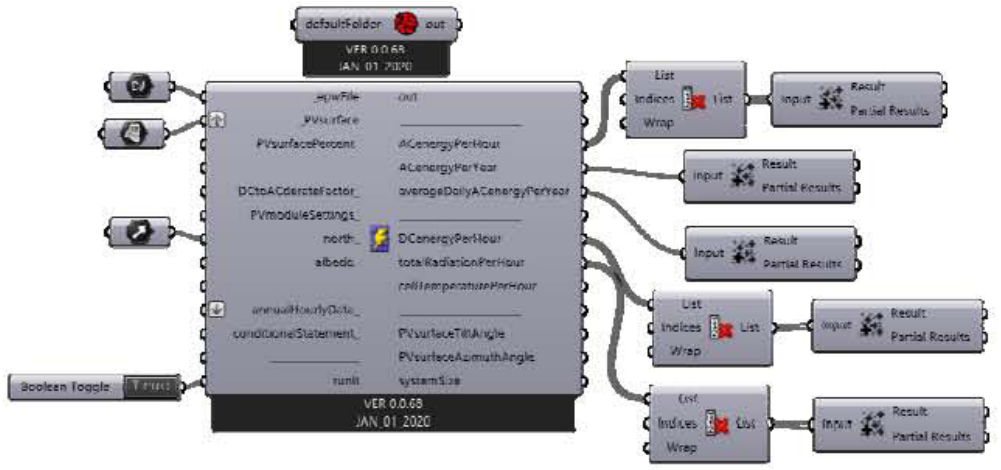

	AC Energy per year (kWh)	Average Daily AC Energy per year (kWh/day)	DC Energy per year (kWh)	Total Radiation per year (kWh/m²)	Total Radiation per year (kWh)
Final Result	322924.56	884.72	368070.02	161.36	2689300

Fig. 12. Algorithm and results of the energy use

BEA RESULTS - Energy Use in Dubai Hotels, Malls and Schools

	Best Performers	Median	Worst Performers
Hotels	< 171 kWh/m².year	249 kWh/m².year	> 414 kWh/m².year
Resorts	< 193 kWh/m².year	334 kWh/m².year	> 444 kWh/m².year
Schools	< 92 kWh/m².year	134 kWh/m².year	> 233 kWh/m².year
Malls	< 378 kWh/m².year	465 kWh/m².year	> 580 kWh/m².year

Fig. 13. Emirates GBC BEA Project from the Emirates GBC 2020 Green Building Market Brief

and environmentally responsive designs. The studies on the effects of these technologies in architecture consisted of two parts. The first part focused on studying how CD could enhance building performance and analyzing some hypothetical scenarios of how it might be implemented. The second part focused on the implementation of the architectural design of a building.

This process used CD technologies to enhance the architectural design process and create more adaptive designs. This stage included three phases:

Phase 1: Using CD tools such as Grasshopper Scripting to design a script that can generate different kinds of adaptable forms.

Phase 2: Performing experimental studies and selecting the best form based on structure, shadow, and radiation analysis.

Phase 3: Developing the skin and the structure of the building, which consisted of triangular panels filled with PV panels from the south and smart glass from the other sides.

After those phases, further analyses were conducted to test the final performance of the building.

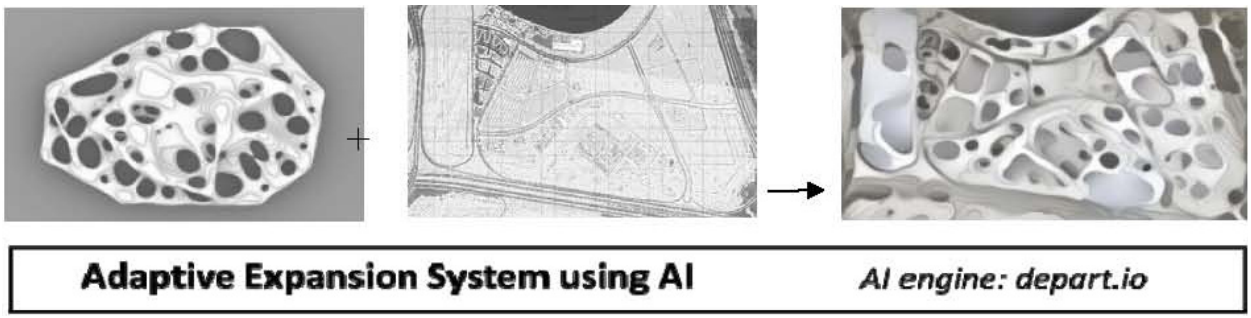

Fig. 14. Using AI to predict the future expansion of the building

The radiation analysis resulted in 161.36 kWh/m^2, which was compared to the values of the Emirates GBC BEA Project from the Emirates GBC 2020 Green Building Market Brief to prove that the resultant form is, in fact, environmentally responsive.

Another analysis was done to test the performance of the PV panels in producing energy for the building, which showed that the PV panels cover 12% of the building's energy.

A CD engine was then used in developing an adaptation system for the building. In conclusion, this research explored the potential of using CD and its technologies in architecture. With the results that showed how the technology helped in creating an environmentally responsive design, it is obvious that these technologies are powerful strategies to be considered and implemented in architecture.

The implementation of CD technologies in architecture starts from the beginning of the design process all the way to the functionality of the actual building. Dubai, being one of the most competitive cities regarding technology, has enormous potential to implement a project like this.

The significant limitation in this field is the scarcity of expertise in CD technology, which makes implementation expensive.

Finally, design and technology are increasingly becoming more connected to each other; it will open doors for new areas of research and redefine how future architecture will look like.

Acknowledgments

This research was partially supported by the University of Sharjah, College of Engineering, Department of Architectural Engineering. We thank our colleagues from the Department of Architectural Engineering, who provided insight and expertise that greatly assisted the research.

References

Abdalla, S.B.; Rashid, M.; Yahia, M.W.; Mushtaha, E.; Opoku, A.; Sukkar, A.; Maksoud, A.; Hamad, R. Comparative Analysis of Building Information Modeling (BIM) Patterns and Trends in the United Arab Emirates (UAE) with Developed Countries. Buildings 2023, 13, 695. doi: 10.3390/buildings13030695

Ahmed, S. N. (2021). Covid, AI, and robotics - a neurologist's perspective. *Frontiers in Robotics and AI*, Vol. 8, 617426. DOI: 10.3389/frobt.2021.617426.

Al-Azzawi, T. and Al-Majidi, Z. (2021). Parametric architecture: the second international style. *IOP Conference Series: Materials Science and Engineering*, Vol. 1067, 012019. DOI: 10.1088/1757-899X/1067/1/012019.

Alexander, D. (2020). *5 ways artificial intelligence is changing architecture*. [online] Available at: https://interestingengineering.com/culture/5-ways-artificial-intelligence-is-changing-architecture [Date accessed 10 December 2022].

Assaf, T. (2021). A frequency modulation-based taxel array: a bio-inspired architecture for large-scale artificial skin. *Sensors*, Vol. 21, Issue 15, 5112. DOI: 10.3390/s21155112.

Birangal, G., Admane, S. V., and Shinde, S. S. (2015). Energy efficiency approach to intelligent building. *International Journal of Engineering Research*, Vol. 4, Issue 7, pp. 389–393. DOI: 10.17950/ijer/v4s7/711.

Caetano, Inês. Santos, Luís. Leitão, António. (2020) Computational design in architecture: Defining parametric, generative, and algorithmic design, Frontiers of Architectural Research, Volume 9, Issue 2, 2020, Pages 287-300, ISSN 2095-2635, https://doi.org/10.1016/j.foar.2019.12.008.https://www.sciencedirect.com/science/article/pii/S2095263520300029)

Caetano, Inês. Leitão, António. (2020) Architecture meets computation: an overview of the evolution of computational design approaches in architecture, Architectural Science Review, 63:2, 165-174, DOI: 10.1080/00038628.2019.1680524

Chen, C., Hu, Y., Karuppiah, M., and Kumar, P. M. (2021). Artificial intelligence on economic evaluation of energy efficiency and renewable energy technologies. *Sustainable Energy Technologies and Assessments*, Vol. 47, 101358. DOI: 10.1016/j.seta.2021.101358.

Chen, D. A., Ross, B. E., and Klotz, L. E. (2015). Lessons from a coral reef: biomimicry for structural engineers. *Journal of Structural Engineering*, Vol. 141, Issue 4, 02514002. DOI: 10.1061/(ASCE)ST.1943-541X.0001216.

Choi, J.-M., Won, M.-C., and Lee, S.-J. (2010). 63906 Vision based self learning mobile robot using machine learning algorithms (Robotics and Mechatronics). In: *The Proceedings of the Asian Conference on Multibody Dynamics*, 2010, Vol. 2010.5, 63906. DOI: 10.1299/jsmeacmd.2010.5._63906-1_.

Chua, S. L. (2013). Behaviour recognition in smart homes. *Journal of Ambient Intelligence and Smart Environments*, Vol. 5, No. 1, p. 133. DOI: 10.3233/AIS-120193.

Cortiços, N. D. (2019). Self-learning and self-repairing technologies to establish autonomous building maintenance. *MATEC Web of Conferences*, Vol. 278, 04004. DOI: 10.1051/matecconf/201927804004.

Cotrufo, N., Saloux, E., Hardy, J. M., Candanedo, J. A., and Platon, R. (2020). A practical artificial intelligence-based approach for predictive control in commercial and institutional buildings. *Energy and Buildings*, Vol. 206, 109563. DOI: 10.1016/j.enbuild.2019.109563.

Cubukcuoglu, C., Ekici, B., Tasgetiren, M. F., and Sariyildiz, S. (2019). OPTIMUS: self-adaptive differential evolution with ensemble of mutation strategies for Grasshopper algorithmic modeling. *Algorithms*, Vol. 12, Issue 7, 141. DOI: 10.3390/a12070141.

Dimitropoulos, K., Daras, P., Manitsaris, S., Fol Leymarie, F., and Calinon, S. (2021). Editorial: artificial intelligence and human movement in industries and creation. *Frontiers in Robotics and AI*, Vol. 8, 712521. DOI: 10.3389/frobt.2021.712521.

Emaminejad, N. and Akhavian, R. (2022). Trustworthy AI and robotics: implications for the AEC industry. *Automation in Construction*, Vol. 139, 104298. DOI: 10.1016/j.autcon.2022.104298.

Emiratesgbc.org (2020). *Emirates GBC 2020 Green Building Market Brief*. [online] Available at: https://emiratesgbc.org/wp-content/uploads/2020/09/UAE-Brief_NewTemplate_electronic_final.pdf [Date accessed 12 December 2022].

Estévez, A. T. and Navarro, D. (2017). Biomanufacturing the future: biodigital architecture & genetics. *Procedia Manufacturing*, Vol. 12, pp. 7–16. DOI: 10.1016/j.promfg.2017.08.002.

Hendy, A. M. (2020). The new design considerations in the residential buildings' interiors at the post-Corona (COVID-19) era. *Journal of Advanced Research in Dynamical and Control Systems*, Vol. 12, Special Issue 8, pp. 444–458. DOI: 10.5373/JARDCS/V12SP8/20202544.

Hutson, M. (2017). *How artificial intelligence could negotiate better deals for humans*. [online] Available at: https://www.science.org/content/article/how-artificial-intelligence-could-negotiate-better-deals-humans [Date accessed 12 December 2022].

Jaruga-Rozdolska, A. (2022). Architektura 4.0: proces projektowania wspierany przez sztuczną inteligencję Potencjał wykorzystania skryptu generatywnego MidJourney w procesie tworzenia koncepcji architektonicznej. *Builder*, Vol. 303, No. 10, pp. 66–69. DOI: 10.5604/01.3001.0015.9893.

Joshi, N. (2019). *How AI is making buildings smart and intelligent*. [online] Available at: https://www.forbes.com/sites/cognitiveworld/2019/08/13/how-ai-is-making-buildings-smart-and-intelligent/?sh=289dcd1e28d7 [Date accessed 1 January 2023].

Kurtoglu, T., Campbell, M. I., and Linsey, J. S. (2009). An experimental study on the effects of a computational design tool on concept generation. *Design Studies*, Vol. 30, Issue 6, pp. 676–703. DOI: 10.1016/j.destud.2009.06.005.

Maksoud, A., Mushtaha, E., Al-Sadoon, Z., Sahall, H., and Toutou, A. (2022). Design of Islamic parametric elevation for interior, enclosed corridors to optimize daylighting and solar radiation exposure in a desert climate: a case study of the University of Sharjah, UAE. *Buildings*, Vol. 12, Issue 2, 161. DOI: 10.3390/buildings12020161.

Maksoud A., Mushtaha E., Chouman L., Al Jawad E., Samra S.A., Sukkar A., Yahia M.W. Study on Daylighting Performance in the CFAD Studios at the University of Sharjah (2022) Civil Engineering and Architecture, 10 (5), pp. 2134 - 2143, DOI: 10.13189/cea.2022.100532.

Mehra, S. and Sharma, R. (2019). Performance analysis of artificial intelligence based MPPT techniques for a solar system under changing environmental conditions. In: *Proceedings of ICAEEC-2019*, IIIT Allahabad, India, May 31 – June 1, 2019. DOI: 10.2139/ssrn.3573604.https://doi.org/10.2139/ssrn.3573604

Mushtaha, Emad; Alsyouf, Imad; Hamad, Rawan; Elmualim, Abbas; Maksoud, Aref ;Yahia Moohammed Wasim (2022). Developing design guidelines for university campus in hot climate using Quality Function Deployment (QFD): the case of the University of Sharjah, UAE, Architectural Engineering and Design Management, 18:5, 593-613, DOI: 10.1080/17452007.2022.2041386

Naboni, R. and Kunic, A. (2017). Design and additive manufacturing of lattice-based cellular solids at building scale. *Blucher Design Proceedings*, Vol. 3, No. 12, pp. 369–375. DOI: 10.5151/sigradi2017-058.

Nisztuk M, Myszkowski PB. Usability of contemporary tools for the computational design of architectural objects: Review, features evaluation and reflection. International Journal of Architectural Computing. 2018;16(1):58-84. doi:10.1177/1478077117738919

Oberste-Ufer, K. (2019). *7 ways artificial intelligence is revolutionizing architecture*. [online] Available at: https://blog.dormakaba.com/7-ways-artificial-intelligence-is-revolutionizing-architecture [1 January 2023].

Oxman, R. (2017). Thinking difference: theories and models of parametric design thinking. *Design Studies*, Vol. 52, pp. 4–39. DOI: 10.1016/j.destud.2017.06.001.

Pala, Z. and Özkan, O. (2020). Artificial intelligence helps protect smart homes against thieves. *DUJE (Dicle University Journal of Engineering)*, Vol. 11, Issue 3, pp. 945–952. DOI: 10.24012/dumf.700311.

Philips, M. (2020). *The present and future of AI in design (with infographic)*. [online] Available at: https://www.toptal.com/designers/product-design/infographic-ai-in-design#:~:text=Designers%20working%20with%20AI%20can,adjustments%20based%20on%20that%20data [4 January 2023].

Rocha, H. R. O., Honorato, I. H., Fiorotti, R., Celeste, W. C., Silvestre, L. J., and Silva, J. A. L. (2021). An Artificial Intelligence based scheduling algorithm for demand-side energy management in Smart Homes. *Applied Energy*, Vol. 282, Part A, 116145. DOI: 10.1016/j.apenergy.2020.116145.

Roudsari, M. S., Pak, M., and Viola, A. (2013). Ladybug: a parametric environmental plugin for Grasshopper to help designers create an environmentally-conscious design. In: *Proceedings of Building Simulation 2013: 13th Conference of IBPSA*, Chambéry, France, August 26–28, 2013, pp. 3128–3135. DOI: 10.26868/25222708.2013.2499.

Shishina, D. and Sergeev, P. (2019). Revit|Dynamo: designing objects of complex forms. toolkit and process automation features. *Architecture and Engineering*, Vol. 4, Issue 3, pp. 30–38. DOI: 10.23968/2500-0055-2019-4-3-30-38.

Wang, H. (2011) Real-time data-based fault diagnosis system. *Advanced Materials Research*, Vol. 189–193, pp. 2621–2624. DOI: 10.4028/www.scientific.net/AMR.189-193.2621.

Wollerton, M. (2018). *Nest Learning Thermostat (3rd Gen) review: same great Nest, now with a temperature sensor.* [online] Available at: https://www.cnet.com/reviews/nest-learning-thermostat-third-generation-review [Date accessed 12 December 2022].

Zhao, Y., Li, T., Zhang, X., and Zhang, C. (2019). Artificial intelligence-based fault detection and diagnosis methods for building energy systems: advantages, challenges and the future. Renewable and *Sustainable Energy Reviews*, Vol. 109, pp. 85–101. DOI: 10.1016/j.rser.2019.04.021.

DOI: 10.23968/2500-0055-2023-8-1-25-36

IMPACT OF WINDOW SHADING ON THE THERMAL PERFORMANCE OF RESIDENTIAL BUILDINGS OF DIFFERENT FORMS IN JORDAN

Esraa Sh. Abbaas*[1], Mazran Ismail**[1], Ala'eddin A. Saif[2], Muhamad Azhar Ghazali[1]

[1]School of Housing, Building and Planning, Universiti Sains Malaysia
Penang, Malaysia

[2]College of Science, University of Jeddah
Jeddah, Saudi Arabia

Corresponding author's e-mail: *esraabbas91@gmail.com, **mazran@usm.my

Abstract
Introduction: Window shading is considered one of the most effective passive design approaches that improves indoor thermal performance, minimizing the usage of HVAC and reducing energy consumption. **Purpose of the study:** We aimed to investigate the impact of external window shading on thermal performance of three existing residential buildings having different forms (rectangular, L-shaped, and U-shaped) in hot-dry climate in Amman, Jordan. **Methods:** Three types of shading, namely: vertical, horizontal, and combined, of different lengths (0.75 m, 1.00 m, and 1.25 m) were introduced to the existing buildings. The effect of those types of shading was studied using the OpenStudio SketchUp 2020 plugin and EnergyPlus simulation program. **Results:** It was established that vertical shading slightly improves the indoor air temperature in all building forms, while horizontal shading and combined shading improve the thermal performance of buildings to a more significant extent. Combined shading of 1.25 m in length shows the optimum behavior in all buildings since it reduces the indoor air temperature in the range of 2.6–3.3°C. Besides, it improves thermal sensation, which seem to be closer to the comfort zone, by reducing the predicted mean vote (PMV) and predicted percentage of dissatisfied (PPD) values as compared with the baseline situation without shading. In addition, the rectangular building demonstrated the best response for shading by showing the largest reduction in the indoor air temperature.

Keywords: EnergyPlus, shading, thermal comfort, PMV, hot-dry climate, residential building.

Introduction

Windows are responsible for a large share of heat gain during summer and heat loss during winter in buildings. A number of solutions have been proposed to minimize energy exchange through windows such as the use double glazing and window shading or decrease in the window-wall ratio (Bataineh and Alrabee, 2018). Shading devices significantly improve the thermal performance of buildings by reducing heat gain since they block direct sunlight in summer and reduce heat losses in winter, thus minimizing the cooling and heating loads and saving energy (Mushtaha et al., 2021). Generally, shading of openings includes exterior and interior window shading. Exterior window shading is more effective in minimizing the heat gain of direct sunlight than interior window shading. However, interior window shading is more advantageous since it offers more user-friendly control (Ohene et al., 2022). There are other types of shading ensured by architectural elements such as Iwan, which is more popular in the Middle Eastern and North African architecture (Eskandari et al., 2018). Shading effect can also be achieved thanks to tall trees improving the thermal performance of the buildings nearby (both residential and commercial) in hot climate (Minangi and Alibaba, 2018). Window shading is considered the most effective since it can be adjusted to minimize solar radiation received by the building (Feng et al., 2021). Besides, the availability of numerous kinds of window shading on the market in a wide range of prices makes them the preferable choice of occupants (especially in residential buildings) who install them even at the late stage of construction to achieve the optimal thermal comfort.

Some researchers investigated the impact of using different types of shading on the thermal performance and energy consumption of various buildings in Jordan. For instance, Freewan (2014) analyzed the effect of using three window shading devices (egg crate, vertical fins, and diagonal fins) on the air temperature of the south-west facade of an office building in Irbid, Jordan. He found that those shading devices can improve the indoor air temperature returning it to the acceptable range compared to the office without shading devices.

Moreover, egg crate and diagonal fins showed better performance in terms of improving air temperature compared to vertical fins. Ali and Hashlamun (2019) studied the effect of adding 100 cm horizontal overhang on the southern facade of a school in Amman on energy saving in terms of both cooling and heating. They established that the proposed shading system can save 20.3% of annual cooling energy but shows minimum effect regarding energy saved on heating, which amounts to 9.8%. Abu Qadourah et al. (2022) examined the impact of such shading devices as horizontal shading on the southern facade and horizontal fins on the eastern facade, having different lengths, in a multi-family apartment building in Amman, Jordan. They found that both types of shading can decrease the cooling energy demand and increase the heating and lighting energy demands. In addition, an increase in the size of the shading devices enhances their effect.

We have noticed that only a limited number of works focused on investigating the effect of window shading on thermal performance and thermal comfort in Jordan, while most of them dealt with window shading devices as passive design strategies to improve energy performance (Abu Qadourah et al., 2022; Bataineh and Alrabee, 2018; Bataineh and Al Rabee, 2021). Therefore, this study addresses the influence of different types of exterior shading, particularly: vertical fins, horizontal overhang, and the combined structure of vertical and horizontal shading, on the thermal performance and thermal comfort of existing residential buildings of different forms (rectangular, L-shaped, and U-shaped) in Amman, the capital of Jordan. To study the impact of shading on the thermal performance of these buildings, we analyzed the indoor air temperature and evaluated its influence on the thermal comfort of the buildings using the predicted mean vote (PMV) and predicted percentage of dissatisfied (PPD) indicators.

Methods

Case studies

We considered three case studies representing different residential building forms, namely: rectangular, L-shaped, and U-shaped, located in the same district of Amman. Fig. 1 shows photos of the main facades of those buildings facing the west. All buildings have the same constructions and consist of three floors. Only three west-facing rooms (one on the middle floor of each building) were taken for this study. We investigated the impact of vertical fins, horizontal overhang, and the combined structure of

Fig. 1. Main facades of the buildings of different forms: (a) rectangular, (b) L-shaped, and (c) U-shaped

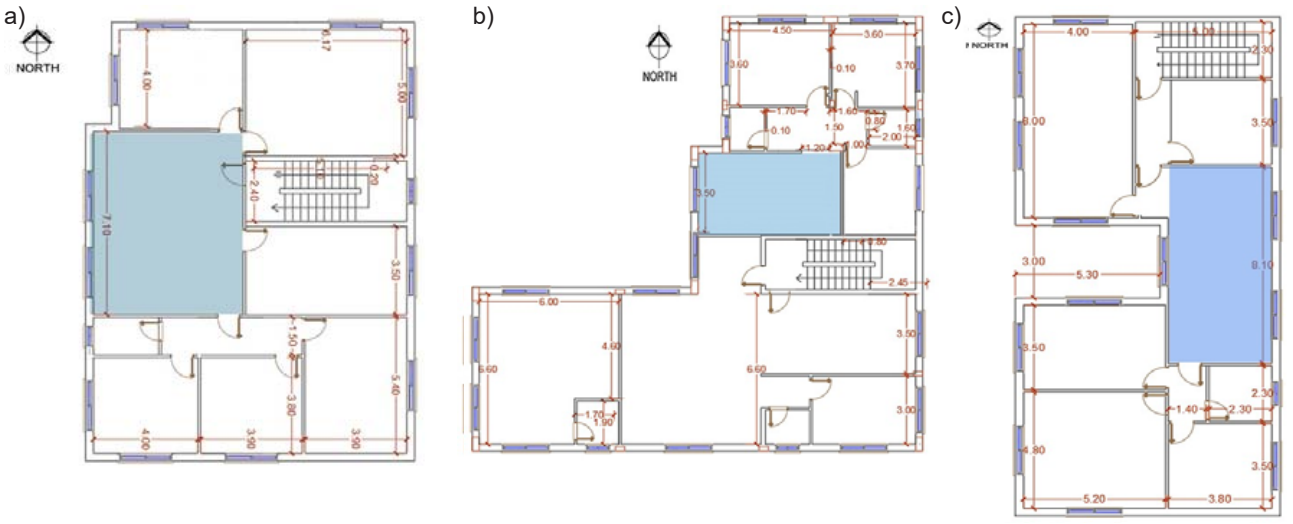

Fig. 2. 2D plans with the rooms in the buildings of different forms: (a) rectangular, (b) L-shaped, and (c) U-shaped

vertical and horizontal shading of different lengths on the thermal performance of these rooms. We also analyzed the thermal comfort of these rooms using the PMV and PPD indicators. Fig. 2 shows the middle floor plan of each of the three buildings where the west-facing rooms under consideration are highlighted with blue color. These rooms were selected since the west facade is facing solar radiation for longer time during the day (see the sun path chart in Fig. 3).

Amman, the capital of Jordan, lies at latitude 31°57′23.76″ North and longitude 35°56′44.52″ East. About 90% of Jordan areas are semi-arid or arid since the climate is mainly of the Mediterranean type, hot in summer and cold in winter (Abdulla, 2020). We focused on the hot-dry summer season, which lasts for three months from June 21 to September 21, where July 21 July was picked as the design day. In summer, the air temperature at peak hours from 1:00 PM to 3:00 PM can be as high as 40°C (Albatayneh et al., 2021). Besides, summer in Amman is known to have long daytime hours, where on July 21 they lasted from 5:45 AM until 7:40 PM, which is about 14 hours (Table 1). This means that the buildings are exposed to sun radiation for long time during the daytime.

For further understanding of summertime and solar radiation in Amman, which is located both in the northern and eastern hemispheres, we need to analyze the sun path. The sun path is the seasonal and daily arc that Sun follows as the Earth goes around the Sun throughout the year. The sun path affects the length of the daytime and the amount of solar radiation received by the buildings at certain time during the day or season. Besides, the sun altitude and azimuth play an important role in the amount of shading cast on a building by the surrounding buildings and trees (Nwankwo et al., 2021).

We downloaded the polar sun path chart for Amman (Fig. 3) using the sun path tool available on sunearthtools.com. Here, the orange line represents the sun path on July 21. The polar chart shows the Sun elevation, azimuth, clock line, and date line. Another type of chart for the Sun path is the Cartesian chart (not shown), where the Sun position is plotted hourly by the solar elevation angle

Table 1. **Amman, Jordan — sunrise, sunset, dawn and dusk times (GIASMA, 2022)**

Date	sunrise	sunset	dawn	dusk
July 21, 2022	5:45	19:40	5:18	20:07

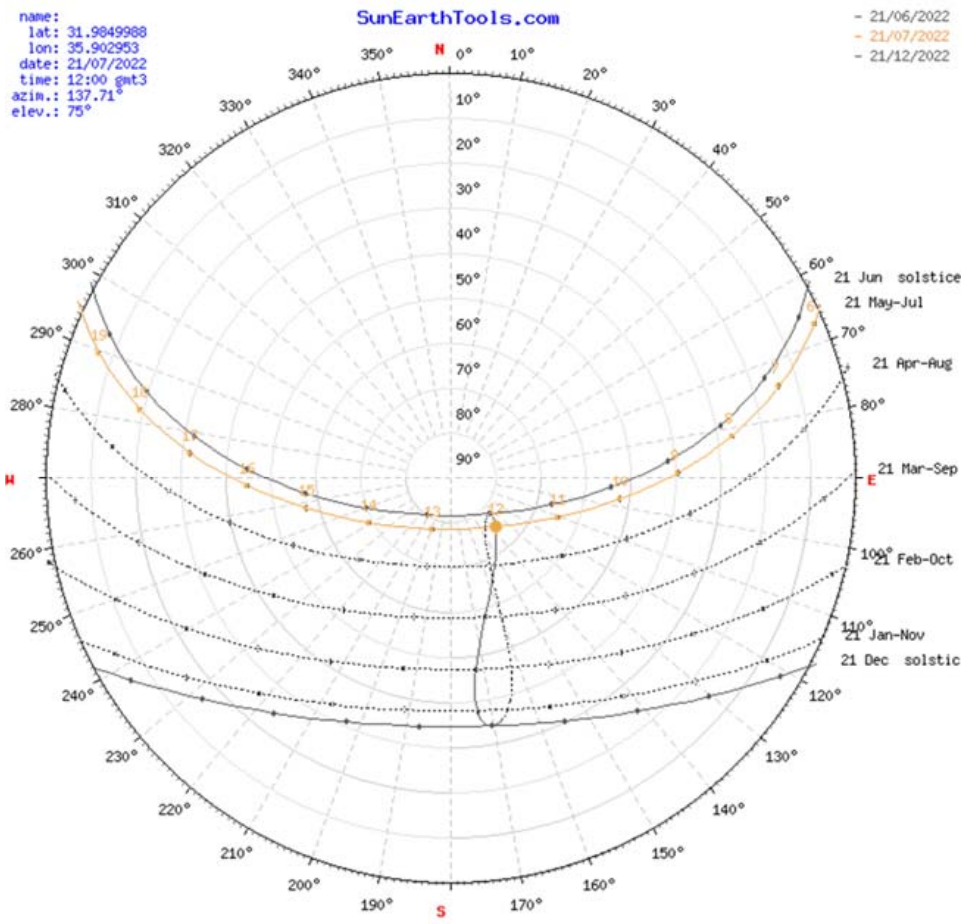

Fig.3. Polar sun path chart for July 21 in Amman, Jordan

as a function of the solar azimuth angle. According to the polar chart, at midday time (12:00 PM), the Sun was located at an azimuth angle of 137.71° and elevation angle of 75°. The estimated track angle for the Sun from 12:00 PM till sunset was 157.1°, while the track angle from sunrise till 12:00 PM was 72.66°. This means that the west facades of the buildings would receive higher solar radiation as compared with the east facades. For further understanding of the Sun position effect during daytime and the times when the building facades are exposed to sun or shaded, the Sun path at 8:00 AM, 12:00 PM, and 4:00 PM was plotted for the buildings under consideration (Figs. 4–6). It should be noted that the azimuth and elevation angles at 8:00 AM were 81.46° and 26.61°, respectively, while at 4:00 PM they were 267.78° and 44.67°, respectively. Based on Figs. 4–6, it can be seen that since the selected rooms face the west, they would be shaded in the morning (except for the room in the U-shaped building, which has two windows facing the east, exposed to sun in the morning) and receive the afternoon sun.

Simulation

We performed a simulation study to investigate the effect of shading devices on the thermal performance and thermal comfort of the residential buildings of different forms located in Amman. To do that, we started with the measurement of environmental parameters at the sites, i.e., air temperature, air velocity, mean radiant temperature, and relative humidity regarding the baseline situation with the windows closed and

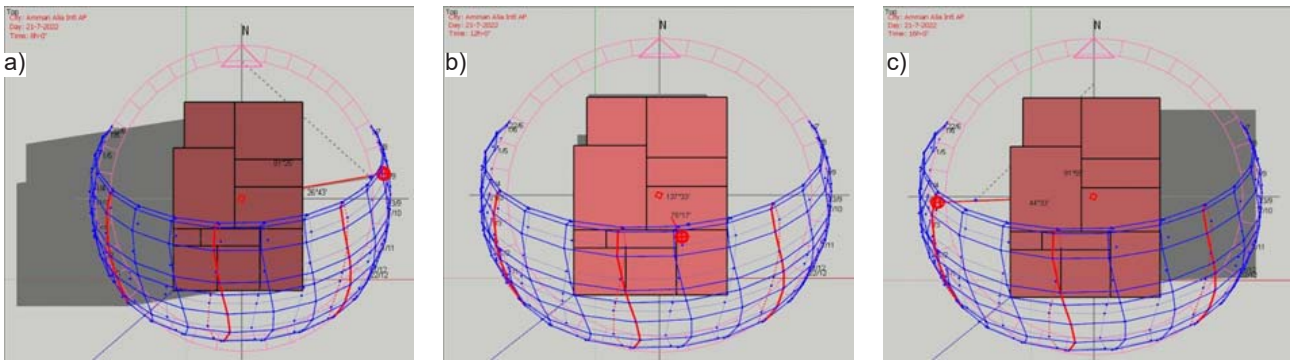

Fig. 4. Sun path diagram for the rectangular building on July 21 at (a) 8:00 AM, (b) 12:00 PM, and (c) 4:00 PM

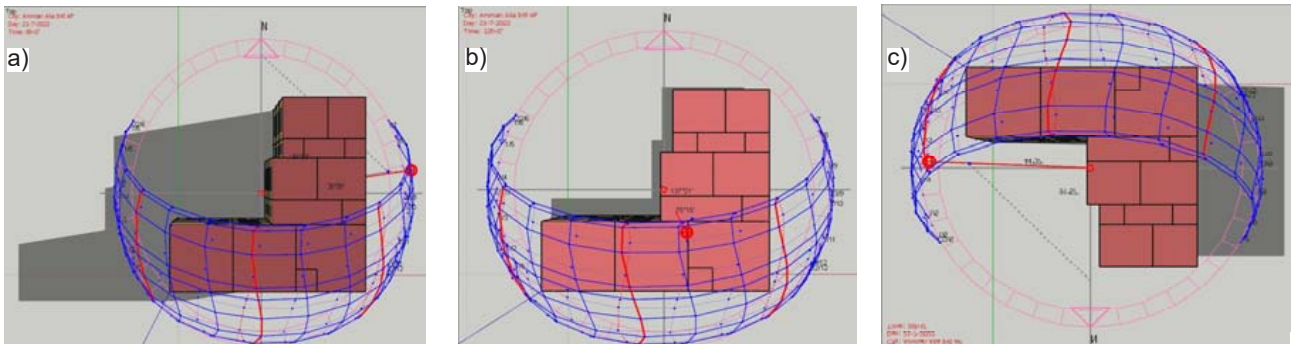

Fig. 5. Sun path diagram for the L-shaped building on July 21 at (a) 8:00 AM, (b) 12:00 PM, and (c) 4:00 PM

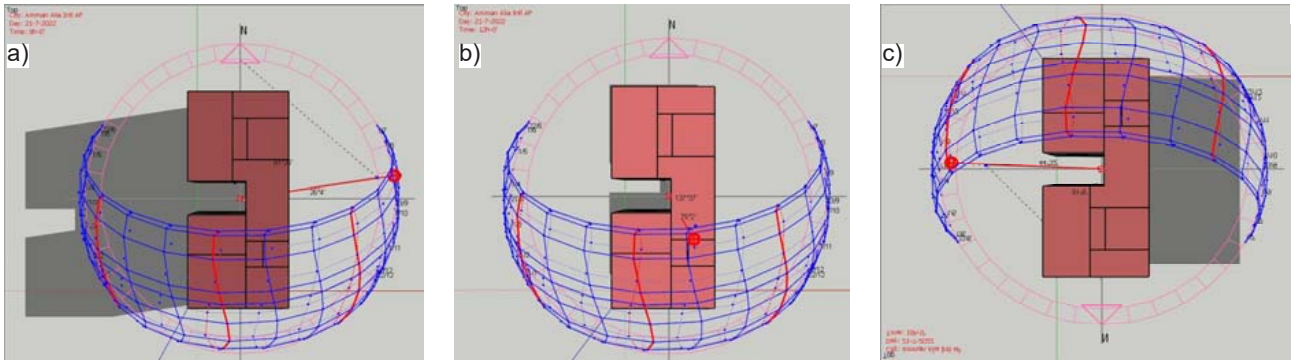

Fig. 6. Sun path diagram for the U-shaped building on July 21 at (a) 8:00 AM, (b) 12:00 PM and (c) 4:00 PM

without shading. These measurements were used to validate the simulation results, and they were found to be very close to each other.

At the early stage of simulation, we drew two-dimensional plans of the buildings of different forms using AutoCAD, and then built three-dimensional models for all the three buildings using the OpenStudio SketchUp 2020 plugin. In the existing buildings, we determined the construction system for the roof, walls, and ground. We also determined characteristics of each building space (where the space type was selected as residential), and set the number of floors to be equal to three. Then we uploaded the climate file for Amman in the EPW format to the OpenStudio platform. July 21 was imported in the DDY format as the summer design day. Besides, we defined the infiltration schedules and internal loads such as people, electric equipment, and light for the spaces. Finally, models were simulated in baseline situations without shading using the EnergyPlus simulation program.

The impact of shading on the thermal performance of the buildings (rooms under consideration) was studied by introducing different types of shading, particularly: vertical fins, horizontal overhang, and combined shading structure. These shading devices had different lengths of 0.75 m, 1.00 m, and 1.25 m. For more accuracy, the output environmental parameters were set to be simulated every 15 minutes, and then four readings per hour were averaged. The thermal performance of the buildings was analyzed based on the indoor air temperature. The air temperature in the rooms was measured with the presence of shading devices while the windows were closed, both individually and compared to the baseline case without shading. Finally, the output environmental parameters were used to evaluate the thermal comfort of the buildings by studying the PMV and PPD indicators for the baseline situation and for the optimum type of shading at its optimum length. Figs. 7–9 show different types of shading devices for three building forms: vertical shading (fins), horizontal shading (overhang), and combined shading, respectively. These types of shading were investigated at three different shading device lengths of 0.75 m, 1.00 m, and 1.25 m.

Results and discussion

Air temperature depending on the type of shading device in the buildings of different forms

Fig. 10 shows the effect of the vertical, horizontal and combined shading devices having different lengths on the thermal performance of the rectangular building. It can be seen that all shading devices have a notable impact on reducing the air temperature in the room as compared with the baseline case without shading. Furthermore, one can notice that as the length of the shading device increases, the indoor air temperature slightly decreases. For instance, in Fig. 10a, the air temperature slightly decreases with the presence of vertical shading fins in the range of 0.4–0.6°C regardless of length as compared with the baseline situation. While in the presence of horizontal overhang shading, the air temperature shows better results since it decreases by 2.1°C, 2.5°C, and 2.8°C at an overhang length of 0.75 m, 1.00 m, and 1.25 m, respectively, as compared with the case without shading at 4:00 PM (Fig. 10b). In case of the combined shading structure, the air temperature shows the largest difference as compared with the case without shading: at a length

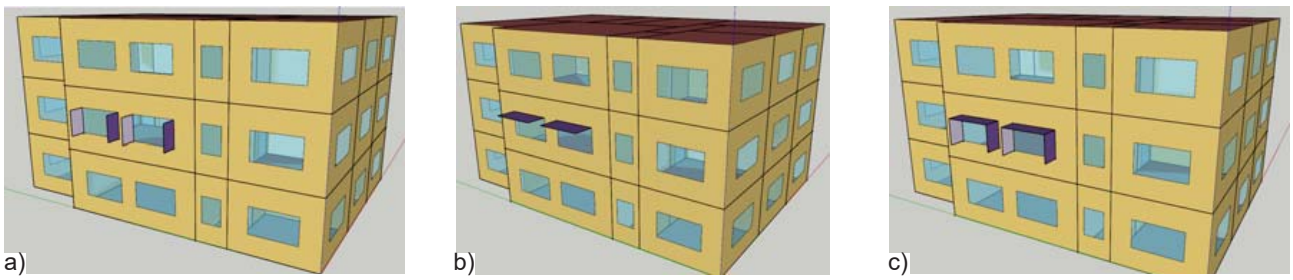

Fig. 7. Shading devices: (a) vertical shading (fins), (b) horizontal shading (overhang), and (c) combined shading for the rectangular building

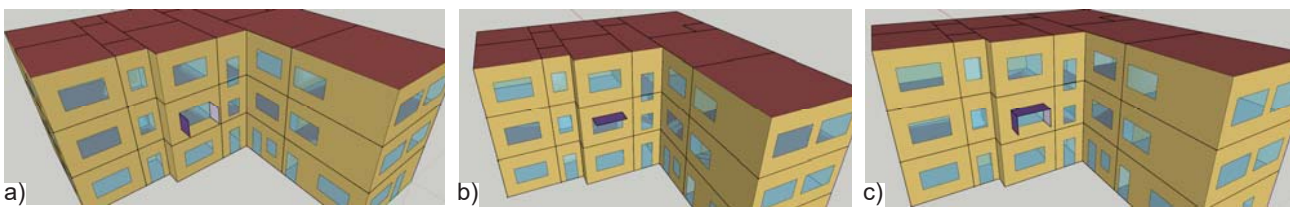

Fig. 8. Shading devices: (a) vertical shading (fins), (b) horizontal shading (overhang), and (c) combined shading for the L-shaped building

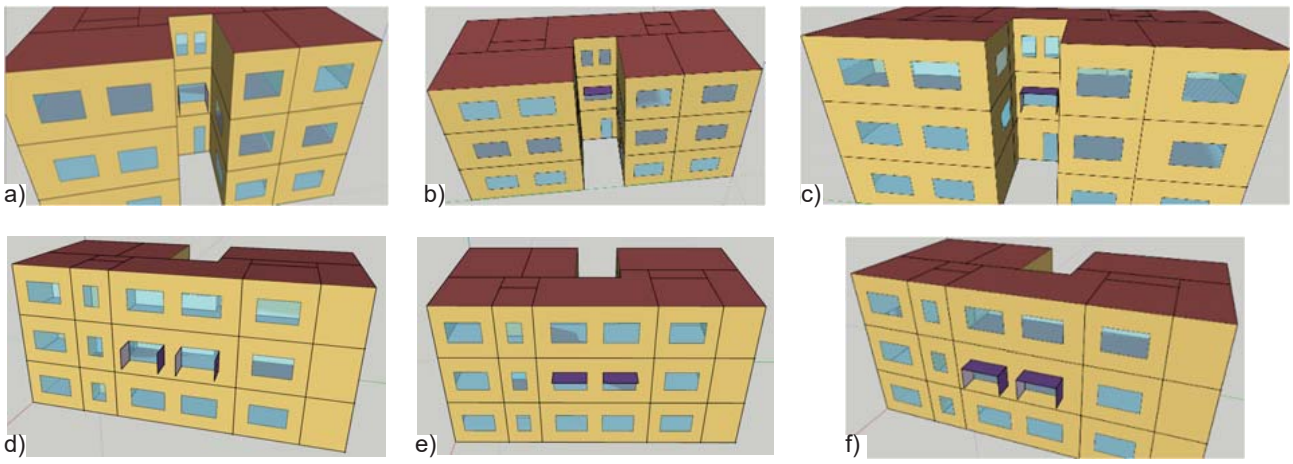

Fig. 9. Shading devices: (a) vertical shading (fins) of a west side window, (b) horizontal shading (overhang) of a west side window, (c) combined shading of a west side window (d) vertical shading (fins) of east side windows, (e) horizontal shading (overhang) of east side windows, and (f) combined shading of east side windows for the U-shaped building

of the shading device of 0.75 m, 1.00 m, and 1.25 m, the air temperature decreases by 2.4°C, 2.9°C, and 3.3°C at 4:00 PM, respectively (Fig. 10c).

A similar trend is observed for the air temperature in the presence of different shading devices as compared with the case without shading for the L-shaped building (Fig. 11). Fig.11a shows almost negligible air temperature reduction in the presence of vertical fins, where it reaches its maximum of 0.3°C at 1.25 m in length. On the other hand, in the presence of horizontal overhang, the air temperature is characterized by a significant reduction of 1.8°C, 2.2°C, and 2.5°C at a length of 0.75 m, 1.00 m, and 1.25 m, respectively, as compared with the case without shading (Fig. 11b). The combined shading device shows the optimum behavior with regard to the air temperature by reducing the temperature by up to 1.9°C, 2.4°C, and 2.7°C at 4:00 PM at a length of 0.75 m, 1.00 m, and 1.25 m, respectively (Fig. 11c).

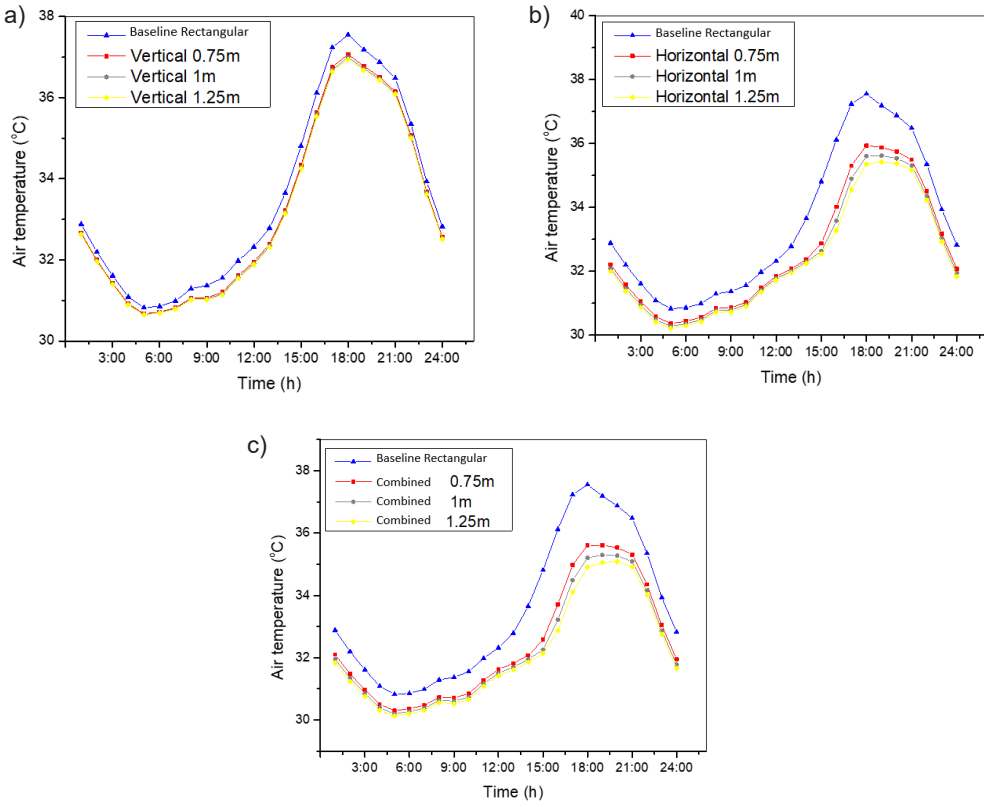

Fig. 10. Comparison of the air temperature in the rectangular building for different shading devices having different lengths: (a) vertical fins, (b) horizontal overhang, and (c) combined shading device

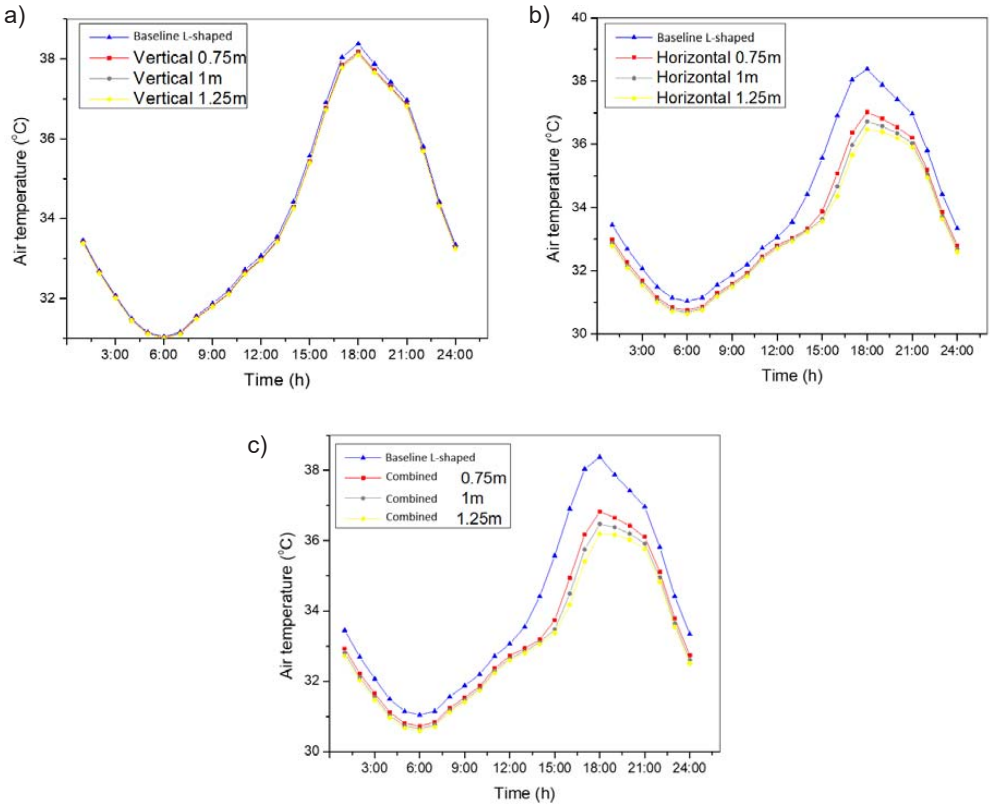

Fig. 11. Comparison of the air temperature in the L-shaped building for different shading devices having different lengths: (a) vertical fins, (b) horizontal overhang, and (c) combined shading device

A similar trend is observed for the indoor temperature reduction in the presence of shading devices in the U-shaped building as compared with the rectangular and L-shaped buildings (Fig. 12). As compared with the case without shading, vertical fins ensure the maximum air temperature difference of 0.35°C at a length of 1.25 m (Fig. 12a). While in case of horizontal overhang, larger air temperature differences are noticed (Fig. 12b), where at 10:00 AM, the temperature difference of 2.2°C, 2.6°C, and 2.9°C is recorded for 0.75 m, 1.00 m, and 1.25 m of length, respectively. At 4:00 PM, the temperature difference of 1.7°C, 2.0°C, and 2.3°C is recorded at the same length values, respectively. Fig. 12c shows the performance of combined shading at different lengths, where the air temperature reduction is also noteworthy: the temperature difference reaches 2.4°C, 2.5°C, and 3.2°C at 10:00 AM and 1.9°C, 2.3°C, and 2.6°C at 4:00 PM at a length of 0.75 m, 1.00 m, and 1.25 m, respectively. These differences in the indoor temperature when using horizontal and combined shading at 10:00 AM in the U-shaped building are attributed to the existence of the east windows in addition to the west window. Moreover, the lower temperature reduction at 4:00 PM as compared with that obtained at 10:00 AM is due to self-shading as a result of the U-shape for the west window, which is predominant during daytime (Fig. 6). Thus, extra shading would have less effectiveness as compared with the east windows exposed directly to the sun during morning hours where shading devices make more obvious difference.

Based on the discussion for Figs. 10–12, it can be concluded that for all proposed types of shading, the optimum length is equal to 1.25 m. This means that the longer the shading device, the better shading effect is obtained, which results in lower temperature values. To determine the optimum shading device to be used for each building form, the air temperature during the day was plotted for different types of shading with a length of 1.25 m for each building form (Fig. 13). The results show that the vertical fins demonstrates the lowest temperature difference of 0.3–0.6°C as compared with the baseline case without shading for all building forms. This indicates that the use of vertical fins on the west facade is not practical. The horizontal overhang shows better performance as it reduces the indoor air temperature by 2.3–2.9°C for all building forms. Besides, it is considered practical for the exterior facade and ensures better view as compared with the vertical fins. The combined shading device shows the optimum results for all building forms in terms of reducing the air temperature since the lowest values of 2.6–3.3°C were recorded. Interestingly, the maximum reduction in the air temperature of 3.3°C was recorded for the rectangular building with combined shading.

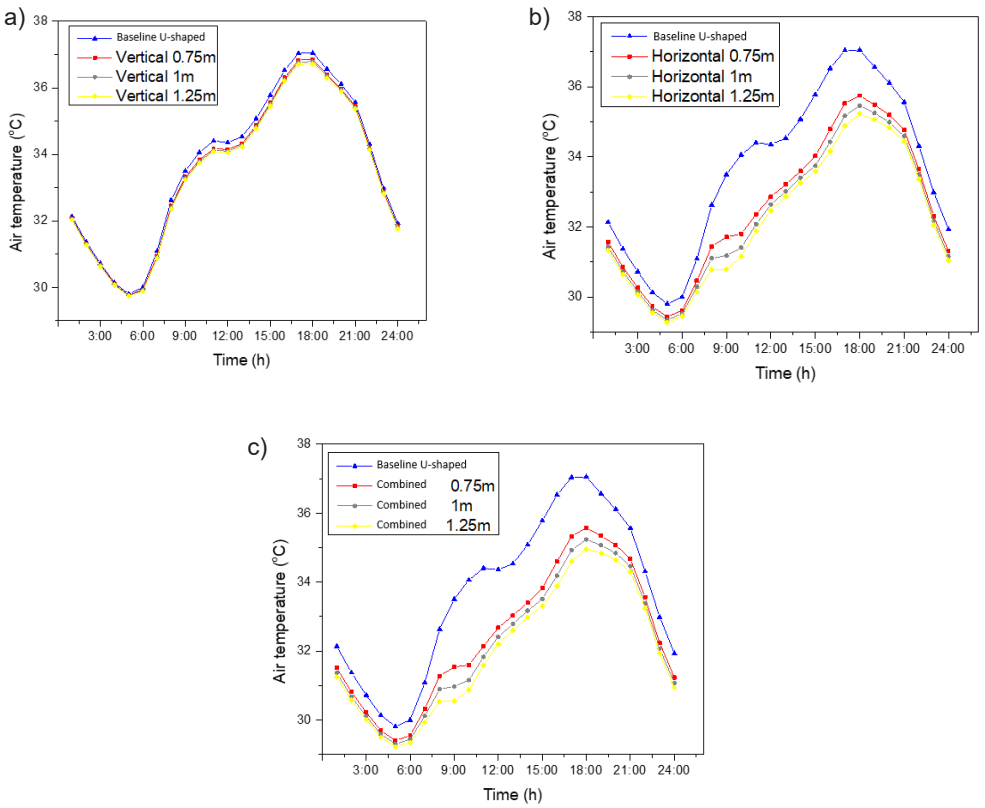

Fig. 12. Comparison of the air temperature in the U-shaped building for different shading devices at various lengths: (a) vertical fins, (b) horizontal overhang, and (c) combined shading device

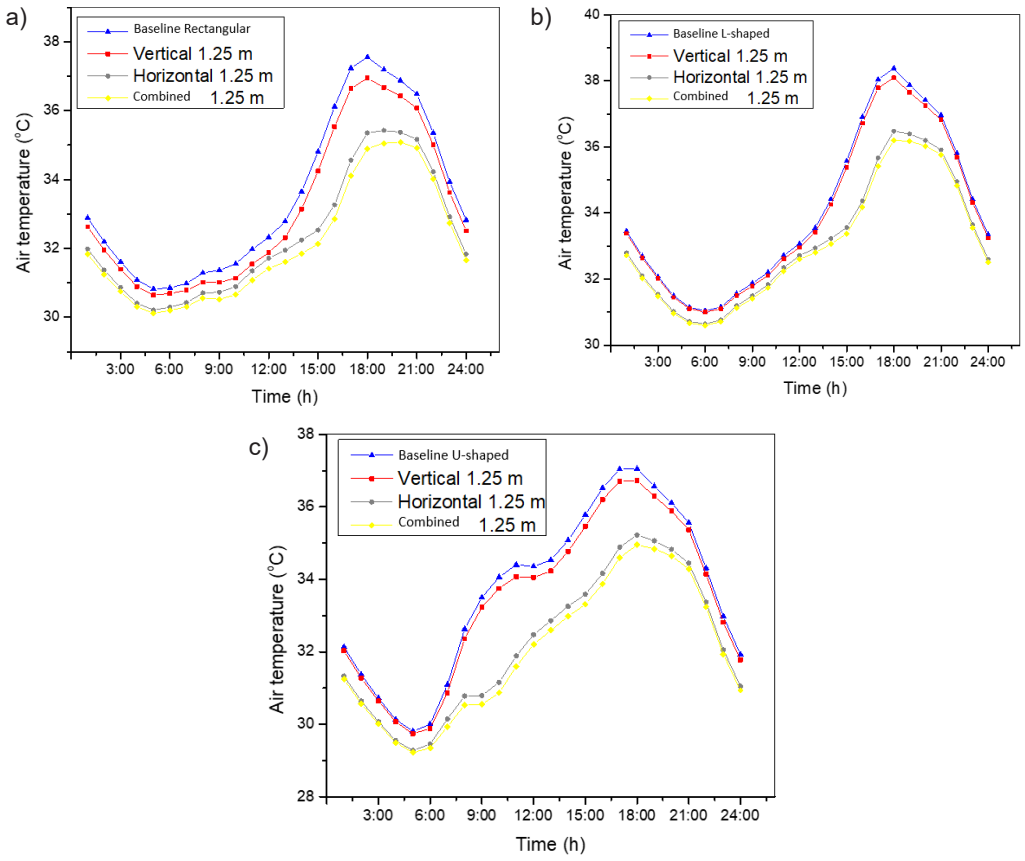

Fig. 13. Comparison of the air temperature for different shading devices with the optimum length (1.25m) for different building forms: (a) rectangular, (b) L-shaped, and (c) U-shaped

Table 2. **Seven-point thermal sensation scale according to Fanger's model (Fanger, 1970)**

Scale	Sensation
3	Hot
2	Warm
1	Slightly warm
0	Neutral
-1	Slightly cool
-2	Cool
-3	Cold

PMV and PPD of different shading devices for different building forms

To gain a better understanding of the impact of shading devices on the thermal performance of the buildings under consideration, the optimal shading device (combined shading) was compared with the baseline case without shading using the predicted mean vote (PMV) and predicted percentage of dissatisfied (PPD) indicators. The PMV and PPD indicators are usually determined with the use of Fanger's model, which was originally developed by collecting data from a large number of surveys on people subjected to different conditions within a climate zone (Emir, 2016). The PMV indicator is the average comfort vote based on the seven-point thermal sensation scale from cold –3 to hot +3 (Table 2), while the PPD indicator is used to evaluate the ability of occupants to withstand high and low air temperatures in terms of thermal comfort conditions (Duan et al., 2022; Fanger and Toftum, 2002; Hailu et al., 2021; Kumar and Sharma, 2022). For an indoor thermal zone to provide comfort sensation, the acceptable range of PMV should be in the range from –1 to +1 and PPD should be less than 26%.

According to Fanger's model, PMV can be calculated by the following equation (Duan et al., 2022; Rînjea et al., 2022):

$$PMV = \left(0.303e^{-0.036M} + 0.028\right) \times \left\{ \begin{array}{c} M - W - 3.05\times10^{-3} \times \\ \times\left[5733 - 6.99\left(M - W\right) - Pa\right] - \\ -0.42\left[\left(M - W\right) - 58.15\right] - \\ -1.72\times10^{-5} M\left(5867 - Pa\right) - \\ -0.0014M\left(34 - t_a\right) - 3.96\times10^{-8} f_{cl} \times \\ \times\left[\left(t_{cl} + 273\right)^4 - \left(t_r + 273\right)^4 - f_{cl} h_c \left(t_{cl} - t_a\right)\right] \end{array} \right\}, \quad (1)$$

where M is the energy metabolic rate in W/m^2, W is the effective mechanical power generated by the

Table 3. **PMV, PPD, and thermal sensation for the west room in the rectangular building in the baseline case and with optimum shading devices 1.25 m long**

Time (h)	PMV Rectangular Baseline	PPD Rectangular Baseline (%)	Sensation Rectangular Baseline	PMV Rectangular Combined	PPD Rectangular Combined (%)	Sensation Rectangular Combined
1:00	2.64	95.9	Warm	2.36	90.1	Warm
2:00	2.45	92.4	Warm	2.2	84.9	Warm
3:00	2.27	87.4	Warm	2.03	78.4	Warm
4:00	2.12	82	Warm	1.91	72.58	Slightly warm
5:00	2.00	76.8	Warm	1.8	67.2	Slightly warm
6:00	1.95	74.7	Slightly warm	1.77	65.7	Slightly warm
7:00	1.96	75.3	Slightly warm	1.78	66.4	Slightly warm
8:00	2.03	78.3	Warm	1.84	69.3	Slightly warm
9:00	2.08	80.3	Warm	1.88	71.1	Slightly warm
10:00	2.12	82.2	Warm	1.92	73	Slightly warm
11:00	2.19	84.6	Warm	1.99	76.3	Slightly warm
12:00	2.26	87.1	Warm	2.07	79.9	Warm
13:00	2.36	90.1	Warm	2.1	81.3	Warm
14:00	2.60	95.2	Warm	2.16	83.5	Warm
15:00	2.92	98.6	Warm	2.23	86.2	Warm
16:00	3.28	99.7	Hot	2.4	91.1	Warm
17:00	3.54	99.96	Hot	2.68	96.4	Warm
18:00	3.58	99.97	Hot	2.86	98.3	Warm
19:00	3.48	99.95	Hot	2.9	98.6	Warm
20:00	3.38	99.90	Hot	2.89	98.5	Warm
21:00	3.28	99.8	Hot	2.86	98.3	Warm
22:00	3.11	99.4	Hot	2.74	97.1	Warm
23:00	2.87	98.3	Warm	2.56	94.6	Warm
0:00	2.65	96.1	Warm	2.35	89.8	Warm

Table 4. **PMV, PPD, and thermal sensation for the west room in the L-shaped building in the baseline case and with optimum shading devices 1.25 m long**

Time (h)	PMV L-shaped Baseline	PPD L-shaped Baseline (%)	Sensation L-shaped Baseline	PMV L-shaped Combined	PPD L-shaped Combined (%)	Sensation L-shaped Combined
1:00	2.75	97.27	Warm	2.6	95.29	Warm
2:00	2.54	94.32	Warm	2.42	91.56	Warm
3:00	2.34	89.67	Warm	2.24	86.45	Warm
4:00	2.18	84.3	Warm	2.1	81.17	Warm
5:00	2.03	78.42	Warm	1.97	75.61	Slightly warm
6:00	1.96	75.07	Slightly warm	1.91	72.66	Slightly warm
7:00	1.95	74.71	Slightly warm	1.9	72.32	Slightly warm
8:00	2.02	77.75	Warm	1.97	75.57	Slightly warm
9:00	2.09	80.79	Warm	2.03	78.5	Warm
10:00	2.16	83.52	Warm	2.1	81.33	Warm
11:00	2.24	86.29	Warm	2.18	84.32	Warm
12:00	2.31	88.68	Warm	2.26	87.06	Warm
13:00	2.41	91.4	Warm	2.28	87.91	Warm
14:00	2.64	95.83	Warm	2.33	89.26	Warm
15:00	3	98.99	Hot	2.41	91.46	Warm
16:00	3.37	99.87	Hot	2.59	95.12	Warm
17:00	3.66	99.98	Hot	2.89	98.45	Warm
18:00	3.73	99.99	Hot	3.09	99.44	Hot
19:00	3.63	99.98	Hot	3.15	99.6	Hot
20:00	3.51	99.96	Hot	3.14	99.57	Hot
21:00	3.4	99.91	Hot	3.09	99.44	Hot
22:00	3.21	99.7	Hot	2.96	98.92	Warm
23:00	2.97	98.92	Warm	2.77	97.48	Warm
0:00	2.74	97.14	Warm	2.56	94.66	Warm

Table 5. **PMV, PPD, and thermal sensation for the west room in the U-shaped building in the baseline case and with optimum shading devices 1.25 m long**

Time (h)	PMV U-shaped Baseline	PPD U-shaped Baseline (%)	Sensation U-shaped Baseline	PMV U-shaped Combined	PPD U-shaped Combined (%)	Sensation U-shaped Combined
1:00	2.43	91.82	Warm	2.15	83.08	Warm
2:00	2.22	85.6	Warm	1.96	75.09	Slightly warm
3:00	2.01	77.31	Warm	1.78	66.01	Slightly warm
4:00	1.84	69.31	Slightly warm	1.63	58.41	Slightly warm
5:00	1.7	61.89	Slightly warm	1.51	51.57	Slightly warm
6:00	1.71	62.32	Slightly warm	1.5	51.03	Slightly warm
7:00	2	76.63	Warm	1.64	59.03	Slightly warm
8:00	2.44	91.93	Warm	1.81	67.91	Slightly warm
9:00	2.71	96.89	Warm	1.83	68.83	Slightly warm
10:00	2.86	98.32	Warm	1.91	72.81	Slightly warm
11:00	2.9	98.63	Warm	2.06	79.59	Warm
12:00	2.87	98.4	Warm	2.22	85.77	Warm
13:00	2.88	98.45	Warm	2.3	88.28	Warm
14:00	3.01	99.15	Hot	2.38	90.58	Warm
15:00	3.21	99.71	Hot	2.46	92.68	Warm
16:00	3.42	99.92	Hot	2.58	94.97	Warm
17:00	3.5	99.96	Hot	2.71	96.94	Warm
18:00	3.46	99.94	Hot	2.77	97.54	Warm
19:00	3.34	99.87	Hot	2.77	97.55	Warm
20:00	3.21	99.72	Hot	2.72	97.08	Warm
21:00	3.07	99.38	Hot	2.65	96.1	Warm
22:00	2.87	98.35	Warm	2.52	93.82	Warm
23:00	2.65	95.97	Warm	2.32	88.85	Warm
0:00	2.41	91.27	Warm	2.09	80.86	Warm

human body in W/m^2, *Pa* is the partial pressure of water vapor in Pa, determined as follows:

$$Pa = 10 - 5\Phi \exp\left[\begin{array}{c} -\frac{5800}{t_a} + 0.048T_a + \\ +4.1\times10^{-8}t_a^3 + 6.545lnT_a \end{array}\right], \quad (2)$$

t_a is the air temperature in °C, Φ is the relative humidity, $T_a = t_a + 273.15$ in K, t_r is the mean radiation temperature in °C, determined as follows:

$$t_r = t_g + 2.4v_a 0.5\left(t_g - t_a\right) \quad (3)$$

v_a is the average air speed in m/s, t_g is the temperature of the black sphere, f_{cl} is the clothing area factor, determined as follows:

$$f_{cl} = 1.0 + 0.3I_{cl} \quad (4)$$

t_{cl} is the clothing area temperature in °C, determined as follows:

$$t_{cl} = 35.7 - 0.028\left(M - W\right) - I_{cl} \times \times\left\{\begin{array}{c} 3.96\times10^{-8} f_{cl} \times \\ \times\left[\left(t_{cl}+273\right)^4 - \left(t_r+273\right)^4 - \left(f_{cl}-t_a\right)\right] \end{array}\right\} \quad (5)$$

and h_c is the surface heat transfer coefficient in W/(m^2·K), determined as follows:

$$h_c = = \begin{cases} 2.38\left(t_{cl}-t_a\right)^{0.25}, \ if\ 2.38\left(t_{cl}-t_a\right)^{0.25} \geq 12.1\sqrt{v_a} \\ 12.1\sqrt{v_a}, \ if\ 2.38\left(t_{cl}-t_a\right)^{0.25} < 12.1\sqrt{v_a} \end{cases} \quad (6)$$

The PPD and PMV indicators have the following relationship (Duan et al., 2022; Rînjea et al., 2022):

$$PPD = 100 - 95e^{-\left[\left(-0.335.PMV^4 - 0.217.PMV^2\right)\right]} \quad (7)$$

In this work, the PMV and PPD values were obtained by setting the environmental variables extracted from the EnergyPlus simulation program (air temperature, relative humidity, air speed, and mean radiant temperature) as well as the personal variables (thermal resistance of clothing and metabolic rate) in the OpenStudio platform. The thermal resistance of clothing was considered to be equal to 0.5, which represents light summer clothing, and the metabolic rate was taken as 1.25 met (1 met = 58 W/m^2) to represent the routine and relaxed state.

The hourly variation of the PMV and PPD values, corresponding to different building forms on July 21, was determined for the baseline case without shading and for the case with the combined shading device 1.25 m long (Tables 3–5). The results show that with the shading device, most of daily hours are brought closer to the comfort zone. In the rectangular building, the sensation percentages for hot, warm, and slightly warm for the baseline case were 29.16%, 62.5%, and 8.33%, respectively. With the combined shading, they became 0% for hot sensation, 66.67% for warm sensation, and 33.33% for slightly warm sensation, indicating significant shifting closer to the comfort zone. In addition, combined shading in the L-shaped building brings daily hours' percentage for indoor sensation from 33.33% in the baseline case to 16.67% in the case with combined shading for hot sensation, 58.33% in the baseline case to 66.67% in the case with combined shading for warm sensation, and 8.33% in the baseline case to 16.67% in the case with combined shading for slightly warm sensation, indicating good shifting for sensation to the comfort zone. Combined shading in the U-shaped building brings daily hours' percentage for indoor sensation from 33.33% for hot sensation, 54.17% for warm sensation, and 12.5% for slightly warm sensation for the baseline conditions to 0%, 62.5%, and 37.5%, respectively, indicating significant shifting for sensation closer to the comfort zone.

Based on these results, it can be concluded that combined shading of an optimal length of 1.25 m obviously improves the sensation feeling in all buildings. The rectangular and U-shaped buildings show better results than the L-shaped building. This can be attributed to the compactness factor of the rectangular building, which has less surface to volume ratio for the building envelope exposed to the direct sunlight, while the U-shaped building is characterized by self-shading since its shape creates more shadows.

Besides, Tables 3–5 it also show that the PPD percentage for all buildings significantly decreases with the presence of shading devices for all day long as compared with the case without shading, which indicates obvious improvement of the thermal comfort in the rooms with shading.

Conclusions

This papers addresses the impact of different shading devices of different length on the thermal performance and thermal comfort of different residential building forms in hot-dry climate in Amman, Jordan. Based on the results, we can draw the following conclusions:

- Vertical fins facing west make almost no difference in all types of buildings except for the rectangular one, which shows maximum reduction in the indoor air temperature of 0.6°C.
- Horizontal and combined shadings demonstrate significant reduction in the indoor air temperature and enhance the thermal performance.
- The length of shading is a significant factor in improving the indoor temperature, and it was found that 1.25 m length ensures the best performance, minimizing the air temperature in all building forms.
- Combined shading shows the best results as compared with other types of shading as it reduces the indoor air temperature by 2.6–3.3°C for all building forms.
- Combined shading with 1.25 m in length can improve the thermal comfort of all buildings, especially in rectangular and U-shaped buildings,

where hot sensation was minimized. This is explained by the compactness and self-shading factors.

- The U-shaped building shows the best PMV and PPD results when using combined shading with 1.25 m in length since 0%, 62.5%, and 37.5% for hot, warm, and slightly warm sensation were recorded, respectively. The rectangular building shows the largest air temperature reduction when using combined shading with 1.25 m in length as it reduces the air temperature by 3.3°C at 4:00 PM.

References

Abdulla, F. (2020). 21st century climate change projections of precipitation and temperature in Jordan. *Procedia Manufacturing*, Vol. 44, pp. 197–204. DOI: 10.1016/j.promfg.2020.02.222.

Abu Qadourah, J., Al-Falahat, A. M., Alrwashdeh, S. S., and Nytsch□Geusen, C. (2022). Improving the energy performance of the typical multi-family buildings in Amman, Jordan. *City, Territory and Architecture,* Vol. 9, 6. DOI: 10.1186/s40410-022-00151-8.

Albatayneh, A., Jaradat, M., Al-Omary, M., and Zaquot, M. (2021). Evaluation of coupling PV and air conditioning vs. solar cooling systems—case study from Jordan. *Applied Science*, *Vol. 11*, Issue 2, 511. DOI: 10.3390/app11020511.

Ali, H. and Hashlamun, R. (2019). Envelope retrofitting strategies for public school buildings in Jordan. *Journal of Building Engineering*, Vol. 25, 100819. DOI: 10.1016/j.jobe.2019.100819.

Bataineh, K. and Alrabee, A. (2018). Improving the energy efficiency of the residential buildings in Jordan. *Buildings*, *Vol. 8*, Issue 7, 85. DOI: 10.3390/buildings8070085.

Bataineh, K. and Al Rabee, A. (2021). Design optimization of energy efficient residential buildings in Mediterranean region. *Journal of Sustainable Development of Energy, Water and Environment Systems,* Vol. 10, Issue 2, 1090385. DOI: 10.13044/j.sdewes.d9.0385.

Duan, X., Yu, S., Chu, J., Chen, D., and Chen, Y. (2022). Evaluation of indoor thermal environments using a novel predicted mean vote model based on artificial neural networks. *Buildings*, *Vol. 12*, Issue 11, 1880. DOI: 10.3390/buildings12111880.

Emir, S. (2016). The evaluation of thermal comfort on primary schools in hot-humid climates: a case study for Antalya. *European Journal of Sustainable Development*, Vol. 5, No. 1, 53. DOI: 10.14207/ejsd.2016.v5n1p53.

Eskandari, H., Saedvandi, M., and Mahdavinejad, M. (2018). The impact of Iwan as a traditional shading device on the building energy consumption. *Buildings,* Vol. 8, Issue 1, *3*. DOI: 10.3390/buildings8010003.

Fanger, P. O. (1970). Thermal comfort. Copenhagen: Danish Technical Press, 244 p.

Fanger, P. O and Toftum, J. (2002). Extension of the PMV model to non-air-conditioned buildings in warm climates. *Energy and Building*, Vol. 34, Issue 6, pp. 533–536. DOI: 10.1016/S0378-7788(02)00003-8.

Feng, F., Kunwar, N., Cetin, K., and O'Neill, Z. (2021). A critical review of fenestration/window system design methods for high performance buildings. *Energy and Buildings*, Vol. 248, 111184. DOI: 10.1016/j.enbuild.2021.111184.

Freewan, A. A. Y. (2014). Impact of external shading devices on thermal and daylighting performance of offices in hot climate regions. *Solar Energy*, Vol. 102, pp. 14–30. DOI: 10.1016/j.solener.2014.01.009.

GIASMA (2022). Sunrise, sunset, dawn and dusk times around the world. [online] Available at: https://www.gaisma.com/en [Date accessed September, 2022].

Hailu, H., Gelan, E., and Girma, Y. (2021). Indoor thermal comfort analysis: a case study of modern and traditional buildings in hot-arid climatic region of Ethiopia. *Urban Science*, Vol. 5*,* Issue 3, 53. DOI: 10.3390/urbansci5030053.

Kumar, P. and Sharma, A. (2022). Assessing outdoor thermal comfort conditions at an urban park during summer in the hot semi-arid region of India. *Materials Today: Proceedings*, Vol. 61, Part 2, pp. 356–369. DOI: 10.1016/j.matpr.2021.10.085.

Minangi, F. S. and Alibaba, H. Z. (2018). Effect of shading on thermal performance of dormitory building on hot climate. *International Journal of Interdisciplinary Research and Innovation,* Vol. 6, Issue 4, pp. 610–621.

Mushtaha, E., Salameh, T., Kharrufa, S., Mori, T., Aldawoud, A., Hamad, R., and Nemer, T. (2021). The impact of passive design strategies on cooling loads of buildings in temperate climate. *Case Studies in Thermal Engineering*, Vol. 28, 101588. DOI: 10.1016/j.csite.2021.101588.

Nwankwo, P. N., Akpado, K. A., Isizoh, A. N., Alumona, T. L., and Oguejiofor, O. S. (2021). Optimization of solar panel tilt and azimuth angle for maximum solar irradiation and minimum loss for rural electrification. *International Journal for Research in Applied Science & Engineering Technology (IJRASET)*, Vol. 9, Issue X, pp. 1852–1868. DOI: 10.22214/ijraset.2021.38665.

Ohene, E., Shu-Chien, H., and Chan, A. P. C. (2022). Feasibility and retrofit guidelines towards net-zero energy buildings in tropical climates: a case of Ghana. *Energy and Buildings*, Vol. 269, 112252. DOI: 10.1016/j.enbuild.2022.112252.

Rînjea, C., Chivu, O. R., Darabont, D.-C., Feier, A. I., Borda, C., Gheorghe, M., and Nitoi, D. F. (2022). Influence of the thermal environment on occupational health and safety in automotive industry: a case study. *International Journal of Environmental Research and Public Health*, Vol. 19*,* Issue 14, 8572. DOI: 10.3390/ijerph19148572.

DOI: 10.23968/2500-0055-2023-8-1-37-43

STRUCTURAL AND PARAMETRIC ANALYSIS OF LEAD RUBBER BEARINGS AND EFFECT OF THEIR CHARACTERISTICS ON THE RESPONSE SPECTRUM ANALYSIS

Faqiri Amanollah, Nadezhda Ostrovskaya*, Yuriy Rutman

Saint Petersburg State University of Architecture and Civil Engineering
Saint Petersburg, Russia

*Corresponding author's e-mail: ostrovskaya.nv@yandex.ru

Abstract

Introduction: Earthquakes are one of the most frequent and potentially disruptive natural disasters. Up to this day, numerous methods have been tested and applied to prevent damage to buildings and structures as a result of earthquakes. Currently, one of the widely used methods is to provide seismic isolation between the building and the ground. Its main purpose is to reduce the interaction between the building and the ground as well as the impact of soil movement on the building. For our study, we chose a system of lead rubber bearings as isolators used to improve the seismic resistance of buildings. **Purpose of the study:** We aimed to expand the tool kit for the analysis of seismic isolation based on rubber bearings and demonstrate the effectiveness of ETABS software. **Methods:** The paper investigates the behavior of an isolation system with lead rubber bearings for various earthquake records with the use of ETABS software according to UBC-97 standards and software developed specifically for this study in Excel. **Results:** Based on the developed software, we analyzed how changes in properties of base isolators affect the behavior of structures exposed to earthquakes.

Keywords: seismic isolation, seismic bearing, rubber bearing, seismic isolation effectiveness.

Introduction

One of the important challenges of structural engineers is to find a suitable solution to reinforce structures so that they could withstand earthquakes. In traditional design methods, the seismic resistance of buildings is provided by the combination of stiffness, plasticity, and energy losses in the main components of the structure. In modern design methods, seismic isolation systems are utilized to ensure the safety and resistance of structural components to earthquakes as well as to reduce material consumption for structural components. Currently, seismic isolation systems are widely used to prevent structural vibrations from earthquakes, which allows structural components to remain in the elastic deformation range and makes it possible to prevent their significant damage and destruction (Tamim Tanwer et al., 2019).

There are many damping devices, including rubber bearings (with/without a lead core), friction and kinematic dampers. In recent decades, they have been used in practical seismic design of structures and are still being developed (Buckle and Mayes, 1990; Rutman and Ostrovskaya, 2019; Tyapin, 2020; Uzdin et al., 2012).

Fig. 1 shows an example of a lead rubber bearing (LRB) widely used all over the world (Jangid, 2007; Tyler and Robinson, 1984). The LRB is made of alternating layers of rubber and steel plates with one or several lead cores inside. The core is deformed, ensures the hysteresis operation of the structure as well as sufficient stiffness, strength and resistance to low lateral loads, light winds, and minor earthquakes (Bhandari et al., 2018).

The LRB force/displacement relationship is non-linear, and the correct prediction for the behavior of isolated base structures under seismic effects depends heavily on the mathematical model chosen to describe the system. For instance, there are several hysteresis models to describe the dynamic behavior of the LRB: linear, polynomial, and curvilinear (Wen, 1980). A suitable model for the dynamic behavior of the system is usually based on the characteristics of pulse energy, obtained as a result of dynamic or static experiments. In recent decades, much effort has been made to develop methods to identify non-linear hysteresis systems. These methods include least squares estimation in the time domain (Kilar et al., 2011; Lin et al., 2001; Wenbin, 2000; Yang and Lin, 2004). Thus, the task of determining the parameters of seismic bearings and simulating the behavior of the structure / seismic isolation system is quite relevant.

Subject, tasks, and methods

Fig. 2 shows a design scheme and main design parameters of the LRB (Sharbatdar et al., 2011). To determine the isolator parameters, Uniform Building Code UBC-97, corresponding to the regulations, was used (ICBO, 1997). *The target period of the building and material properties* were determined based on the following considerations: the values from 2 to 3 seconds are the desired values of the

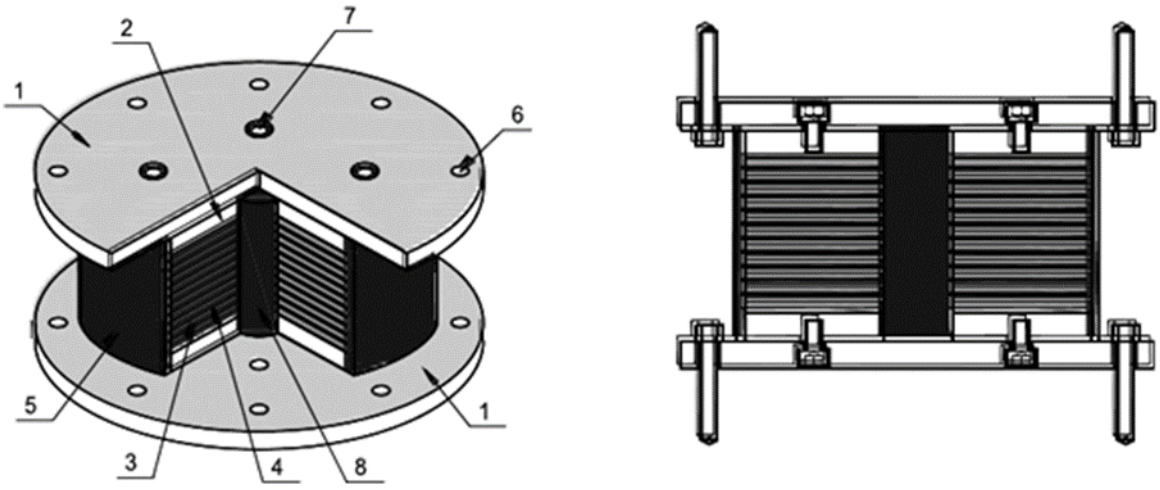

Fig. 1. Schematic diagram of the LRB (Smirnov and Bubis, 2014):
1 — support plates fastened to the non-seismically isolated and seismically isolated parts of the structure; 2 — flanged steel plates; 3 — steel plates located between rubber plates; 4 — rubber plates; 5 — a rubber cover protecting the inner layers of rubber and metal; 6 — holes for anchor bolts required to fasten the bearing to the non-seismically isolated and seismically isolated parts of the structure; 7 — key holes; 8 — a lead core.

isolation system oscillation period. The modulus of elasticity *E*, the shear modulus *G*, and the maximum shear strain γ_{max} differ depending on the type of the LRB selected.

The main stages of the calculation were as follows: first, a building with rigid fixing was modeled, and vertical loads in the interior, exterior and corner columns were determined. After that, the design parameters of the LRB were calculated using an Excel spreadsheet. Then those parameters were used to determine the LRB parameters in ETABS. As a result, the following design parameters were obtained for three different types of the LRB (Table 1).

Description of the design solutions adopted with the use of the LRB. To test the model, we considered a standard 10-story reinforced concrete building located in the earthquake-prone area V, with an open floor, as shown in Figs. 3 and 4. The dimensions of the building in plan view are 30 and 24 m in the x and y directions, respectively (Ferraioli and Mandara, 2017). The height of the first floor is 3.6 m, and the height of the rest floors is 3 m. Thus, the total height of the building is 30.6 m. The slab thickness is 0.150 m. The design static loads are taken to be equal to 3.4 kPa for the partitions and 1.5 kPa for the floors and the roof. Table 2 shows other characteristics of concrete and reinforcement. The axial load for the interior, exterior and corner columns is 5332.06 kN, 4529.19 kN, and 3911.39 kN, respectively. The design was performed as per American standard ASCE07 and UBC-97 (ICBO, 1997). In the calculations, concrete of grade M35 was used, and high yield strength deformed (HYSD) bars with a minimum yield strength of 415 MPa were utilized as both longitudinal and transverse reinforcement.

Modeling and design of a building with an LRB**.** ETABS software was used for the calculation. Fig. 5 shows a design scheme in the form of a spatial frame. It should be noted that in ETABS (and in some foreign design programs), static non-linear pushover analysis is implemented by introducing plastic hinges into the sections of the design scheme components where, from the point of view of the program user, inelastic deformations should

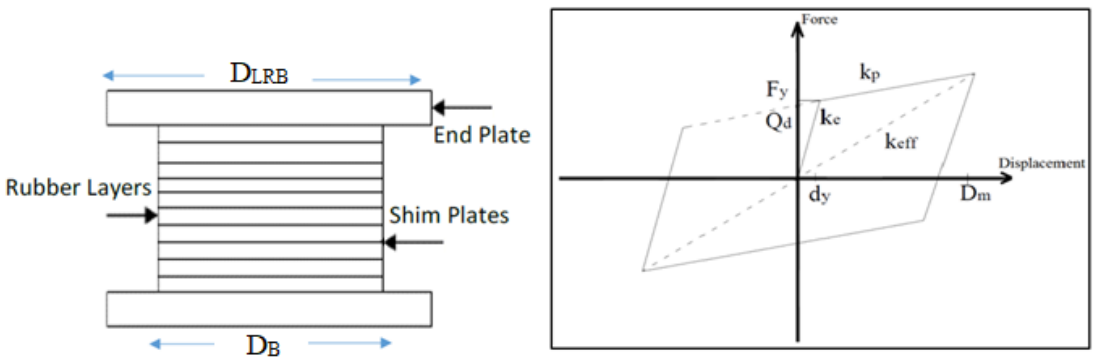

Fig. 2. Design scheme and main design parameters of the LRB

Table 1. **Design parameters of the LRB for ETABS**

Final input data for ETABS	Exterior columns	Interior columns	Corner columns
Rotational inertia (kN/m)	0.0146	0.0207	0.0107
U1 Effective stiffness (kN/m)	721.991	849.977	623.510
U2 & U3 Effective stiffness (kN/m)	2913	3430	2516
U2 & U3 Effective damping	0.1	0.1	0.1
U2 & U3 Distance from the end — J (m)	0.0058	0.0058	0.0058
U2 & U3 Stiffness (kN/m)	24.559	28.913	21.209
U2 & U3 Yield strength (kN)	142.2	167.4	122.8
Bearing diameter, DLRB (m)	0.789	0.856	0.75
Total height of the LRB, h (m)	0.34	0.35	0.34

develop. This significantly increases the error probability since it is almost impossible to define an appropriate mechanism for the destruction of a complex structure and criteria for the transition of its components into plastic condition.

The use of the response spectrum function in accordance with the standards is a more unified procedure, which does not require additional user control over the structure operation, and that creates the advantage of using the response spectrum analysis method compared with the calculation according to the plastic mechanism.

Table 2. **Initial data for structural modeling**

No.	Parameter	Value
1	First floor height (m)	3.6
2	Floor height (m)	3
3	Building height (m)	30.6
4	Column size (m)	0.6×0.6 or 0.5×0.5
5	Number of floors	10
6	Beam size (m)	0.4×0.5
7	Floor slab thickness (m)	0.150
8	Modulus of elasticity of concrete Ec (GPa)	25
9	Design strength of concrete Fck (MPa)	30
10	Reinforcement yield strength (MPa)	415
11	Poisson's ratio	0.2
12	Dead load on the slab (kN/m^2)	4.5
13	Load on the floor with partitions (kN/m^2)	3.4
14	Load on the roof (kN/m^2)	1.5
15	Load on the walls (kN/m)	7.5
16	Specific weight of reinforced concrete (kN/m^3)	25.00
17	Material	Concrete M35 and reinforcement Fe-415 (HYSD, compliant with IS-2002)
18	Reinforcement	High strength deformed steel compliant with IS-2002. Modulus of elasticity — 200 kN/mm^2

Results and discussion

The spectral analysis of the structure isolated with the use of the LRB and the non-isolated structure yielded the following results presented in Figs. 6–10.

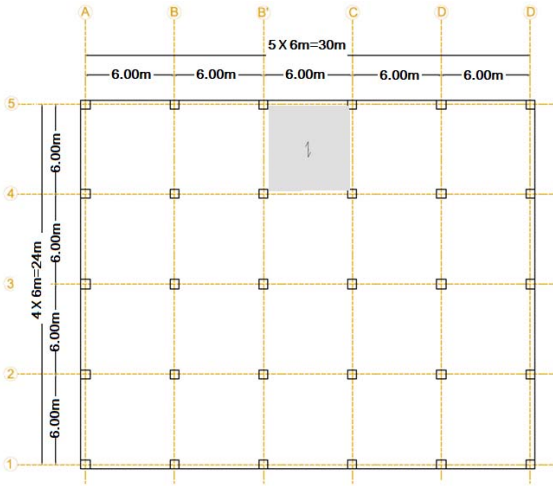

Fig. 3. Standard floor plan

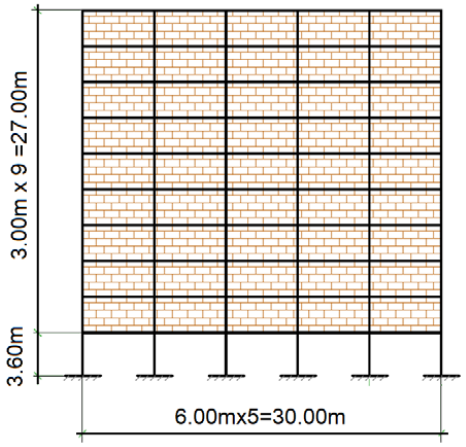

Fig. 4. Scheme of the transverse frame of the reinforced concrete building structure

Table 3. **Seismic characteristics of the construction facility as per UBC-97**

No.	Parameter	Value	Remark
1	Seismic zone factor (Z)	0.36	(UBC 97, Table 16-I)
2	Seismic load	As per ASCE07	
3	Seismic source type	B	(UBC 97, Table 16-S)
4	Distance to a known source	5	(UBC 97, Table 16-S)
5	Soil profile type	S_D	(UBC 97, Table 16-J)
6	Near-source factor (Na)	1.2	(UBC 97, Table 16-S)
7	Near-source factor (Nv)	1.6	(UBC 97, Table 16-T)
8	Seismic coefficient (Ca)	0.36	(UBC 97, Table 16-Q)
9	Seismic coefficient (Cv)	0.56	(UBC 97, Table 16-R)
10	Design period TD, s	2.5	
11	Behavior coefficient	1.25	
12	Effective damping (βd or βm)	0.05	
13	Damping coefficient (βd or βm)	1	

The following designations are used in these figures: FB — a system without seismic isolation; LRB — a system with seismic isolation using the LRB. The results are given for the effects of an operating basis earthquake as well as for the system response spectrum analysis.

A comparison of the values of the maximum displacement for story drift and the shear force for each story, obtained based on the response spectrum analysis, makes it possible to note that displacement, drift, and shear forces decrease by 30% or more when the LRB is used. In the assessment of the maximum displacement of the LRB system, which is one of the main parameters in the design of seismic

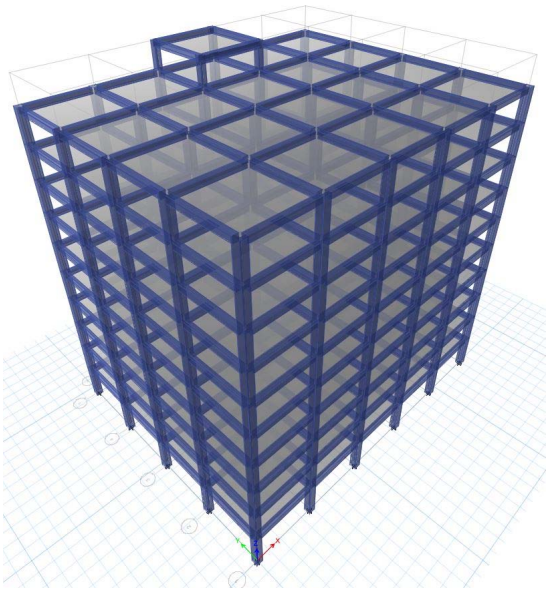

Fig. 5. Scheme of the spatial frame of the reinforced concrete building structure with the LRB

isolation, as well as the maximum displacement of the base section of the structure and the building as a whole, the spectrum analysis method proved to be a simple and effective method.

In conclusion, it should be noted that it is important to choose the right parameters of seismic isolators. The system response spectrum analysis is one of the easiest and effective tools to determine the required properties of isolators, taking into account the complex movement of the structure. The proposed method for determining the LRB parameters using Excel in accordance with UBC-97 has acceptable accuracy in terms of assessing the design parameters of the LRB. Considering the behavior of the isolated structure and the fact that the bearings have non-linear characteristics, it is possible to choose the most effective model for the seismic bearing and structure by analyzing the response spectrum of the system.

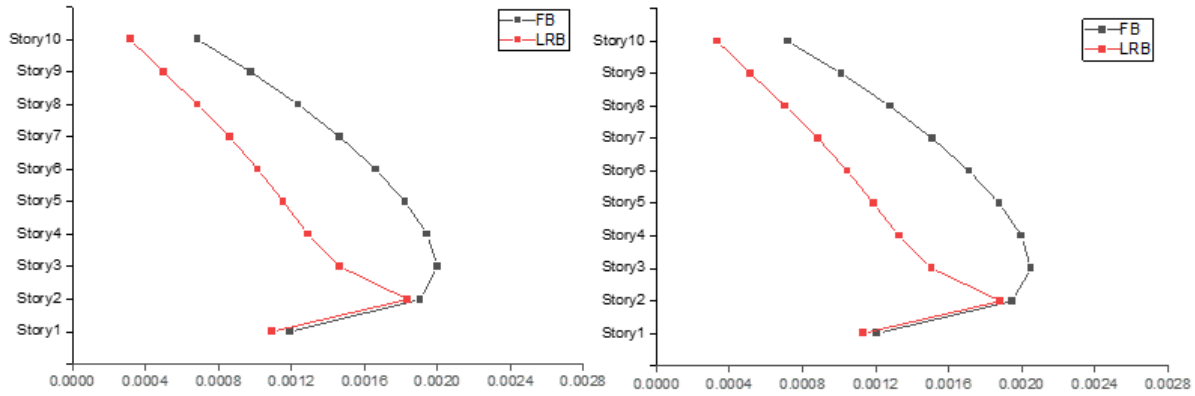

Fig. 6. Drift in the X and Y directions (earthquake)

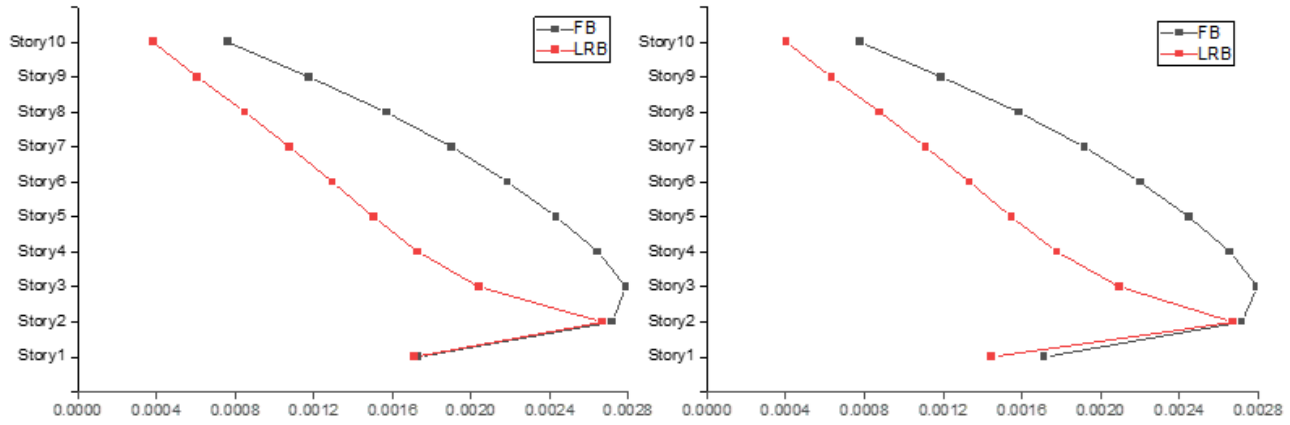

Fig. 7. Drift in the X and Y directions (spectrum analysis)

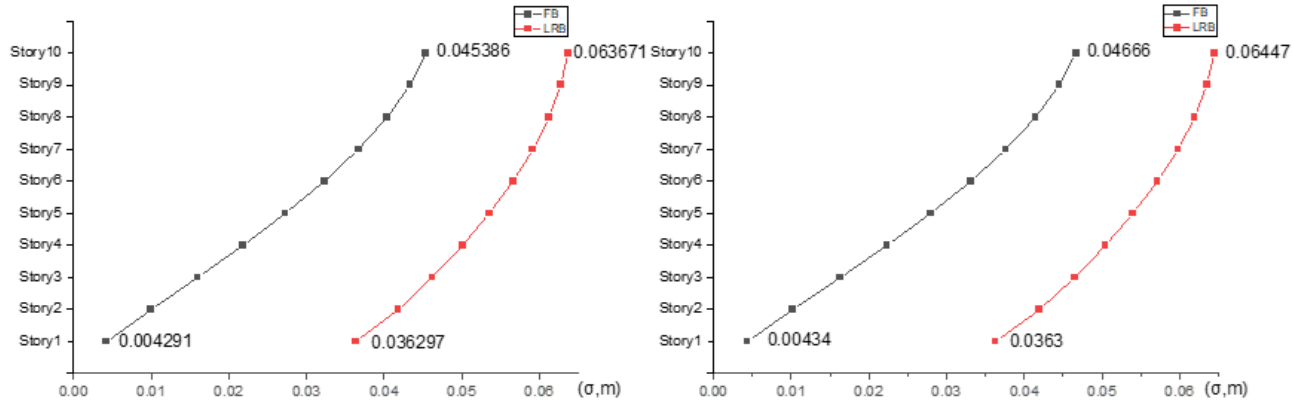

Fig. 8. Displacement in the X and Y directions (earthquake)

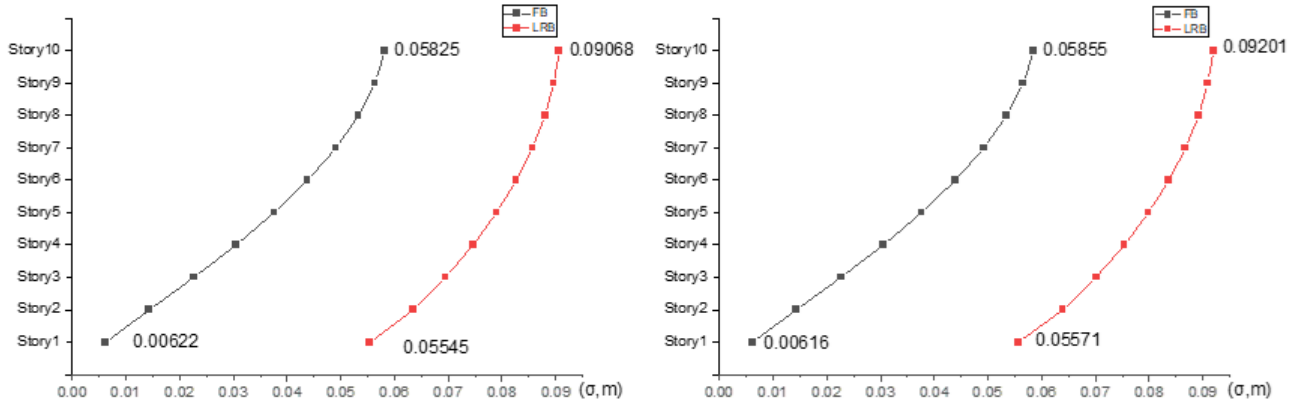

Fig. 9. Displacement in the X and Y directions (spectrum analysis)

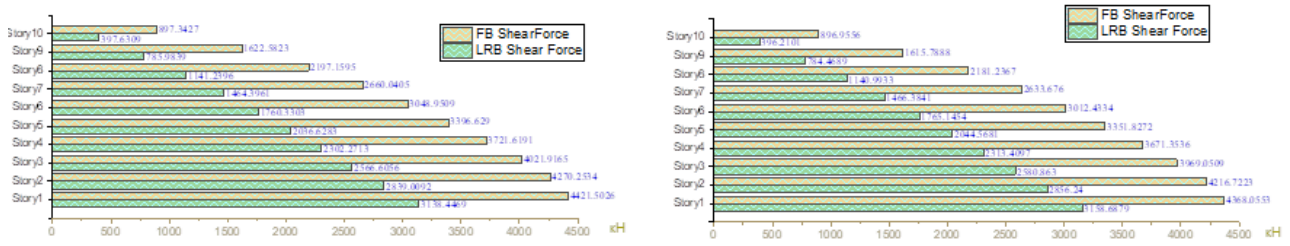

Fig. 10. Shear force in X and Y directions (spectrum analysis)

References

Bhandari, M., Bharti, S. D., Shrimali, M. K. and Datta, T. K. (2018). Assessment of proposed lateral load patterns in pushover analysis for base-isolated frames. *Engineering Structures*, Vol. 175, pp. 531–548. DOI: 10.1016/j.engstruct.2018.08.080.

Buckle, I. G. and Mayes, R. L. (1990). Seismic isolation: history, application, and performance — a world view. *Earthquake Spectra*, Vol. 6, Issue 2, pp. 161–201. DOI: 10.1193/1.1585564.

Ferraioli, M. and Mandara A. (2017). Base isolation for seismic retrofitting of a multiple building structure: design, construction, and assessment. *Mathematical Problems in Engineering*, Vol. 2017, 4645834. DOI: 10.1155/2017/4645834.

ICBO (1997). *Uniform Building Code (UBC-97). Vol. 2. Structural Engineering Design Provisions.* Whittier, California: International Conference of Building Officials, 492 p.

Jangid, R. S. (2007). Optimum lead–rubber isolation bearings for near-fault motions. *Engineering Structures*, Vol. 29, Issue 10, pp. 2503–2513. DOI: 10.1016/j.engstruct.2006.12.010.

Kilar, V., Petrovčič, S., Koren, D., and Šilih, S. (2011). Seismic analysis of an asymmetric fixed base and base-isolated high-rack steel structure. *Engineering Structures*, Vol. 33, Issue 12, pp. 3471–3482. DOI: 10.1016/j.engstruct.2011.07.010.

Lin, J.-W., Betti, R., Smyth, A. W., and Longman, R. W. (2001). On-line identification of non-linear hysteretic structural systems using a variable trace approach. *Earthquake Engineering & Structural Dynamics*, Vol. 30, Issue 9, pp. 1279–1303. DOI: 10.1002/eqe.63.

Rutman, Yu. L. and Ostrovskaya, N. V. (2019). *Dynamics of structures: earthquake resistance, seismic protection, wind loads*. Saint Petersburg: Publishing House of the Saint Petersburg State University of Architecture and Civil Engineering, 253 p.

Sharbatdar, M. K., Hoseini Vaez, S. R., Amiri, G.G., and Naderpour, H. (2011). Seismic response of base-isolated structures with LRB and FPS under near fault ground motions. *Procedia Engineering*, Vol. 14, pp. 3245–3251. DOI: 10.1016/j.proeng.2011.07.410.

Smirnov, V. I. and Bubis, A. A. (2014). Discussion of the draft national standard: “Anti-seismic and seismically isolated construction design code. Design rules”. *Earthquake Engineering. Constructions Safety*, No. 3, pp. 22–33.

Tamim Tanwer, M., Kazi, T. A., and Desai, M. (2019). A study on different types of base isolation system over fixed based. In: Satapathy, S. and Joshi, A. (eds.). *Information and Communication Technology for Intelligent Systems. Smart Innovation, Systems and Technologies*, Vol. 106. Singapore: Springer, pp. 725–734. DOI: 10.1007/978-981-13-1742-2_71.

Tyapin, A. G. (2020). Equation of planar vibrations of rigid structure on kinematic supports after A.M. Kurzanov. *Earthquake Engineering. Constructions Safety*, No. 5, pp. 19–31.

Tyler, R. G. and Robinson, W. H. (1984). High-strain tests on lead-rubber bearings for earthquake loadings. *Bulletin of the New Zealand Society for Earthquake Engineering*, Vol. 17, No. 2, pp. 90–105. DOI: 10.5459/bnzsee.17.2.90-105.

Uzdin, A. M., Yelizarov, S. V., and Belash, T. A. (2012). *Earthquake-resistant constructions of transport buildings and structures*. Moscow: Rail Transport Training Center, 501 p.

Wen, Y. K. (1980). Equivalent linearization for hysteretic systems under random excitation. *Journal of Applied Mechanics*, Vol. 47, Issue 1, pp. 150–154. DOI: 10.1115/1.3153594.

Wenbin, Q. J. L. (2000). Static Pushover Analysis-an analytical tool for performance/displacement-based seismic design. *Building Structure*, Vol. 30, No. 6, pp. 23–26.

Yang, J. N. and Lin, S. (2004). On-line identification of non-linear hysteretic structures using an adaptive tracking technique. *International Journal of Non-Linear Mechanics*, Vol. 39, Issue 9, pp. 1481–1491. DOI: 10.1016/j.ijnonlinmec.2004.02.010.

КОНСТРУКТИВНЫЙ И ПАРАМЕТРИЧЕСКИЙ АНАЛИЗ СВИНЦОВЫХ РЕЗИНОМЕТАЛЛИЧЕСКИХ ОПОР И ВЛИЯНИЕ ИХ ХАРАКТЕРИСТИК НА АНАЛИЗ СПЕКТРА ОТКЛИКА

Факири Амоналлах, Надежда Владимировна Островская*, Юрий Лазаревич Рутман

Санкт-Петербургский государственный архитектурно-строительный университет
Санкт-Петербург, Россия

*E-mail: ostrovskaya.nv@yandex.ru

Аннотация
Введение: Землетрясения являются одним из часто наблюдаемых стихийных бедствий, которые могут иметь весьма разрушительные последствия. До сегодняшнего дня было опробовано и применено множество различных методов для предотвращения повреждений сооружений и конструкций, которые могут возникнуть в результате землетрясений. Одним из широко используемых в настоящее время методов является применение сейсмоизоляции между зданием и грунтом, основной целью которого является уменьшение взаимодействия между ними и уменьшение влияния движения грунта на здание. В качестве изоляторов, применяемых в сейсмостойких зданиях, была выбрана система резинометаллических опор со свинцовым сердечником. **Цель исследования:** настоящая статья ставит целью расширить инструментарий средств расчета сейсмоизоляции на базе резинометаллических опор и показать эффективность применения программного комплекса ETABS. **Методы:** в статье проводится исследование поведения системы изоляции с применением резинометаллических опор со свинцовым сердечником для различных записей землетрясений с использованием программного комплекса ETABS согласно нормам UBS-97 и программного обеспечения, разработанного специально для этого исследования в Exel. **Результаты:** с помощью разработанного программного обеспечения анализировалось влияние изменения различных свойств изоляторов основания на поведение конструкции под действием землетрясений.

Ключевые слова: сейсмоизоляция, сейсмоопора, резинометаллическая опора, эффективность сейсмоизоляции.

DOI: 10.23968/2500-0055-2023-8-1-44-50

USEFUL STRATEGIES FOR LOW-COST CONSTRUCTION

Omar Moustafa Alomari*[1], A M Faten Albtoush[2], Mohammad Al-Rawashdeh[1]

[1] Al-Balqa Applied University, Alsalt, Jordan

[2] Jadara University, Irbid, Jordan

*Corresponding author's e-mail: omar.alomari@bau.edu.jo

Abstract

Introduction: Everyone, regardless of culture, seeks a dwelling that provides comfort and safety at an affordable cost. Many countries worldwide have witnessed increased demand for residential buildings due to population growth. However, because of the economic conditions that most countries suffer from, the search for low-cost housing without compromising the quality of construction and materials has become extremely essential. Low-cost construction meets the demand for cost-effective design solutions without prejudice to quality. **Purpose of the study:** We aimed to determine the applicability of building materials and technologies used in low-cost construction. **Methods:** In the course of the study, we thoroughly reviewed literature sources addressing low-cost construction. **Results:** Based on the review, we determined six strategies of low-cost construction: effective planning, use of low-cost materials, use of environmentally-friendly materials, use of cost-efficient construction techniques, use of available alternative construction methods, and sustainable community through involvement and training. All over the world, knowledge exchange and technology development within local societies are considered techniques that reduce the cost of buildings at the expense of local manpower. We recommend governments to enhance the involvement of local resources by developing training programs in cooperation with local communities. Besides, governments should provide opportunities for the application of environmentally-friendly construction materials and encourage their use. This study will help researchers delve deeper into the issues and obstacles occurring in low-cost construction.

Keywords: low-cost construction, sustainability, environmentally-friendly materials.

Introduction

In all parts of the world, housing is not only a place of residence but also a place where one can live calmly, in prosperity and development. It is a place where people feel safe and enjoy privacy and sense of belonging. Besides, adequate housing allows people achieve their environmental, economic, and security needs. Therefore, everyone seeks a home that guarantees basic requirements for living a decent life. One of the most pressing challenges faced by developing countries is the provision of adequate shelter for all people (Tam, 2011). For these reasons, housing is one of the essential components of any country's national strategy. To stay healthy, people need a proper place to live for the rest of their lives, and that is home (Srivastava and Kumar, 2018).

According to Adeniyi et al. (2020), there is a major problem with providing adequate housing to the population globally. As the worldwide population increases, there is an increase in the demand for housing, leading to a massive demand for construction materials, such as cement, wood, steel, etc. This means that the consumption of natural resources to produce these materials increases as well. The continuous exploitation and depletion of natural resources damage the environment (Srivastava and Kumar, 2018). The production of construction materials from natural resources results in emissions of toxic gases harmful to the environment: nitrogen oxides, sulfur oxides, and carbon monoxide. These toxic substances contaminate soil, water, air, and aquatic life, affecting the human health and standards of living (Srivastava and Kumar, 2018). Besides, the process of producing construction materials from natural resources is costly. Thus, it is necessary to adopt cost-effective, advanced, and environmentally-friendly housing technologies enabling ordinary people to build houses at affordable cost (Tam, 2011). Many studies have addressed the possibility of using new technologies based on cost-effective materials in construction to design low-cost and efficient housing.

Low-cost architecture emerges as a response to the demand for economical construction solutions that still ensure good visual, hygrothermal, and acoustic performance (Oliveira et al., 2013). Cost-effective construction is a relative concept that has more to do with budgeting and seeks to reduce construction costs through better management and appropriate use of local materials, skills, and technology while maintaining performance and structure life (Tiwari et al., 1999). With the current economic crisis, this concept is becoming increasingly important in all areas and social strata (Oliveira et al., 2013). Low-cost housing is also a philosophy of cutting-edge budgeting ideas and

strategies that help to minimize construction costs by developing expertise and technology while utilizing locally accessible materials without compromising the structure's effectiveness, existence, or strength (Varun Raj et al., 2021). Accordingly, high-quality construction materials are long-lasting, have appealing features, and require only a little maintenance (Bredenoord, 2017). Cost reduction can be achieved through the effective use of locally available construction materials and techniques that are durable, economical, accepted by users, and do not require costly maintenance (Tam, 2011). The study conducted by Tam (2011) demonstrated that using low-cost housing technologies is a cost-effective construction approach for the industry. In the case studies for walling and roofing, it was found that by employing low-cost housing technologies, it is possible to reduce construction costs by about 26.11% and 22.68%, respectively, in comparison with traditional construction methods.

There is a huge misconception that low-cost housing can only be a result of substandard works when constructed from low-quality materials (Srivastava and Kumar, 2018). Thus, it is important first to understand the concept of low-cost construction to determine its benefits. That is why this study focuses on providing a clear concept of low-cost construction in addition to determining its importance and strategies required to construct affordable housing.

Literature review

Governments around the world, and particularly in developing countries, are concerned with the rising cost of construction (Danso, 2013). Most countries are aware of the importance of affordable housing, especially those with a huge population. For example, India is currently facing a housing shortage of approximately 17.6 million houses (Tam, 2011). For this reason, some studies focus on the adoption of low-cost construction in India. Osman et al. (2017) conducted a study in Malaysia and established that despite the affordable housing policy for the state of Johor, house prices are still quite high, making it difficult for most people to reach their goal of owning a home. This is evidenced by the fact that the housing affordability index for some areas was in the unaffordable category.

Low-cost construction technologies seek to reduce construction costs by replacing traditional methods and materials. Effective planning and project management, low-cost materials, cost-effective construction technologies, and the use of alternative available construction methods can help to provide low-cost housing. In this paper, we aim to present different strategies to achieve the goal of low-cost construction. It is about using local and indigenous building materials, local skills, energy-saving, and environmentally-friendly options (Tam, 2011). That is why in the next sections, we will focus on those strategies in more detail, in addition to presenting some practical ideas about low-cost construction at this stage of development.

Effective planning

There is a widespread misconception that low-cost housing involves only substandard work and uses cheap, low-quality building materials. But the fact is that it is implemented by appropriate planning and efficient management of resources. Effective planning of a low-cost building actually starts from site selection. The nature of soil at the construction site plays an important role in reducing the cost of construction. It is worth noting that the foundation takes approximately 11–16% of the total construction cost. Therefore, it is essential to choose such a construction site where it is not necessary to lay foundations at such a high cost. In case of soft soil, the goal of cost reduction may not be fully achieved or implemented properly. As known, this type of soil requires original designs and large volumes of reinforcement steel and concrete.

It is also important to select simple drawings, which do not demand additional materials. As for building materials, their selection and purchase require prior knowledge that allows a specialist to choose high-quality and, at the same time, low-cost materials. This can be achieved through effective planning at each stage of construction, which makes it possible to avoid numerous costly changes throughout the structure's life cycle.

Low-cost materials

Due to the economic factors that most countries suffer from, which have also clearly affected the construction industry, a serious search for ways to reduce the cost of construction has started. It should be noted that one of the important factors affecting the final cost of construction is the cost of building materials. It is actually the single most important factor in carrying out a project (Ugochukwu and Chioma, 2015). The cost of materials takes more than one-third of the overall cost of erecting a structure. Thus, the use of low-cost materials can be one the ways to obtain a low-cost building without compromising the desired quality. Based on the source of building materials, Srivastava and Kumar (2018) classified low-cost building materials into natural and man-made ones.

There are several options to obtain low-cost and effective materials: producing low-cost building materials by recycling construction waste, using local building materials, or using energy-efficient materials that consume less energy.

It is common for most countries, especially developing ones, to rely on importing construction materials from other countries. Such materials usually turn out to be quite expensive. Therefore, the use of locally available materials will help to

reduce construction costs since transportation takes approximately 30% of the total construction budget (Chowdhury and Roy, 2013). Furthermore, rather than importing from elsewhere, it is also possible to build a cooperative to supply alternative raw materials and thus save 20–30% of the costs (Srivastava and Kumar, 2018). Moreover, the introduction of technological improvements to local building materials can improve traditional construction techniques in local communities (Bredenoord, 2017). Ideally, low-cost housing should use locally available raw materials. It also would be preferable if those raw materials were abundantly available or renewable in nature (Danso, 2013).

Numerous researchers have investigated the use of natural fibers derived from various plants in building materials. When compared with concrete blocks, fiber cement composites show better properties. This is primarily due to the presence of fibers in them (Moslemi, 2008). Some of those properties include better workability, resistance to cracking, a lighter weight, high fracture toughness, and a greater degree of flexibility, which are quite important in the market. Thus, those materials can be used in low-cost construction. Table 1 shows the performance profiles of some important fibers produced in India, as compiled by Chowdhury and Roy (2013).

Use of environmentally-friendly materials

The majority of resources required to build houses are non-renewable. These issues highlight the necessity to reconsider the promotion of materials that result in lower construction costs and minimal environmental costs (Adegun and Adedeji, 2017). Green building materials are environmentally-friendly, which means that they are characterized by low environmental impact. Potential green building materials should be locally available and composed of renewable resources (Hebatalrahman and Mahmoud, 2016). In their work, Adeniyi et al. (2020) demonstrated that green materials are cost-effective, readily available, energy efficient, adaptable to the environment, eco-friendly, reduce construction costs and waste, improve the economy of the community, promote cultural heritage, enhance social well-being, and reduce carbon dioxide emissions. Moreover, the use of green materials cuts the costs of building a structure to a bare minimum, while also increasing cost-effectiveness and making houses affordable for more people (Ugochukwu and Chioma, 2015). Some researchers agree that the use of green materials provides a cost-effective solution when it comes to affordable housing (Adegun and Adedeji, 2017; Danso, 2013; Shen et al., 2019).

In various countries, such as Zimbabwe, Botswana, Mozambique, South Africa, Egypt, Tanzania, Kenya, and Nigeria, such environmentally-friendly building materials as earthen materials are used. Studies show that earthen materials are relatively clean to produce because the process involves little or no fossil fuel (Atolagbe and Fadamiro, 2005; Elkhalifa, 2011; Henry et al., 2014). In the production of 25 kg of ordinary Portland cement, approximately 2 kg of CO_2 are emitted (which is up to 900 kg per ton) (Browne, 2009). As a result, cement use reduction means lower carbon emissions and embodied energy in housing construction (Adegun & Adedeji, 2017).

Table 1. **Performance profiles of some important fibers produced in India**

Building materials	Properties				
	Structural	Thermal	Temperature and water resistance	Buildability	Cost (in Rs/ square meter)
Bamboo	Works better with moisture in shear forces; has a higher flexibility than steel and a lower Young's modulus.	Excellent	Moderate	Moderate	Depends on thickness
Concrete blocks	Strength may be added as needed; less mortar joint as the size grows, which increases stability	Excellent	Excellent	Excellent	31.25
Ferrocement and aerocon panels	Lightweight, does not require wet plastering (aerocon); high strength, low density, and high mortar crack resistance (ferrocement)	Excellent	Excellent	Excellent	Depends on thickness
Mud blocks (compressed)	Economic and energy efficient	Excellent	Excellent	Excellent	15.625
Straw bales (with bricks)	Stable, high load bearing power	Moderate	Also depends on brick composition as it is mixed with bricks and mud	Moderate	NA

Source: (Chowdhury & Roy, 2013).

According to Srivastava and Kumar (2018), the following environmentally-friendly building material technologies for low-cost housing can be adopted: paint for interior and exterior walls, wall plaster, cement-waste slag brick, lightweight concrete block, decorative concrete block, concrete paving block, lime- sand brick, and concrete hollow block.

Cost-effective construction technologies

To reach the goal of low-cost construction, in addition to the use of low-cost materials, new and advanced construction technologies must be followed without compromising the quality of materials and construction. It was found that cost-effective and alternative construction technologies, in addition to lowering construction costs by reducing the quantity of building materials though improved techniques, can play a significant role in providing better housing as well as protecting the environment. It is worth noting that cost-effective construction technologies do not compromise the security and safety of buildings and generally comply with the applicable building codes (Tam, 2011). Tam (2011) also found that the use of low-cost housing technologies instead of traditional construction methods for walling and roofing can save approximately 26.11% and 22.68% of the construction cost, respectively, including material and labor costs.

Precast concrete technology is an example of advanced construction technology. It is one of the technologies used in low-cost construction (Adabre et al., 2020). It is also one of the only to combine a whole range of benefits. Precast concrete technology is also a proven solution like rapid construction and mass production.

Although bricks remain the backbone of the building industry, the quantity of blocks that are broken into different sizes to fit into position at site is very large, which results in material waste. Increased wall block size will be more cost-effective due to faster construction and less mortar consumption, which can be achieved by producing low-density larger-size wall blocks from industrial wastes such as blast furnace slag and fly ash (Srivastava and Kumar, 2018).

To design buildings that meet the requirements of technical standards at the lowest possible cost, many researchers have sought to evaluate the application of construction technologies. In this section of the paper, we review a number of technologies currently applied, which make it possible to reduce the total cost of construction.

There are various construction techniques, which can be used for affordable housing (Kshirsagar et al., 2018), such as:

- On a terraced site, it is less expensive to build a house in the middle of the terrace.
- If a building is placed parallel to the contours rather than crossing them on a sloped site, less excavation and filling up will be required.

Among other techniques, the following, investigated by Manoj and Mohd (2016), can be mentioned:

- Rat-trap bond technology: This masonry technique uses bricks to create a cavity within the wall while maintaining the same wall thickness as for a conventional brick masonry wall. Because of the cavity formed in the wall, the main advantage of rat-trap bond is reduction in the number of bricks and mortar as compared to English/Flemish bond.
- Solid concrete and stone blocks: Walls can be built using modern methods that combine solid blocks with both lean concrete and stones.
- Filler slab technology: Part of concrete in a conventional reinforced cement concrete slab is replaced with a filler material, which can be waste material, to provide an economical advantage over an RCC slab.

It is worth mentioning through the proper management of resources, which contributes to reducing waste of various materials, it is possible to obtain a low-cost building. Besides, developing an effective plan to determine project's requirements corresponding to actual conditions makes it possible to avoid a lot of risks leading to continuous losses during building operation. For instance, it is suggested not to use wood for doors and windows. Instead, concrete or steel section frames shall be used to reduce costs by up to 30–40%. It is also suggested to use burnt bricks, which are immersed in water for 24 hours and then shall be used for the walls.

Use of alternative available construction methods

Low-cost housing can be implemented by the application of particular techniques and effective planning reducing the construction budget thanks to the use of locally available materials and economical construction technologies without compromising the structure's performance, strength, and service life. Profits from the use of such methods can decrease construction costs and make low-cost housing available to all (The Constructor, 2015).

3D printing is a computer-controlled manufacturing technique used to construct a product in layers from a CAD model or a digital 3D model (Varun Raj et al., 2021). By detecting and eliminating errors early in the design process, it is possible to reduce the costs associated with incorrect design (Varun Raj et al., 2021). Han et al. (2021) found that 3D printed concrete requires a larger amount of cement than cast-in-situ construction. However, they also concluded that 3D printed concrete is more cost-effective since it helps to reduce the cost of heavy formwork and labor (Han et al. 2021). Varun Raj et al. (2021) stated that such building components as windows, doors, etc. can be produced quickly and economically with technology in the future.

Haselau (2013) summarized five alternative construction methods, which can be used to erect low-cost buildings. They include: Moladi housing technology, speedwall building systems, hydraform interlocking bricks, modular and timber construction, and straw bale construction, as shown in Table 2.

Sustainable community through involvement and training

To provide low-cost housing, local communities can be engaged, educated, and trained since exchange of knowledge and technology plays an important role in the development of various economic sectors. Bredenoord (2017) proved that using local workforce and involving local residents in housing construction is beneficial for developing the communities. Local residents, craftspeople, and businesses can all be involved in procuring raw materials and their processing into ready-to-use building materials. This way, local residents can reduce their housing costs, which is the underlying goal of self-help housing and self-reliance (Bredenoord and van Lindert, 2014).

When local residents participate in housing construction as much as possible and gain knowledge and skills, we can talk about long-term socioeconomic development. There are, however, some excellent examples of corporate involvement in housing construction. For instance, a Mexican cement company developed a social aid program (Patrimonio Hoy) that provides self-builders with building materials and technical assistance as well as credit for home renovations (Bredenoord, 2017; CEMEX, 2023). Another example is a cement company in Malawi and other East African countries that provides durable soil and cement construction solutions for affordable housing, such as earth brick production, soil analysis and mix design training, and project technical assistance. The product is called Stabilized Compressed Earth Bricks (Bredenoord, 2017). The municipal training program 'Escuela Taller' in León, Nicaragua, among other things, provides young people with opportunities to learn basic carpentry, masonry, electricity, and welding. Practical training is provided in inner city renovation projects that restore traditional style housing.

Conclusions

Given the increasing population growth around the world, the future focus on providing low-cost buildings will be a challenge for most countries. Therefore, it is necessary to search for techniques, materials, methods and strategies that would provide buildings at a low cost. In this paper, we have presented the findings of previous studies addressing low-cost construction methods. The results show that it is possible to provide low-cost dwelling through the use of effective planning and project management, low-cost materials, cost-effective construction technologies, and the use of alternative available construction methods. Recent advancements gave a boost to many new materials and technologies, which can significantly reduce the cost of construction. It should be noted that it is not necessary to use low-cost materials and technologies to obtain low-cost buildings. The use

Table 2. **Summary of alternative construction methods**

Alternative construction method	Description	Construction cost reduction
Moladi housing technology	Moladi technology involves easy-to-use plastic panels joined to create plastic structures/forms of any length and height for various walls in a building.	It is 50% cheaper than ordinary brick wall methods.
Speedwall building systems	Speedwall construction technology uses a mobile panel manufacturing machine to manufacture the floor, wall, and roof panels on site.	Speedwall structures are characterized by high energy efficiency reducing energy costs, which is an advantage for low-cost homes.
Hydraform interlocking bricks	Hydraform blocks are used in strip footing foundations, eliminating the use of mortar in 70% of the building structure with no need for concrete or steel columns.	Hydraform machines are perfect for remote sites with high transportation, cement and sand costs since the dry-stacking technique ensures savings (by 30%) in time and construction costs.
Modular and timber construction	Timber homes were reintroduced as an alternative to traditional brick and mortar dwellings.	In comparison to bricks, blocks, and concrete, which have an embodied energy of 80%, and steel, which has an embodied energy of 95%, manufactured timber components have an embodied energy of 14%.
Straw bale construction	Straw bale structures represent a low-cost alternative for building highly insulating walls by constructing a frame (usually out of wood) and stacking straw bales as if they were cement bricks to create walls.	This technique can save up to 50% of the cost of traditional wall materials.

of sustainable materials, which consume less energy, significantly reduces the cost of buildings and their maintenance. Besides, the quality of construction is not compromised. We argue that it is important to use environmentally-friendly materials, which contribute to the sustainability of buildings and reduce energy consumption. In addition, governments should encourage the use of local materials and workforce to enable them to compete with imported materials. Governments can also develop training programs to prepare the local workforce and involve them in construction, which in the end will be less costly. The study will help other researchers investigate the obstacles that developing countries face when adopting low-cost construction technologies.

References

Adabre, M. A., Chan, A. P. C., Darko, A., Osei-Kyei, R., Abidoye, R., and Adjei-Kumi, T. (2020). Critical barriers to sustainability attainment in affordable housing: International construction professionals' perspective. *Journal of Cleaner Production*, Vol. 253, 119995. DOI: 10.1016/j.jclepro.2020.119995.

Adegun, O. B. and Adedeji, Y. M. D. (2017). Review of economic and environmental benefits of earthen materials for housing in Africa. *Frontiers of Architectural Research*, Vol. 6, Issue 4, pp. 519–528. DOI: 10.1016/j.foar.2017.08.003.

Adeniyi, S. M., Mohamed, S. F., and Rasak, K. O. (2020). Socio-economic benefits of using green materials for the construction of low-cost buildings in Nigeria. *American Academic Scientific Research Journal for Engineering, Technology, and Sciences*, Vol 67, No. 1, pp. 99–108.

Atolagbe, A. M. O. and Fadamiro, J. A. (2005). Energy policy for building materials technology: a global imperative for sustainable architecture. *Elektro Mesin Arsitektur Sipil (EMAS) Jurnal Sains Dan Teknologi*, Vol. 15, Issue 3, pp. 45–57.

Bredenoord, J. (2017). Sustainable building materials for low-cost housing and the challenges facing their technological developments: examples and lessons regarding bamboo, earth-block technologies, building blocks of recycled materials, and improved concrete panels. *Journal of Architectural Engineering Technology*, Vol. 6, Issue 1, 187. DOI: 10.4172/2168-9717.1000187.

Bredenoord, J. and van Lindert, P. (2014). Backing the self-builders: assisted self-help housing as a sustainable housing provision strategy. In: Bredenoord, J., van Lindert, P., and Smets, P. (eds.). *Affordable Housing in the Urban Global South*. London and New York: Routledge, pp. 81–98. DOI: 10.4324/9781315849539-16.

Browne, G. (2009). Stabilised interlocking rammed earth blocks: alternatives to cement stabilisation. In: *11th International Conference on Non-Conventional Materials and Technologies (NOCMAT, 2009)*, September 6–9, 2009, Bath University, pp. 25–26.

CEMEX (2023). *Patrimonio Hoy*. [online] Available at: https://www.cemexmexico.com/sostenibilidad/vivienda/patrimonio-hoy [12 December 2022].

Chowdhury S. and Roy S. (2013). Prospects of low cost housing in India. *Geomaterials*, Vol. 3, No. 2, 30868. DOI: 10.4236/gm.2013.32008.

Danso, H. (2013). Building houses with locally available materials in Ghana: benefits and problems. *International Journal of Science and Technology*, Vol. 2, No. 2, pp. 225–231.

Elkhalifa, A. A. (2011). *The construction and building materials industries for sustainable development in developing countries. Appropriate and innovative local building materials and technologies for housing in the Sudan*. DSc Thesis in Architecture and Design, 412 p.

Han, Y., Yang, Z., Ding, T., and Xiao, J. (2021). Environmental and economic assessment on 3D printed buildings with recycled concrete. *Journal of Cleaner Production*, Vol. 278, 123884. DOI: 10.1016/j.jclepro.2020.123884.

Haselau, J. (2013). *Alternative construction methods for low-cost housing in South Africa*. [online] Available at: https://icoste.org/wp-content/uploads/2012/09/ASAQS-Paper-1-Haselau.pdf [24 November 2022].

Hebatalrahman, A. and Mahmoud, M. (2016). Green building material requirements and selection (a case study on a HBRC building in Egypt). In: *6th International Engineering and Construction Conference (IECC'6)*, June 28–30, 2010, Cairo, Egypt, pp. 80–91.

Henry, A. F., Elambo, N. G., Tah, J. H. M., Fabrice, O. E. N., and Blanche, M. M. (2014). Embodied energy and CO2 analyses of mud-brick and cement-block houses. *AIMS Energy*, Vol. 2, Issue 1, pp. 18–40. DOI: 10.3934/energy.2014.1.18.

Kshirsagar, S., Patil, J., Chaudhari, S., and Kumbhar, S. (2018). Affordable housing materials and techniques. *International Journal of Scientific Research in Science, Engineering and Technology*, Vol. 4, Issue 1, pp. 999–1011.

Manoj, K. and Mohd, A. (2016). An overview: low cost house materials & techniques. RIET-*IJSET International Journal of Science Engineering and Technology*, Vol. 3, No. 2, 97. DOI: 10.5958/2395-3381.2016.00012.5.

Moslemi, A. (2008). Technology and market considerations for fiber cement composites. In: *11th International Inorganic-Bonded Fiber Composites Conference*, November 5–7, 2008, Madrid, Spain, pp. 113–129.

Oliveira, M., Couto, J. P., Mendonça, P., Branco, J., Silva, M., and Reis, A. P. (2013). Low cost construction: state of the art and prospects for using structure wood apartment buildings in Portugal. In: *Structures and Architecture: Concepts, Applications and Challenges*. London: Taylor & Francis Group, pp. 2168–2175.

Osman, M. M., Ramlee, M. A., Samsudin, N., Rabe, N. S., Abdullah, M. F., and Khalid, N. (2017). Housing affordability in the state of Johor. *Planning Malaysia*, Vol. 15, Issue 1, pp. 347–356. DOI: 10.21837/pm.v15i1.251.

Shen, L., Yang, J., Zhang, R., Shao, C., and Song, X. (2019). The benefits and barriers for promoting bamboo as a green building material in China—An integrative analysis. *Sustainability*, Vol. 11, Issue 9, 2493. DOI: 10.3390/su11092493.

Srivastava, M. and Kumar, V. (2018). The methods of using low cost housing techniques in India. *Journal of Building Engineering*, Vol. 15, pp. 102–108. DOI: 10.1016/j.jobe.2017.11.001.

Tam, V. W. Y. (2011). Cost effectiveness of using low cost housing technologies in construction. *Procedia Engineering*, Vol. 14, pp. 156–160. DOI: 10.1016/j.proeng.2011.07.018.

The Constructor (2015). *Building materials for low-cost housing construction*. [online] Available at: https://theconstructor.org/building/low-cost-building-materials/5352/#:~:text=Natural%20fiber%20materials%20are%20coming,are%20made%20from%20natural%20fibers [24 November 2022].

Tiwari, P., Parikh, K., and Parikh, J. (1999). Structural design considerations in house builders' model: optimization approach. *Journal of Infrastructure System*, Vol. 5, Issue 3, pp. 75–90. DOI: 10.1061/(ASCE)1076-0342(1999)5:3(102).

Ugochukwu, I. B. and Chioma, M. I. B. (2015). Local building materials: affordable strategy for housing the urban poor in Nigeria. *Procedia Engineering*, Vol. 118, pp. 42–49. DOI: 10.1016/j.proeng.2015.08.402.

Varun Raj, P., Surya Teja, P., Sai Siddhartha, K., Kalyana Rama, J. S. (2021). Housing with low-cost materials and techniques for a sustainable construction in India-A review. *Materials Today: Proceedings*, Vol. 43, Part 2, pp. 1850–1855. DOI: 10.1016/j.matpr.2020.10.816.

DOI: 10.23968/2500-0055-2023-8-1-51-59

SIMULATION OF WATER FLOW IN A CAVITATION REACTOR

Andrey Belyaev[1], Aleksey Aleshkin[1], Elena Kuts*[2], Vladimir Shabalin[2]

[1]Vyatka State University, Kirov, Russia

[2]Saint Petersburg State University of Architecture and Civil Engineering
Saint Petersburg, Russia

*Corresponding author's e-mail: kouts@yandex.ru

Abstract
Introduction: Searching for methods to improve the efficiency of water treatment with reagents is quite important in both water conditioning and industrial wastewater purification. Among the technologies providing high efficiency and reducing resource consumption in combination with reagent methods, hydrodynamic cavitation water treatment is of particular interest. The analysis of scientific and technical data made it possible to determine the main indicators of hydrodynamic cavitation water treatment that can affect the efficiency of reagent purification. Extreme parameters occurring during intense cavitation are associated with the formation of high temperatures up to 2000°C and high pulse pressures of 100–1500 MPa in local areas of hydrodynamic systems. In such conditions, the initiation and intensification of the physical and chemical processes of water treatment are observed. **Purpose of the study:** Improving the efficiency of existing traditional water purification technologies, allowing to improve its quality at the lowest cost. **Methods:** To study the parameters affecting water treatment efficiency and occurring with the cavitation flow of water, simulation in Ansys CFX was performed with the use of the finite volume method. The calculation was carried out with account for the turbulent nature of the flow based on the k-ε turbulence model. The cavitation process was calculated with the use of the Rayleigh-Plesset cavitation model. **Results:** Steam formation in the cavitation reactor promotes sufficiently complete absorption of the gaseous disinfectant by water. An increase in temperature is also considered as one of the factors increasing the efficiency of water treatment with reagents. During cavitation, water temperature increases in local micro-volumes. Thus, to intensify the process, there is no need to heat the entire volume of liquid, and, as a result, the total energy consumption for water treatment is reduced.

Keywords: cavitation reactor, cavitation parameters, water treatment processes, simulation.

Introduction

Since clean water is becoming one of the most valuable and expensive natural resources, great attention has been recently paid to the issues of drinking water treatment and industrial wastewater treatment. The current trends are moving in the direction of tightening regulatory requirements for the quality of water used for various purposes. That is why specialists focus on enhancing the efficiency of the existing traditional water purification technologies, which will make it possible to improve water quality in the least-cost manner.

To achieve those goals, in terms of environmental, process, and operational advantages, the use of physical methods seems the most appropriate. To increase the efficiency of processes and, as a consequence, reduce operating costs, it is required to develop and utilize efficient devices characterized by relatively low energy and material consumption and ensuring intensive impact on the treated medium. The development of devices providing energy impact on the treated media due to the pulsed flow conditions is one of the promising technical directions in purification intensification. Such devices include hydrodynamic cavitation reactors where the intensification of processes is provided by special flow conditions with mechanical and acoustic effects (Carpenter et al., 2017; Holkar et al., 2019; Pandit et al., 2021; Patil et al., 2021).

Extreme parameters occurring during intense cavitation are associated with the formation of high temperatures up to 2000°C and high pulse pressures of 100–1500 MPa in local areas of hydrodynamic systems (Belyaev and Flegentov, 2014; Chandra et al., 2019). In such conditions, the initiation and intensification of the physical and chemical processes of water treatment are observed. The authors conducted numerous experimental studies confirming the possibility of intensifying water treatment with reagents by applying hydraulic cavitation in a flow reactor. Those studies were carried out both during water conditioning and wastewater treatment (water disinfection by ozonation and chlorination (Belyaev and Flegentov, 2014); silica removal from water with magnesium oxide (Gimranov et al., 2014b), swimming pool water disinfection (Lysov et al., 2016), removal of phenol and petroleum products (Kuts, 2003), ammonium compounds from water (Gimranov et al., 2013)).

The technology for removal of organic compounds from water with simultaneous water disinfection can be improved by intensifying the mixing of disinfectant

(ozone, chlorine) with treated water through the use of hydrodynamic cavitation (Belyaev and Flegentov, 2014; Belyaev et al., 2012; Fleguentov et al., 1997; Gogate et al., 2014). This technology can improve the quality of water treatment at water treatment facilities and in industrial wastewater treatment systems of chemical and machine-building enterprises, thermal power and other plants. Intensification of mixing two-phase flows by hydrodynamic cavitation can also be used to reduce disinfectant consumption when introducing it into the treated water at water purification plants (Belyaev et al., 2012).

The use of underground water sources for the needs of heat and power facilities as well as chemical and pharmaceutical, pulp and paper industry often requires silicon compounds to be removed from water in water conditioning (Huuha et al., 2010). Therefore, the search for ways to upgrade the existing technologies of silica removal from water and improve the efficiency of treatment with reagents in the applied technologies remains quite urgent. The authors also studied intensification of the process of silica removal from water of underground sources by its additional exposure to hydrodynamic cavitation in a flow reactor (Belyaev et al., 2019). It was established that the rate of silica removal from water using magnesium oxide with additional cavitation treatment increases by 17.1%.

The authors also studied the use of hydrodynamic cavitation to intensify swimming pool water purification (Gimranov et al., 2014a; Lysov et al., 2016). The possibility of obtaining aqueous suspensions of metals with oligodynamic effect by cavitation erosion was considered. The sizes of silver and copper particles formed during cavitation treatment in a hydrodynamic flow unit of original design were experimentally evaluated using a scanning microscope.

Subject and methods

We aimed to study the parameters occurring with the cavitation flow of water and affecting the efficiency of water conditioning and purification.

To do that, we considered the flow of water in a cavitation reactor, the parameters of which were proposed in the patent by Belyaev and Flegentov (2012) (Fig. 1). The flow of water in the unit was determined in Ansys CFX (Abdulin et al., 2011) with the use of the finite volume method (Zamankhan, 2015).

The calculation was carried out with account for the turbulent nature of the flow based on the k–ε turbulence model (Ranade, 2022). The cavitation process was calculated with the use of the Rayleigh-Plesset cavitation model (Hilgenfeldt et al., 1998). The differential equation serving as the basis of this model takes the following form:

$$R\frac{d^2R}{dt^2}+\frac{2}{3}\left(\frac{dR}{dt}\right)^2+\frac{2\sigma}{\rho R}=\frac{p_S-p}{\rho}, \qquad (1)$$

where R — the radius of a steam bubble formed during cavitation, m; t — time, s; σ — the coefficient of surface tension in a steam bubble at the liquid boundary, N/m; ρ — liquid density, kg/m^3; p_s — pressure of saturated vapors, Pa, (assumed to be equal to p_S = 3169 Pa); p — absolute pressure in the flow point, Pa.

In the model put in Ansys CFX, an approximate solution of Eq. (1) is used to determine the rate of steam bubble formation and collapse depending on the pressure difference in the right part. The average diameter of a steam bubble, taken as nominal, was assumed to be equal to $2\cdot10^{-6}$ m (Rooze, 2012).

In each finite volume, it was assumed possible to find water and steam parameters at the same time, the proportions between which depend on the rate of vaporization, while water enters the reactor as a liquid.

Figs. 2 and 3 show the division into finite volumes. The number of division elements was m = 114061, and the number of nodes was n = 231263.

Along the solid walls, no-slip conditions and mesh refinement in the boundary layer were set. The number of boundary layers was 5, the element height in the boundary layer did not exceed 1 mm. A uniform velocity field was set at the inlet to the cavitation reactor, and zero relative pressure was set at the outlet from the cavitation reactor (Fig. 4). The calculation was performed at two water flow velocity modes at the inlet: at 15 and 23 m/s. The studies were carried out with a reactor previously used in other works (Belyaev and Flegentov, 2014; Belyaev et al., 2012; Fleguentov et al., 1997; Gimranov et al., 2013, 2014a, 2014b; Kuts, 2003), with parameters as per Fig. 1: H = h = D = 10 mm, b = 20 mm.

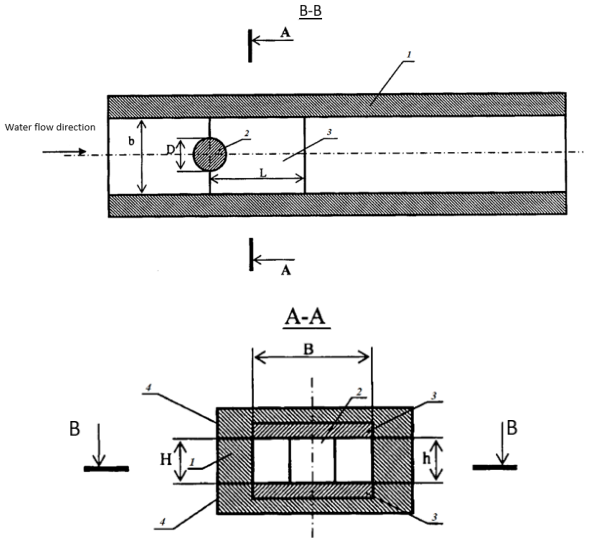

Fig. 1. Scheme of the cavitation reactor according to patent RU 2445272: 1 — walls of the reactor channel; 2 — a cylindrical cavitation exciter; 3 — metal substrates; 4 — a reactor vessel; H and D — height and diameter of the cavitation exciter, respectively; h and b — height and width of the cavitation channel, respectively; L — length of the metal substrate

Results and discussion

At the first stage of the calculations, we studied the flow of water without cavitation effect. Then the calculation results were set as initial conditions for the flow with account for cavitation.

As a result of the calculations, absolute pressure distribution fields were obtained, shown in Figs. 5 and 6.

It can be seen from the pressure distribution fields that pressure does not drop below the boiling point of water. The highest values p = 1.291 MPa (Fig. 5) and p = 0.5524 MPa (Fig. 6) are reached in front of the cylinder, and as the flow flows around, they drop to the boiling point p = 3169 Pa.

Figs. 7 and 8 show distribution of the volume fractions of steam in the flow.

Figs. 9 and 10 show distribution of the volume fractions of steam in the longitudinal section passing through the axis of the cylinder. The study of this parameter showed that boiling is more intense on the back side of the cylinder and at the channel walls behind it, which are parallel to the bases. It is expedient to install substrates with active materials for chemical reactions in these zones.

Figs. 11, 12, 13, and 14 show distribution of steam bubble and water velocities in the cavitation area.

Figs. 15–22 show distribution of the calculated values of steam and water temperature in the corresponding longitudinal sections of the reactor.

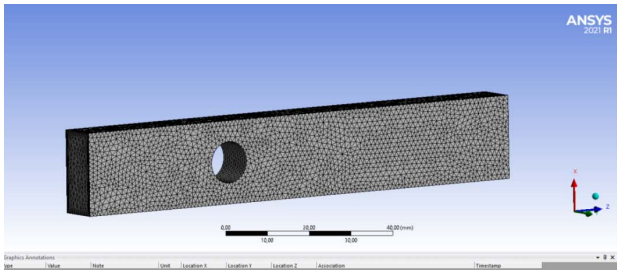

Fig. 2. Scheme of division into finite volumes

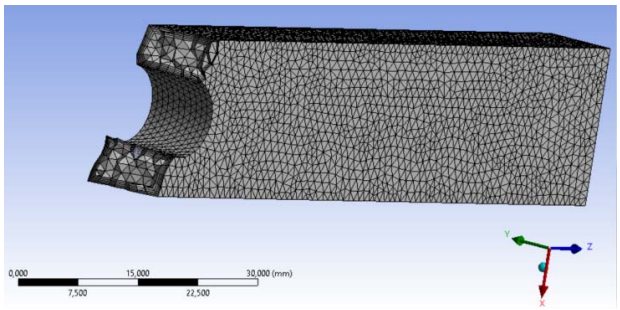

Fig. 3. Cross-section of the mesh model for visualization of the boundary layer

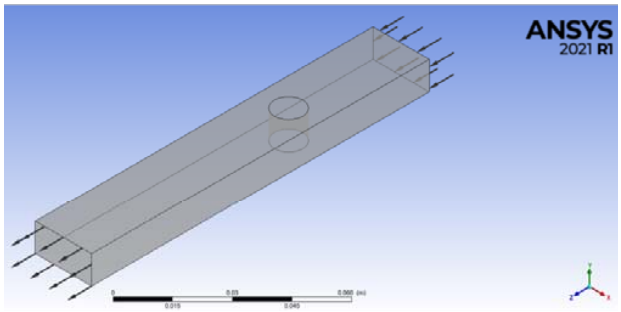

Fig. 4. Boundary conditions

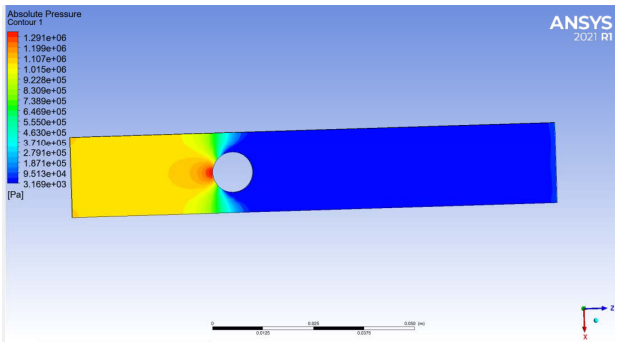

Fig. 5. Absolute pressure distribution in the axial section of the cavitation reactor, perpendicular to the axis of the cylinder at a water velocity at the inlet of 23 m/s

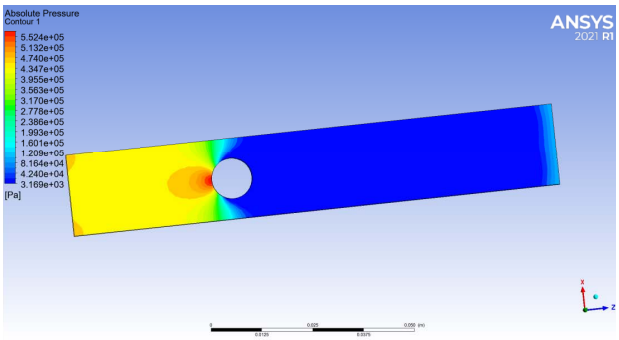

Fig. 6. Absolute pressure distribution in the axial section of the cavitation reactor, perpendicular to the axis of the cylinder at a water velocity at the inlet of 15 m/s

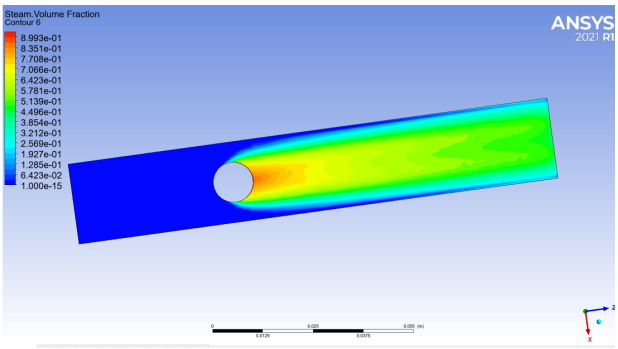

Fig. 7. Steam volume fraction distribution in the axial section of the cavitation reactor, perpendicular to the axis of the cylinder at a water velocity at the inlet of 23 m/s

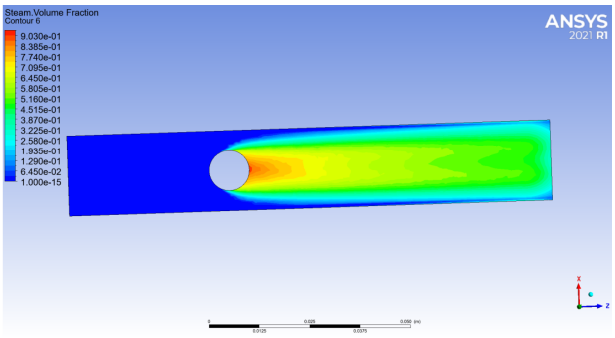

Fig. 8. Steam volume fraction distribution in the axial section of the cavitation reactor, perpendicular to the axis of the cylinder at a water velocity at the inlet of 15 m/s

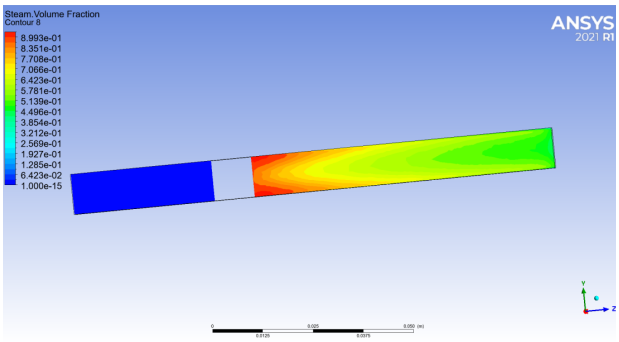

Fig. 9. Steam volume fraction distribution in the axial section of the cavitation reactor, passing through the axis of the cylinder at a water velocity at the inlet of 23 m/s

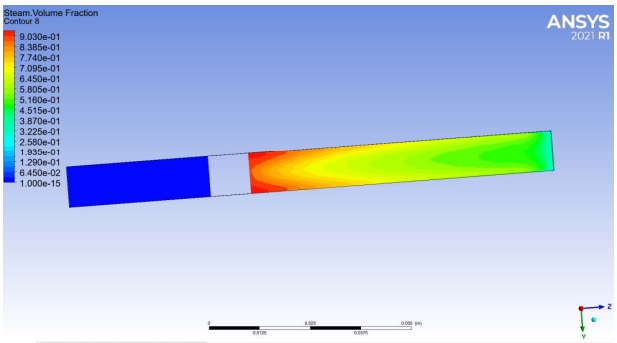

Fig. 10. Steam volume fraction distribution in the axial section of the cavitation reactor, passing through the axis of the cylinder at a water velocity at the inlet of 15 m/s

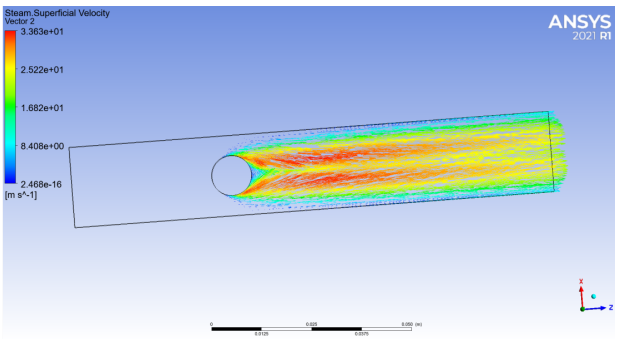

Fig. 11. Steam bubble velocity distribution in the axial section of the cavitation reactor, perpendicular to the axis of the cylinder at a water velocity at the inlet of 23 m/s

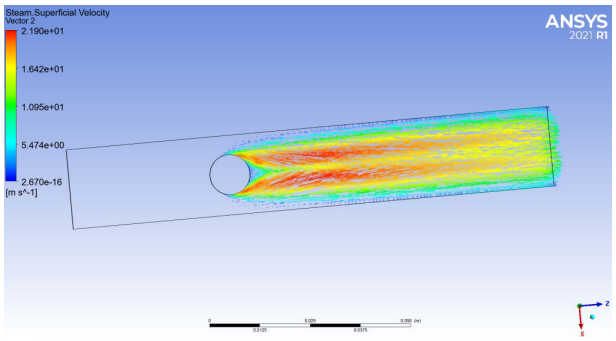

Fig. 12. Steam bubble velocity distribution in the axial section of the cavitation reactor, perpendicular to the axis of the cylinder at a water velocity at the inlet of 15 m/s

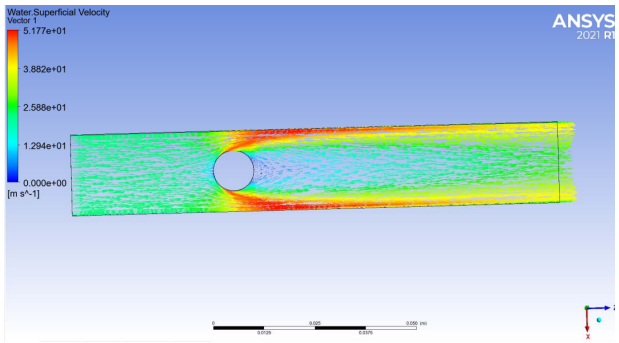

Fig. 13. Water velocity distribution in the axial section of the cavitation reactor, perpendicular to the axis of the cylinder at a water velocity at the inlet of 23 m/s

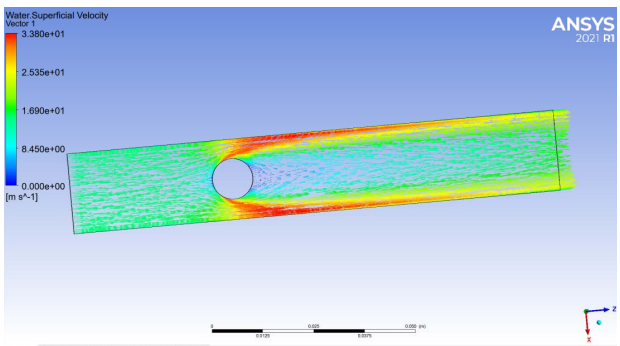

Fig. 14. Water velocity distribution in the axial section of the cavitation reactor, perpendicular to the axis of the cylinder at a water velocity at the inlet of 15 m/s

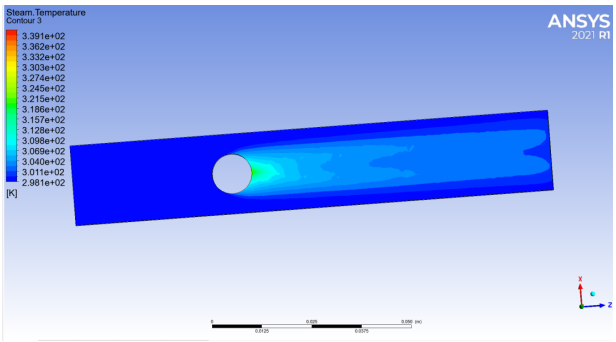

Fig. 15. Steam temperature distribution in the axial section of the cavitation reactor, perpendicular to the axis of the cylinder at a water velocity at the inlet of 23 m/s

Let us take a look at a three-dimensional image of elements with a steam volume fraction of more than 0.7 (Figs. 23, 24)

With an increase in the input flow rate from 15 to 23 m/s, an increase in the length of the steam bubble plume is observed. Besides, there is a slight increase in the temperature of water in the flow when the absolute pressure required to create a velocity of 23 m/s is doubled.

The obtained results allow us to see the data obtained during field studies (conducted earlier with the use of the same cavitation reactor design) in the new light. For instance, in experiments to obtain aqueous suspension of silver (Gimranov et al., 2014a). Fig. 25 shows the surface of a silver substrate located at the base of the cavitation exciter.

On the left, we can see a plume of half of the base of the cylindrical exciter with a diameter of D = 8 mm; in the center, above and below, we can see clear outlines of an erosive plume from the cavitation torch, flowing around the exciter at a flow rate in the channel of 23 m/s. By comparing the sizes of this plume and distribution of the steam volume fraction in the axial section of the cavitation reactor, shown in Figs. 9 and 10, we can see a clear correspondence between the sizes of the red/orange zone (see Figs. 9–10) in the lower part of the channel and cavitation deformations observed at a distance up to 3D.

A more detailed study of erosive surfaces in the areas of initial deformation with the use of a JSM-6510 LV electronic scanning microscope (JEOL, Japan) with 500x magnification (Fig. 26) shows the presence of mechanical deformations caused by the separation of silver microparticles under the influence of water micro-jets due to the collapse of cavitation steam bubbles (Gimranov et al., 2014a). The thermal nature of the deformations in the image shall be ruled out with a high probability because of the absence of particular characteristic features.

The low effect of the temperature component on the cavitation deformations of the silver substrate is confirmed by images of temperature fields in the cavitation reactor, shown in Figs. 21 and 22. Here we can see the temperature dynamics in the cavitation zone at maximum deviation values of 43.6°C and maximum absolute value of 65.2°C, which is not sufficient for thermal deformations on the surface of the silver substrate. However, such dynamics causes changes in the cavitation conditions of the liquid flow in the reactor channel and contributes to the formation of cavitation cavities collapsing with an increase in pressure with the formation of micro-jets, thus facilitating the formation of erosive deformations.

In other studies on silica removal from water with magnesium oxide (Belyaev and Flegentov, 2014; Belyaev et al., 2019; Gimranov et al., 2014b) conducted with the use of the same cavitation reactor design (Belyaev and Flegentov, 2012), the

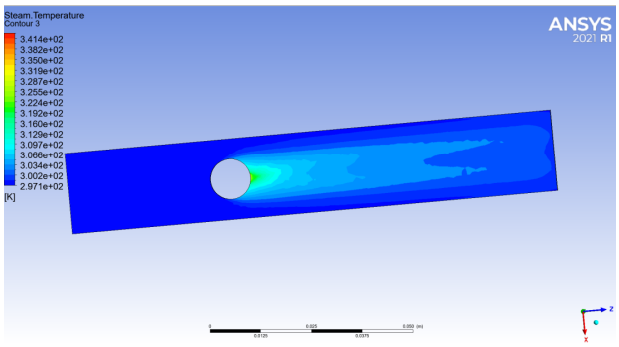

Fig. 16. Steam temperature distribution in the axial section of the cavitation reactor, perpendicular to the axis of the cylinder at a water velocity at the inlet of 15 m/s

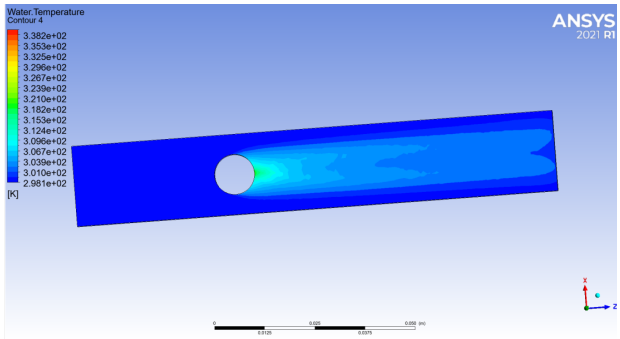

Fig. 17. Water temperature distribution in the axial section of the cavitation reactor, perpendicular to the axis of the cylinder at a water velocity at the inlet of 23 m/s

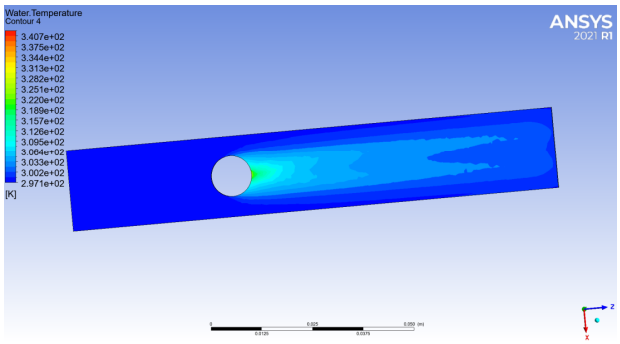

Fig. 18. Water temperature distribution in the axial section of the cavitation reactor, perpendicular to the axis of the cylinder at a water velocity at the inlet of 15 m/s

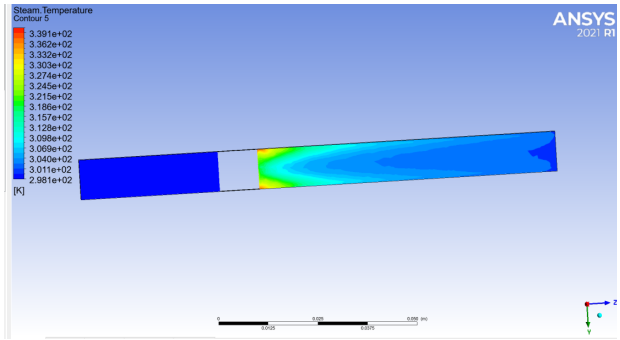

Fig. 19. Steam temperature distribution in the section of the cavitation reactor, passing through the axis of the cylinder at a water velocity at the inlet of 23 m/s

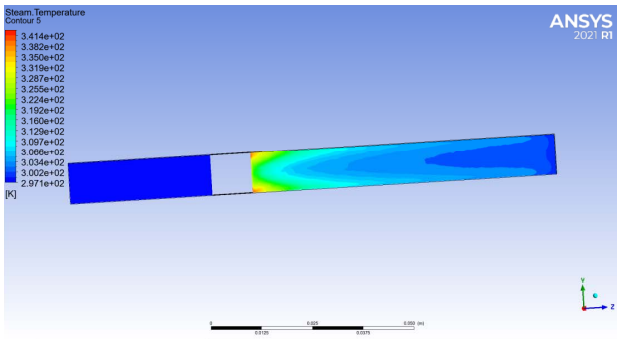

Fig. 20. Steam temperature distribution in the section of the cavitation reactor, passing through the axis of the cylinder at a water velocity at the inlet of 15 m/s

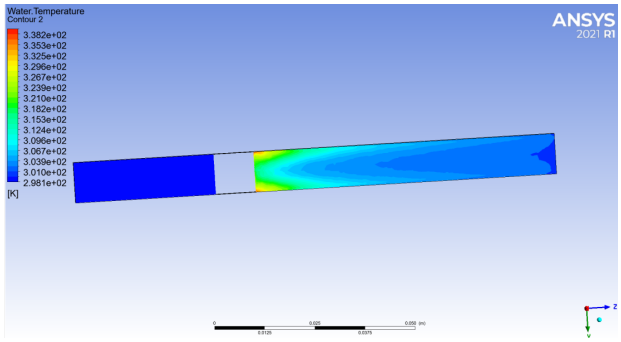

Fig. 21. Water temperature distribution in the section of the cavitation reactor, passing through the axis of the cylinder at a water velocity at the inlet of 23 m/s

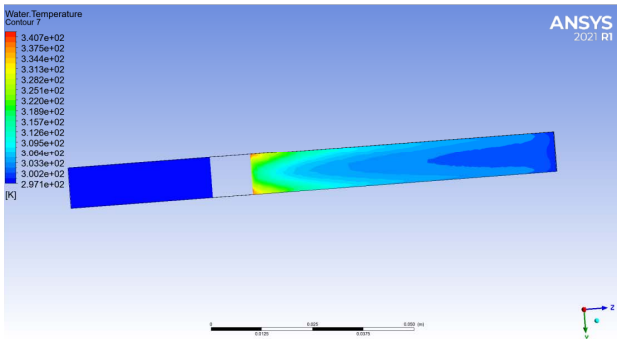

Fig. 22. Water temperature distribution in the section of the cavitation reactor, passing through the axis of the cylinder at a water velocity at the inlet of 15 m/s.

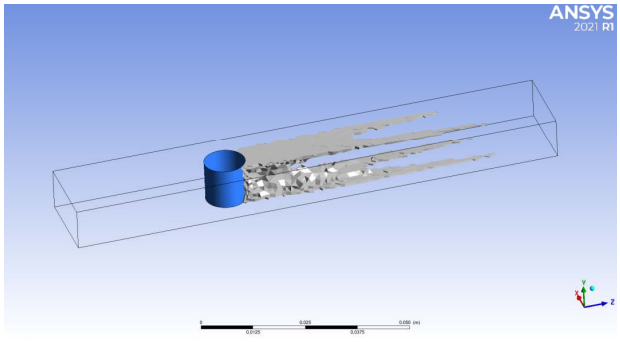

Fig. 23. Distribution of elements with a steam volume fraction of more than 0.7 in the cavitation reactor at a water velocity at the inlet of 23 m/s

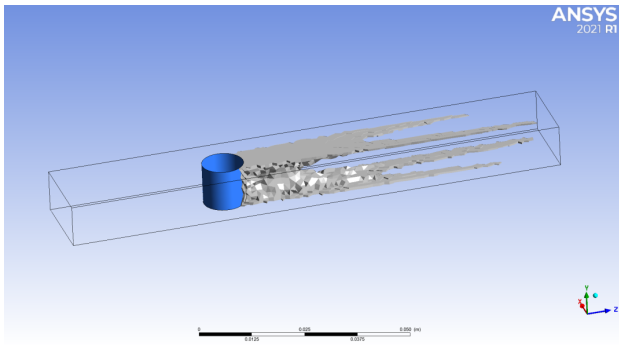

Fig. 24. Distribution of elements with a steam volume fraction of more than 0.7 in the cavitation reactor at a water velocity at the inlet of 15 m/s

Fig. 25. Silver substrate with traces of cavitation erosion

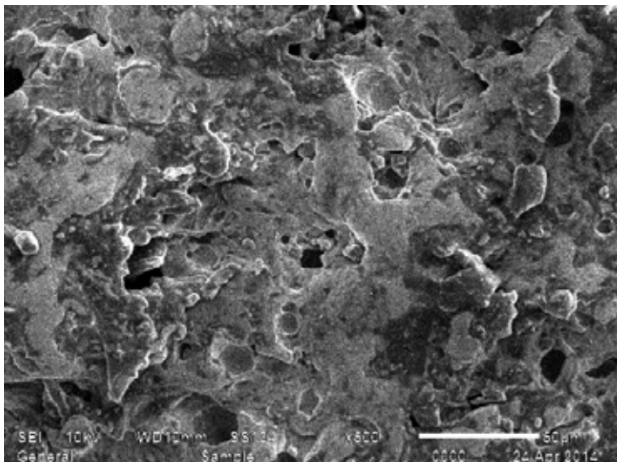

Fig. 26. Photo of the cavitation zone of the silver substrate at 500x magnification

temperature component had to play a key role in reaction intensification. In the course of the studies, the linear dependence between the changes in the rate of heating dynamics and the duration of treatment, expressed by the number of cycles, was determined. As a result, the dynamics of water heating per one cycle did not exceed 2.9°C at an initial temperature of 15°C (Belyaev and Flegentov, 2014). Its low values caused the need for multi-cycle treatment to obtain the required parameters necessary for efficient

reactions during silica removal from water with magnesium oxide. This fact is also confirmed by the built model, which indicates the possibility of its use when applying cavitation in practice.

Conclusions

1. In the course of the study, we analyzed the parameters occurring with the cavitation flow of water and affecting the efficiency of water conditioning and purification. It was established that it is expedient to install substrates with active materials for chemical reactions on the back side of the cylindrical exciter and at the walls of the channel behind it, parallel to its bases, since intense boiling occurs in those very areas. The length of the zone is 7...9 cylinder diameters at water velocities at the inlet to the cavitation reactor of 15...23 m/s.

2. It is expedient to introduce liquid or gaseous reagents directly into the cavitation zone where pressure drop is the highest.

3. The resistance of the cavitation reactor increases significantly from 0.4 to 1.1 MPa with an increase in water velocity at the inlet from 15 m/s to 23 m/s, but the cavitation zone increases to a lesser extent, therefore, the rational value of velocity at the inlet is 15 ...18 m/s.

4. The increase in the flow temperature is most manifested in the section of the channel along the axis of the cylinder and along the walls parallel to its bases. The maximum value of 67°C is observed at the boundary of the back edge of the cavitation exciter and the side walls of the channel (at a water temperature at the inlet to the cavitator of 24°C)

5. In a cavitation reactor, the treated water flow passes through a zone with fast changes in velocities and pressures as well as fast formation and collapse of vapor/gas microspheres, which has a synergistic effect in water treatment technologies.

Thus, the use of highly intense cavitation in hydrodynamic flow units intensifies the physical and chemical processes of water purification and can be used in technologies of water treatment with reagents.

References

Abdulin, A. Y., Proskurina, N. B., Senyushkin, N. S., and Yamaliev, R. R. (2011). Estimation of program complex ANSYS CFX for calculation of centrifugal compressors usage possibility. *Bulletin of Voronezh State Technical University*, Vol. 7, No. 3, pp. 215–219.

Belyaev, A. N., Degterev, B. I., and Kuts, E. V. (2019). Improving efficiency of silica removal from water using magnesium oxide. *Water and Ecology*, No. 1 (77), pp. 10–16. DOI: 10.23968/2305-3488.2019.24.1.10-16.

Belyaev, A. N. and Flegentov, I. V. (2012). *Method of decontaminating water with synergetic action. Patent RU2445272C1*.

Belyaev, A. N. and Flegentov, I. V. (2014). Hydrodynamic cavitation treatment as a tool for intensification of reagent processes in commercial technologies. *Russian Journal of Applied Chemistry*, Vol. 87, Issue 8, pp. 1077−1084. DOI: 10.1134/S1070427214080126.

Belyaev, A. N., Flegentov, I. V., and Suslov, A. S. (2012). Evaluating the effectiveness of the use of hydrodynamic cavitation in the chlorination of water. *Global Scientific Potential*, No. 4 (13), pp. 20–22.

Carpenter, J., Badve, M., Rajoriya, S., George, S., Saharan, V. K., and Pandit, A. B. (2017). Hydrodynamic cavitation: an emerging technology for the intensification of various chemical and physical processes in a chemical process industry. *Reviews in Chemical Engineering*, Vol. 33, Issue 5, pp. 433–468. DOI: 10.1515/revce-2016-0032.

Chandra, M. S., Naresh, R. K., Mahajan, N. C., Kumar, R., Kumar, A., Singh, S. P., Kumar, Y., and Navsare, R. I. (2019). A review on hydrodynamic cavitation – a promising technology for soil and water conservation in inceptisol of North West IGP. *International Journal of Current Microbiology and Applied Sciences*, Vol. 8, Issue 8, pp. 739–753. DOI: 10.20546/ijcmas.2019.808.084.

Fleguentov, I. V., Degterev, B. I., Kouts, E. V., and Akchurin, R. Y. (1997). Treatment of waste waters with ozone using cavitation. In: *International Conference on Ozonation and Related Oxidation Processes in Water and Liquid Waste Treatment, April 21–23, 1997, Berlin*, pp. II.6.1–II.6.12.

Gimranov, F. M., Belyaev, A. N., Flegentov, I. V., and Kuts, E. V. (2014a). Prospects of using cavitation erosion in obtaining aqueous metal suspensions. *Bulletin of Kazan Technological University*, Vol. 17, No. 23, pp. 65–67.

Gimranov, F. M., Belyaev, A. N., Flegentov, I. V., and Kuts, E. V. (2014b). Use of cavitation treatment to reduce silicon content in drinking water. *Bulletin of Kazan Technological University*, Vol. 17, No. 19, pp. 210–214.

Gimranov, F. M., Belyaev, A. N., Flegentov, I. V., Musikhina, T. A., and Lysov, D. S. (2013). Possibility of water treatment to remove ammonia nitrogen by cavitation and oxidation. *Bulletin of Kazan Technological University*, Vol. 16, No. 19, pp. 108–111.

Gogate, P. R., Mededovic-Thagard, S., McGuire, D., Chapas, G., Blackmon, J., and Cathey, R. (2014). Hybrid reactor based on combined cavitation and ozonation: From concept to practical reality. *Ultrasonics Sonochemistry*, Vol. 21, Issue 2, pp. 590–598. DOI: 10.1016/j.ultsonch.2013.08.016.

Hilgenfeldt, S., Brenner, M. P., Grossman, S., and Lohse, D. (1998). Analysis of Rayleigh–Plesset dynamics for sonoluminescing bubbles. *Journal of Fluid Mechanics*, Vol. 365, pp. 171–204. DOI: 10.1017/S0022112098001207.

Holkar, C. R., Jadhav, A. J., Pinjari, D. V., and Pandit, A. B. (2019). Cavitationally driven transformations: A technique of process intensification. *Industrial & Engineering Chemistry Research*, Vol. 58, Issue 15, pp. 5797–5819. DOI: 10.1021/acs.iecr.8b04524.

Huuha, T. S., Kurniawan, T. A., and Sillanpää, M. E. T. (2010). Removal of silicon from pulping whitewater using integrated treatment of chemical precipitation and evaporation. *Chemical Engineering Journal*, Vol. 158, Issue 3, pp. 584–592. DOI: 10.1016/j.cej.2010.01.058.

Kuts, E. V. (2003). *Methods of drinking and waste water treatment to remove phenols and ways of their intensification. Deposited manuscript. No. 2136-B2003*. Russian Institute of Research and Technical Information, 63 p.

Lysov, D. S., Belyaev, A. N., and Flegentov, I. V. (2016). Cavitation erosion of metals in swimming pool water treatment. In: Litvinets, S. G. (ed.). *All-Russian Annual Scientific and Practical Conference "Society, Science, Innovations". 2nd edition*. Kirov: Vyatka State University, pp. 750–755.

Pandit, A. V., Sarvothaman, V. P., and Ranade, V. V. (2021). Estimation of chemical and physical effects of cavitation by analysis of cavitating single bubble dynamics. *Ultrasonics Sonochemistry*, Vol. 77, 105677. DOI: 10.1016/j.ultsonch.2021.105677.

Patil, P. B., Bhandari, V. M., and Ranade, V. V. (2021). Wastewater treatment and process intensification for degradation of solvents using hydrodynamic cavitation. *Chemical Engineering and Processing - Process Intensification*, Vol. 166, 108485. DOI: 10.1016/j.cep.2021.108485.

Ranade, V. V. (2022). Modeling of hydrodynamic cavitation reactors: reflections on present status and path forward. *ACS Engineering Au*, Vol. 2, Issue 6, pp. 461–476. DOI: 10.1021/acsengineeringau.2c00025.

Rooze, J. (2012). *Cavitation in gas-saturated liquids. PhD Thesis in Chemical Engineering and Chemistry*. Eindhoven: Eindhoven University of Technology. DOI: 10.6100/IR732583.

Zamankhan, P. (2015). Simulation of cavitation water flows. *Mathematical Problems in Engineering*, 872573. DOI: 10.1155/2015/872573.

МОДЕЛИРОВАНИЕ ТЕЧЕНИЯ ВОДЫ В КАВИТАЦИОННОМ РЕАКТОРЕ

Андрей Николаевич Беляев[1], Алексей Владимирович Алешкин[1], Елена Владиславовна Куц*[2], Владимир Владимирович Шабалин[2]

[1]Вятский государственный университет, г. Киров, Россия

[2]Санкт-Петербургский государственный архитектурно-строительный университет Санкт-Петербург, Россия

*E-mail: kouts@yandex.ru

Аннотация
Введение: Поиск путей повышения эффективности реагентных методов обработки воды является актуальной задачей как в процессах водоподготовки, так и в процессах очистки производственных сточных вод. Среди технологий, способных в комплексе с реагентными методами обеспечить высокую производительность и снижение ресурсных затрат, особый интерес представляет гидродинамическая кавитационная обработка воды (ГДК). Анализ научно-технической информации позволил выделить основные показатели процесса гидродинамической кавитационной обработки воды, способные повлиять на эффективность процесса реагентной очистки. Экстремальные параметры, которые возникают при интенсивной кавитации, связаны образованием на локальном участке гидродинамической системы высоких температур до 2000 °С и импульсных давлений больших величин 100-1500 МПа. В таких условиях происходит инициация и интенсификация протекания физико-химических процессов обработки воды. **Цель исследования:** Повышение эффективности существующих традиционных технологий очистки воды, позволяющих улучшить ее качество с наименьшими затратами. **Методы:** Для исследования параметров, влияющих на эффективность процессов водоподготовки и возникающих при кавитационном течении воды было проведено моделирование в пакете Ansys CFX, в котором применен метод конечных объемов. Расчет проводился с учетом турбулентного характера течения по модели турбулентности k-ε. Процесс кавитации рассчитывался с использованием модели кавитации Релея-Плесета. **Результаты:** Процесс парообразования в кавитационном реакторе способствует достаточно полному поглощению газообразного дезинфектанта водой. Повышение температуры так же рассматривается как один из факторов повышения эффективности методов реагентной обработки воды. При кавитации повышение температуры воды происходит в локальных микрообъемах, поэтому для интенсификации процесса отсутствует необходимость осуществления нагрева всего объема жидкости и, как следствие, снижаются общие энергозатраты на процесс водоподготовки.

Ключевые слова: кавитационный реактор, параметры кавитации, процессы обработки воды, моделирование.

DOI: 10.23968/2500-0055-2023-8-1-60-70

ON THE POSSIBILITY OF USING TIMBER STRUCTURES IN THE CONSTRUCTION OF HIGH-RISE BUILDINGS IN SEISMIC AREAS

Aleksandr Chernykh, Tatiana Belash, Viktor Tsyganovkin*, Anton Kovalevskiy

Saint Petersburg State University of Architecture and Civil Engineering
Saint Petersburg, Russia

*Corresponding author's e-mail: viktorts@bim-structure.ru

Abstract
Introduction: Part of the territory of Russia is located in a seismically dangerous area. In recent years, glued laminated wood has been gaining popularity in private housing construction as well as other construction sectors. However, Russian standards lack design and structural requirements for buildings and structures made of glued laminated wood**. Methods:** The paper reviews the foreign experience in construction with the use of glued laminated wood and presents seismic design for a multi-story building made of wood and materials based on it. **Results:** We considered the seismic design of a multi-story timber building and reviewed foreign experience in the construction of buildings made of glued laminated wood. Besides, we analyzed how the choice of the material for individual load-bearing structures affects seismic resistance.

Keywords: glued laminated wood, seismic resistance, earthquakes, multi-story buildings.

Introduction

Climate changes on our planet are forcing the population and the governments of various countries to pay more attention to environmental issues directly related to human construction activities. The increase in temperature is largely due to anthropogenic emissions of greenhouse gases into the atmosphere. Compared with concrete and steel, the use of wood as a building material is the most preferable since it reduces carbon dioxide emissions into the atmosphere. Wood production waste is environmentally friendly and can be used in the future as biofuel or for other industrial purposes. All this testifies to the relevance of using wood in the construction of buildings for various purposes. Besides, due to its high performance characteristics, wood has a huge potential in the field of building construction in specific climatic and seismic conditions, reducing the risks of structural collapse and minimizing economic costs of restoration after potential natural disasters, e.g., after violent earthquakes (Black et al., 2010; Goda and Yoshikawa, 2013; Goda et al., 2011; Şahin Güçhan, 2007).

Centuries of experience in the operation of timber buildings show that they can last for hundreds of years. Modern studies on the fire resistance of timber constructions allow us to consider timber buildings quite fire-resistant. This is mainly due to the moisture content in the wood, including the most dried samples. As the research results show, glued laminated wood is characterized by the greatest resistance.

Despite the positive experience of using wood in civil engineering, its use in multi-story or high-rise construction is still quite problematic. This is related to one of the significant disadvantages of wood, i.e., limited choice of geometric dimensions of structures, which increases the cost of wood harvesting and processing. Among other disadvantages of timber structures, the following can be mentioned: changes in the geometric shape as a consequence of shrinkage or swelling, persisting during the operation of structures. As known, additional stresses occur in the nodal joints as a result of shrinkage and settlement, which significantly increase throughout the height of the building. These negative factors are mainly typical for solid wood. They can be largely overcome by using a wide range of wood composite materials, which are quite popular abroad. These include glulam (glued laminated wood), CLT (cross laminated timber) plates, plate materials capable of withstanding loads in loaded structures (OSB plywood), parallel strand lumber (PSL), etc. The main feature of the developed wood composite materials is the possibility of their use in the construction of multi-story and high-rise buildings due to their high performance characteristics, which primarily include strength, rot resistance, corrosion resistance, high vapor permeability, fire resistance, unlimited cross-section sizes, and low specific weight compared with reinforced concrete and steel. Products made of wood composite materials can be used as load-bearing and enclosing structures.

As an example, we considered the multi-story Brock Commons Tallwood House consisting mainly of timber structures, shown in Fig. 1. The building has a hybrid structure consisting of PSL beams, CLT floors, and reinforced concrete stiffening cores where escape routes and elevator shafts are located.

The first floor is also made of reinforced concrete. The structural system is frame, post-and-beam. The used PSL material is isotropic, so it can be used in structures without preferred load direction. Wood fibers in the longitudinal direction are characterized by the best strength indicators at tension and bending. Besides, these products have increased moisture resistance.

Glued laminated wood (glulam) (Fig. 2) is a structural material made by linking individual wood segments glued together using special industrial adhesives, e.g., polyurethane adhesives.

The obtained products are characterized by high strength, fire and moisture resistance. These segments can be used to create construction facilities of various shapes and sizes. One of the main advantages of this type of materials is that it is light and easy to assemble. The joints between various elements can be made not only with adhesives but also with steel dowel pins. An important property of this material is its stable behavior; shrinkage and swelling are minimized.

Another popular wood composite material is cross laminated timber (multilayer cross laminated wooden panels), better known as CLT. This technology was first developed and used in the early 1990s in Germany and Austria and became widespread in the 2000s.

CLT is a wooden panel made of timber layers glued together, with each layer oriented perpendicular to adjacent layers. Panels are made from layers of wood dried to optimum moisture content. The cross arrangement of the longitudinal and transverse layers reduces the shrinkage and swelling of wood in the panel plane to insignificant values, which increases the bearing capacity and minimizes changes in the geometric sizes of the elements. CLT panels can be used as load-bearing and enclosing structures. Due to stiffness and the absence of residual deformations, structures made of this material also found their use in seismic areas. In Japan, a 7-story building made of CLT panels was tested on special equipment simulating earthquake conditions. The results showed high seismic resistance of CLT elements at 7–8 earthquake magnitudes (Porcu et al., 2018; Shen et al., 2013).

Fig. 3 shows the Mjøstårnet building. It is the 18-story building built in Norway, with a total height of 84.5 m. To erect this large object, load-bearing columns, beams, and massive diagonal members made of glued laminated wood were used.

The total area of living space in the building is ca. 11,300 m^2. The building is based on the post-and-beam structural scheme. The posts and beams are made of glued laminated timber and reinforced with additional braces. The floor slabs are made of CLT panels. However, reinforced concrete structures were also used in the construction. Up to the 12^{th} floor, wooden beams are covered with laminated veneer and a 50 mm concrete layer to improve acoustic properties and reduce oscillations. From the 12^{th} to the 18^{th} floor, the floor slabs are reinforced concrete. Thanks to this structural solution, it is possible to erect a building with such a height and ensure optimal wind load resistance. The semi-basement floor, the foundation, and the slab of the first floor are also made of reinforced concrete. The building has a stiffening core made of CLT panels, where a staircase and an elevator shaft are located. Fig. 4 shows the general view of the load-bearing structures.

Another example of using CLT is the Via Cenni residential complex in Milan. It is based on the technology for the construction of high-rise buildings with the use of CLT panels. The residential complex consists of four 9-story towers, each 28 m high, connected by two-story buildings. The structural scheme used in the design is panel-wall. This technology made it possible to erect the residential complex in just 14 weeks. The construction area is located in a 7-magnitude seismic zone. The building (except for the semi-basement floor, the floor of the first story, and the foundation) is completely made of CLT panels. To ensure the required horizontal

Fig. 1. Brock Commons Tallwood House

Fig. 2. Glued laminated wood

Fig. 3. Mjøstårnet Tower, Norway

stiffness, each panel has at least 5 layers. Reinforced concrete stiffening cores play an important role in the seismic vulnerability of the building since they resist horizontal loads transmitted from the CLT floor panel through steel joints (resistance bars), thus ensuring the frame resistance to loads of this nature. To avoid the transmission of vertical loads in the bearing areas of the columns to the CLT panels, a steel bond is provided, directly connecting the upper and lower columns, thereby preventing the deformation of the floor panels due to the pressure from the columns. The enclosing structures of the building consist of CLT-based prefabricated panels finished with refractory materials. The erection of the building took only 70 days. As of today, the seismic resistance of buildings made of reinforced concrete and steel is most extensively studied, and those studies are systemic and reflected in Russian and foreign standards. The studies addressing the seismic resistance of timber buildings are either local or deal with local issues of wooden house construction (Belash and Ivanova, 2006, 2019; Belash et al., 2010, Kirkham et al., 2014). Those studies also do not provide the specifics of structural engineering with regard to buildings made of glued laminated wood: methods for accounting the anisotropic properties of wood or methods for accounting the mutual arrangement of fibers. Based on the aforesaid, we aimed to study the seismic resistance of a multi-story building with load-bearing structures made of glued laminated wood and determine the possibility of using this material in large-scale construction at the current level of science and technology development.

Subject, methods and materials

To assess the load-bearing capacity of the analyzed structural solutions under seismic impacts, we performed calculations and theoretical studies. The subject of the study is an 18-story building with load-bearing structures made of glued laminated wood (Fig. 5). The floors of the building are made of CLT panels consisting of 5 layers of 40 mm each.

The vertical load-bearing structures (with the transmission of vertical loads as the main function) are columns made of glued laminated wood of first grade with a cross-section of 600x600 mm.

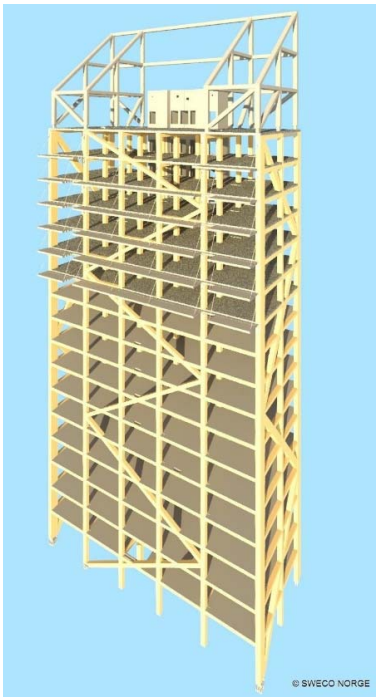

Fig. 4. Mjøstårnet Tower, general view of the load-bearing structures

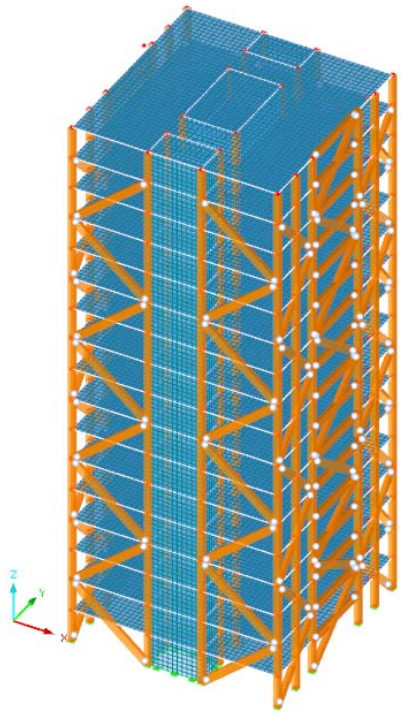

Fig. 5. Building under consideration. General view

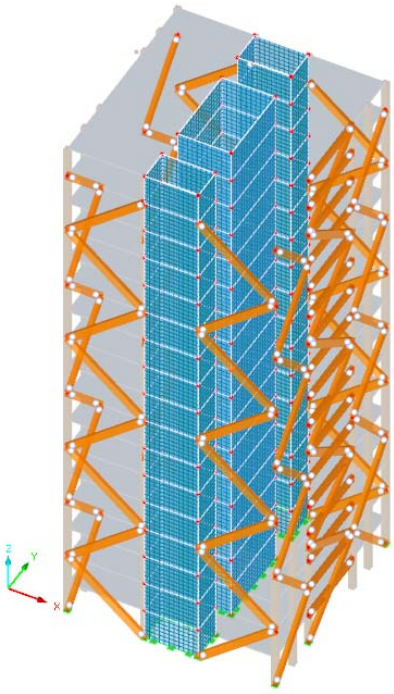

Fig. 6. Horizontal load resistance system

To increase the stiffness of the building as a whole to horizontal loads as well as to increase its seismic resistance, it is necessary to provide a transverse load resistance system in the building (hereinafter — the TLRS). In this building, the TLRS elements are the walls of the elevator shafts made of CLT panels as well as external diagonal members forming vertical trusses (Fig. 6). For comparison, a design scheme was developed where only reinforced concrete stiffening cores act as the TLRS, and the walls of the elevator shafts are made of reinforced concrete with a thickness of 200 mm.

The design model does not take into account the ductility of the element joints, which can affect the stress-strain state of individual elements (Astakhova et al., 2022). The design model adopts completely hinged and completely rigid joints. The braces in the bases of the columns are rigid. To simulate the seismic impact, we used the accelerogram for Friuli, Italy (Finetti et al., 1979). Based on this accelerogram, the response spectrum of the system was generated (Fig. 7).

Based on the given response spectrum, equivalent loads were formed, which were applied to the joints of the finite elements. The design scheme of the adopted structural system was analyzed using the finite element method. The design scheme was built by replacing horizontal and vertical elements modeled in the academic version of Autodesk Revit with rods, and flat structures — with flat elements, and assigning to them stiffness characteristics in accordance with design solutions for each type of load-bearing elements (Chernykh et al., 2020). The calculations were performed using the academic version of DLUBAL RFEM software.

Results and discussion

An analysis of the existing materials in high-rise wooden housing construction shows that most developments were carried out abroad (Filiatrault et al., 2003; Leimke et al., 2017). This is primarily due to the fact that Russia has not yet developed the production of more innovative types of timber structures, and regulatory documents are still under development. Meanwhile, the interest of specialists in these products is quite high (Benin and Ivanova, 2000; Ivanova, 2005) since the use of timber structures is one of the most popular and priority directions in the field of building materials widely used in Russia.

Based on the calculation results, we determined horizontal displacements caused by a specific combination of loads (Fig. 8). We also determined stresses in the multilayer CLT panel of the floor (Fig. 9).

As the isofields of stresses in the slab show, the maximum stresses are observed only in the bearing areas of the columns (Fig. 10).

Let us consider the stress-strain state of the main vertical load-bearing structures as well as the elements of the transverse load resistance system. Figs. 11–13 show forces arising in the columns.

As can be seen, the columns of the multi-story building mainly act as a compressed-bent rod. Figs. 14–18 show forces in the elements of the vertical truss.

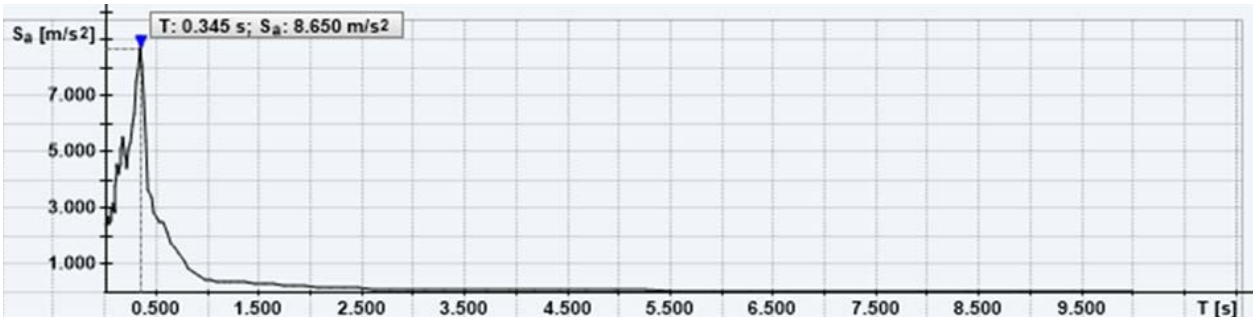

Fig. 7. Synthesized response spectrum from the seismogram

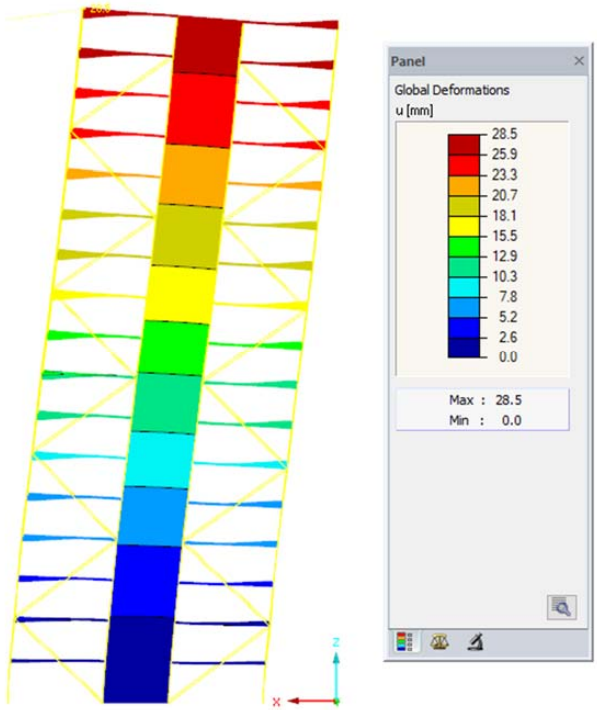

Fig. 8. Deformed scheme of the building as a result of a specific combination of loads

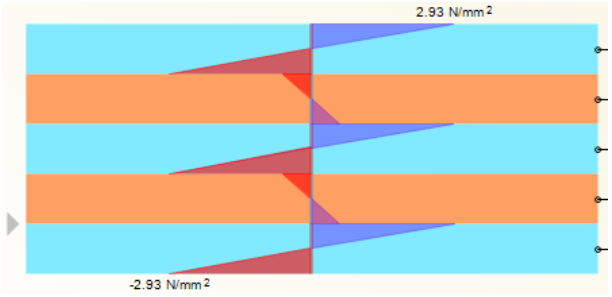

Fig. 9. Maximum normal stresses in the cross-section of the CLT panel of the floor

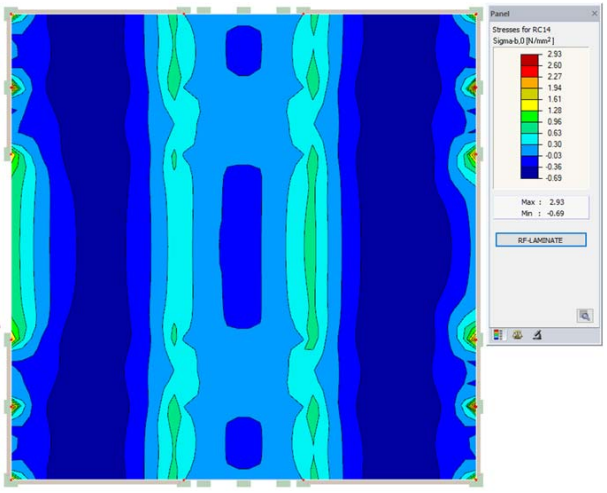

Fig. 10. Isofields of stresses in the CLT panel of the floor

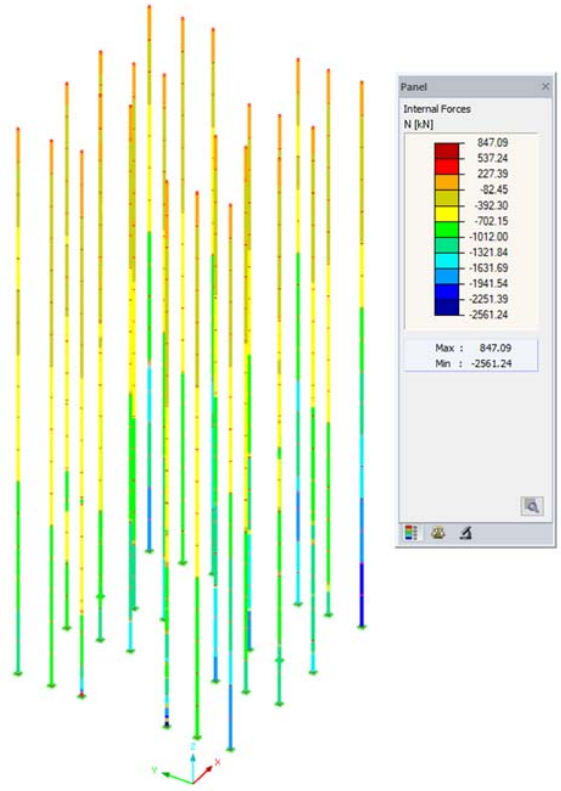

Fig. 11. Diagram of longitudinal force N in the columns of the building

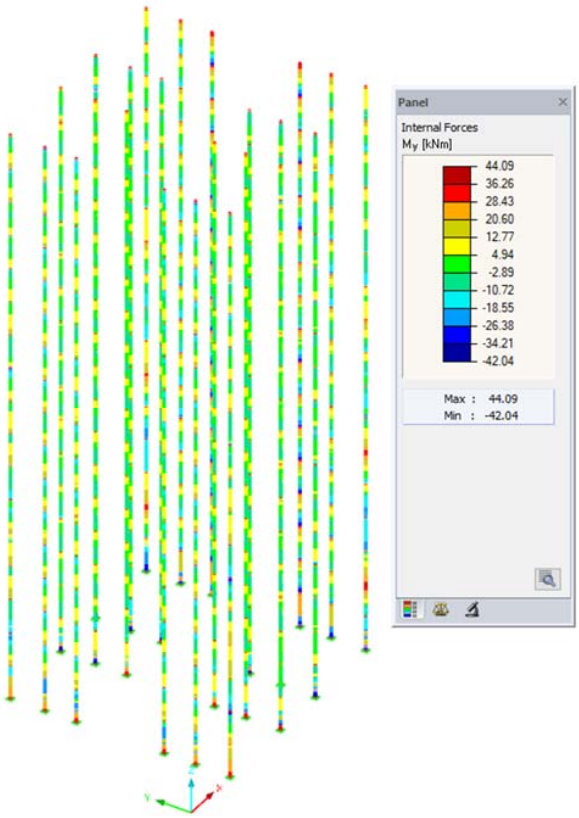

Fig. 12. Diagram of bending moments M_y of force in the columns of the building

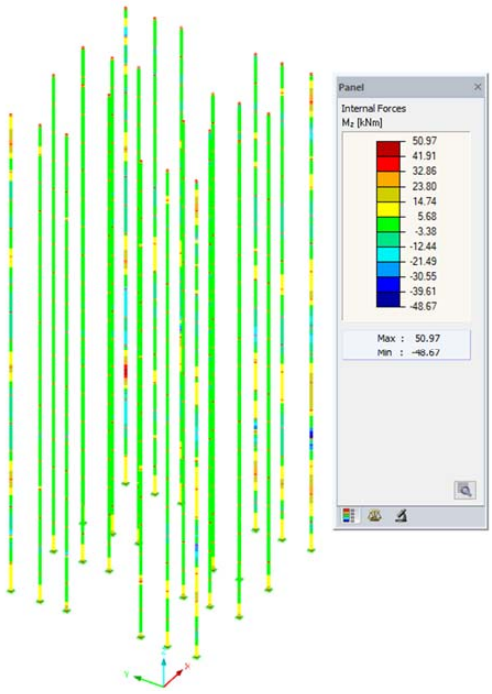

Fig. 13. Diagram of bending moments M_z of force in the columns of the building

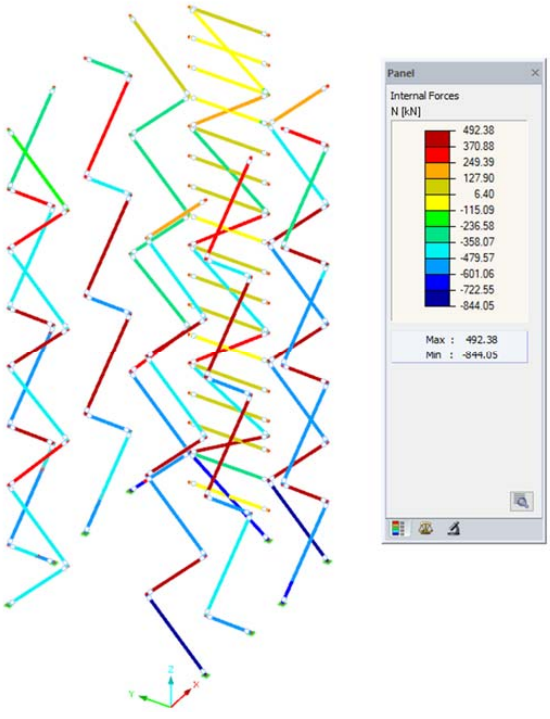

Fig. 14. Force N in the elements of the vertical truss of the building

Based on the presented values of internal forces arising in the mesh elements, we can conclude that the mesh elements act as a compressed-bent or stretched-bent element. The bending moment acts in two planes, being caused under the action of a load equivalent to seismic impact.

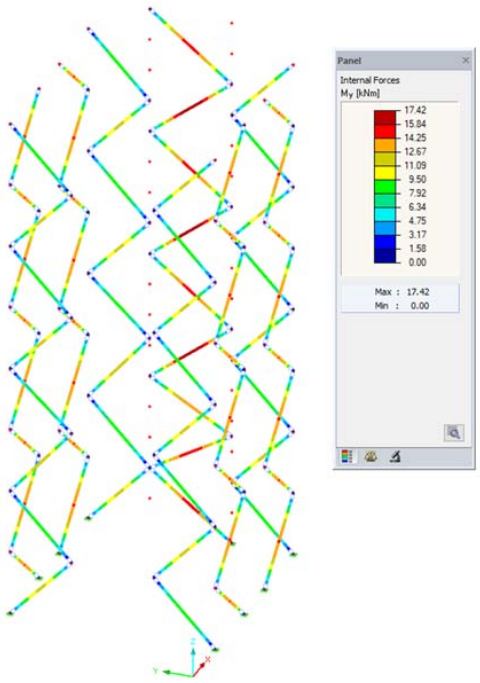

Fig. 15. Force My in the elements of the vertical truss of the building

Let us consider the modes of the building oscillations calculated during the intermediate modal analysis of the scheme. The first two modes of oscillations with the greatest contribution in dynamic analysis are shown in Figs. 19–20.

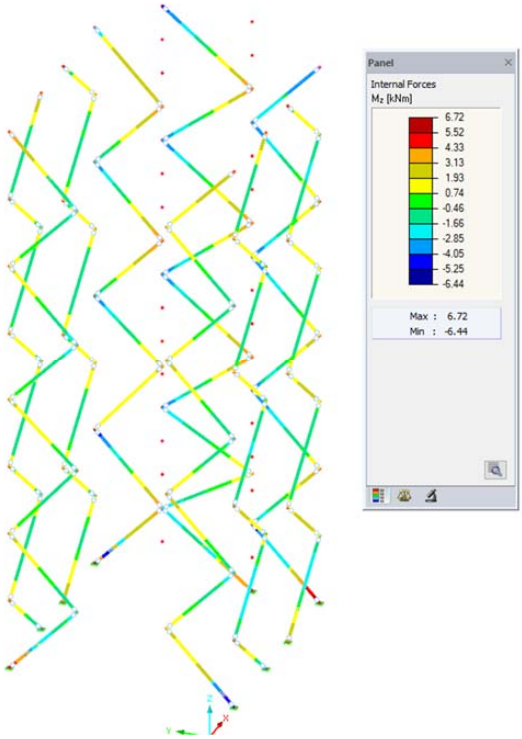

Fig. 16. Force M_z in the elements of the vertical truss of the building

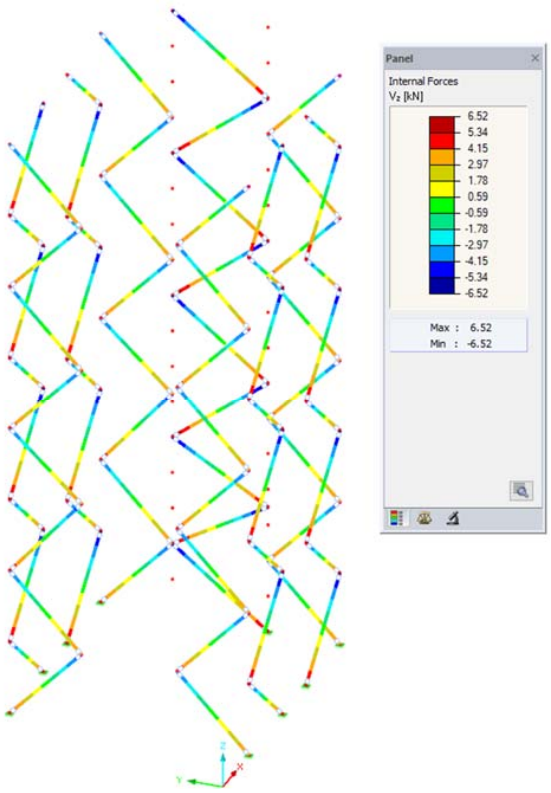

Fig. 17. Force Q_z in the elements of the vertical truss of the building

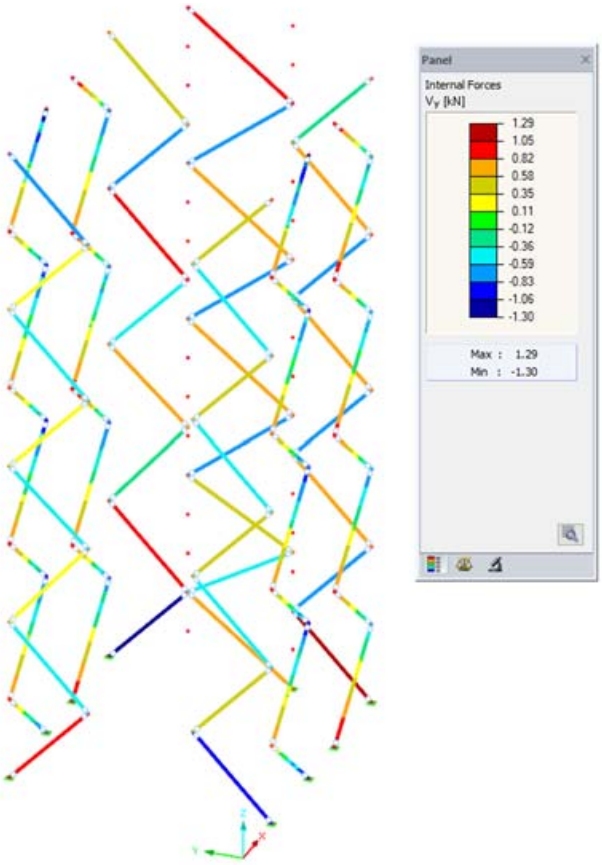

Fig. 18. Force Q_y in the elements of the vertical truss of the building

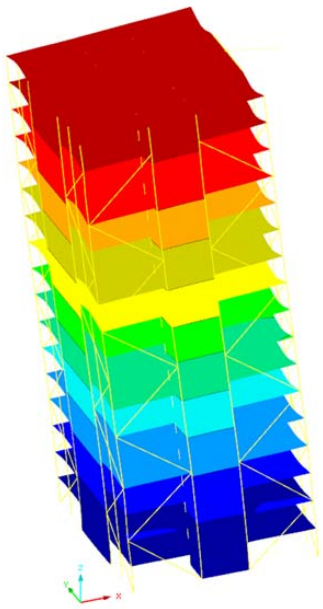

Fig. 19. The first mode of the building oscillations

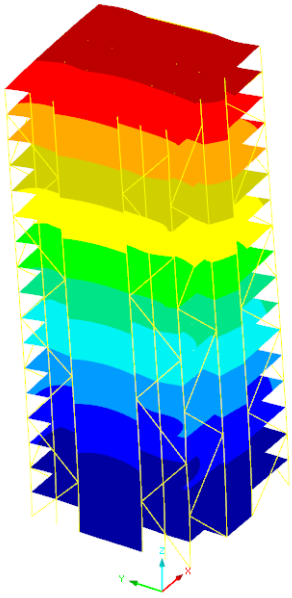

Fig. 20. The second mode of the building oscillations

The oscillation modes presented above represent bending-translational modes of possible oscillations in this building. It should be noted that in the third possible mode of oscillations, the oscillations are bending-torsional. This mode is shown in Fig. 21.

This mode does not affect the final stress-strain state in the elements, since the effective mass inclusion factor for this mode of oscillations is zero or has a near-zero value. Fig. 22 shows the values of the modal mass inclusion factor according to the modes of oscillations. The values in the frame correspond to the effective modal mass factors in the bending-torsional mode of oscillations.

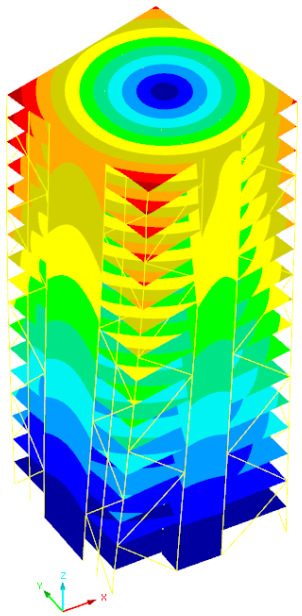

Fig. 21. The third mode of the building oscillations

It should be noted that bending-torsional modes of oscillations should be avoided in multi-story as well as high-rise buildings to prevent the occurrence of significant torsion forces, which are the cause of a significant increase in the cross-sections of the bearing elements of the building.

Let us consider the natural oscillations of a building with reinforced concrete stiffening cores. The first two modes of oscillations with the greatest contribution in dynamic analysis are shown in Figs. 23–24. The first two modes are bending-translational modes of oscillations.

The third mode of oscillations is bending-torsional. This mode does not affect the stress-strain state in the elements of the building, since the effective mass inclusion factor for this mode of oscillations is zero (Fig. 25). Figs. 26–28 show forces arising in the columns.

The horizontal displacements of the scheme with the reinforced concrete stiffening core amount to 25.7 mm (Fig. 29).

Mode No.	To Generate	Frequency ω [rad/s]	Frequency f [Hz]	Period T [s]	Acceleration S_a [m/s²]	Effective Modal Mass Factor [-] f_{meX} [-]	f_{meY} [-]	f_{meZ} [-]
1	☑	9.853	1.568	0.638	1.894	0.725	0.000	0.000
2	☑	11.131	1.771	0.564	2.467	0.000	0.689	0.000
3	☑	21.835	3.475	0.288	6.290	0.000	0.002	0.000
4	☑	31.333	4.987	0.201	5.106	0.164	0.000	0.001
5	☑	36.495	5.808	0.172	5.096	0.000	0.182	0.000
6	☑	49.051	7.807	0.128	4.509	0.001	0.000	0.422
7	☑	53.668	8.541	0.117	3.961	0.002	0.000	0.041
8	☑	54.339	8.648	0.116	3.864	0.015	0.000	0.036
9	☑	54.564	8.684	0.115	3.832	0.000	0.000	0.000
10	☑	54.625	8.694	0.115	3.824	0.000	0.000	0.000
11	☑	54.722	8.709	0.115	3.810	0.000	0.000	0.000
12	☑	54.847	8.729	0.115	3.793	0.000	0.000	0.000
13	☑	54.982	8.751	0.114	3.757	0.000	0.000	0.000
14	☑	55.133	8.775	0.114	3.713	0.000	0.000	0.001

Fig. 22. Effective modal mass inclusion factors according to the modes of oscillations

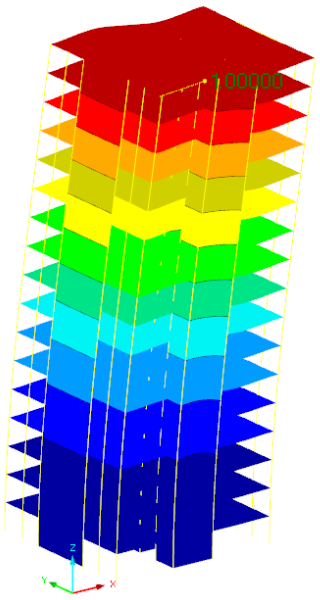

Fig. 23. The first mode of the building oscillations

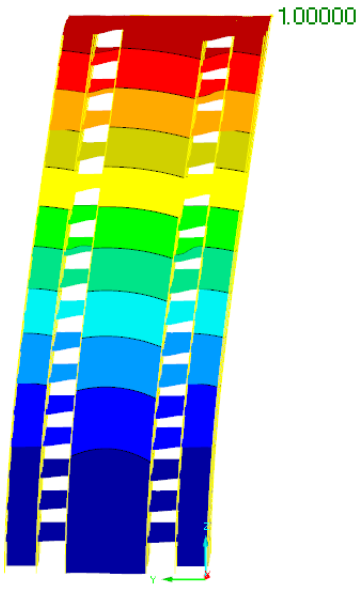

Fig. 24. The second mode of the building oscillations

Mode No.	To Generate	Frequency ω [rad/s]	Frequency f [Hz]	Period T [s]	Acceleration S_a [m/s²]	Effective Modal Mass Factor [-] f_{meX} [-]	f_{meY} [-]	f_{meZ} [-]
1	☑	6.990	1.113	0.899	0.636	0.628	0.000	0.000
2	☑	8.094	1.288	0.776	1.071	0.000	0.634	0.000
3	☑	17.916	2.851	0.351	8.481	0.000	0.000	0.000
4	☑	37.256	5.929	0.169	4.905	0.202	0.000	0.000
5	☑	40.563	6.456	0.155	4.367	0.000	0.200	0.000
6	☑	47.608	7.577	0.132	4.510	0.000	0.000	0.080
7	☑	53.533	8.520	0.117	3.980	0.000	0.003	0.000
8	☑	56.547	9.000	0.111	3.313	0.000	0.000	0.000
9	☑	57.599	9.167	0.109	3.028	0.000	0.000	0.144
10	☑	58.054	9.240	0.108	2.907	0.000	0.000	0.002
11	☑	58.360	9.288	0.108	2.877	0.000	0.000	0.000
12	☑	58.674	9.338	0.107	2.871	0.000	0.000	0.010
13	☑	58.699	9.342	0.107	2.870	0.001	0.000	0.001
14	☑	58.972	9.386	0.107	2.864	0.000	0.000	0.000

Fig. 25. Effective modal mass inclusion factors according to the modes of oscillations for buildings with reinforced concrete stiffening cores

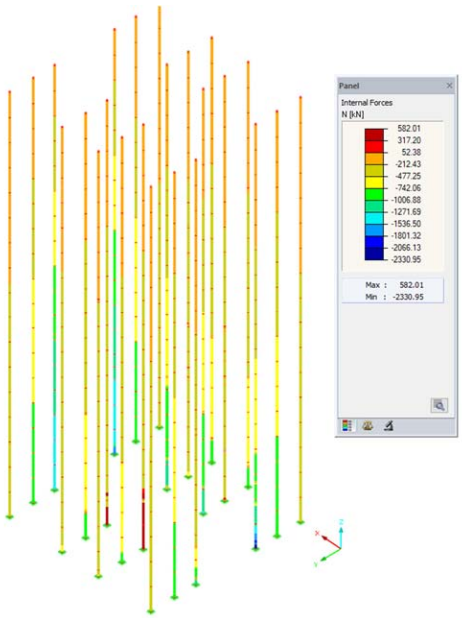

Fig. 26. Diagram of longitudinal force N in the columns of the building

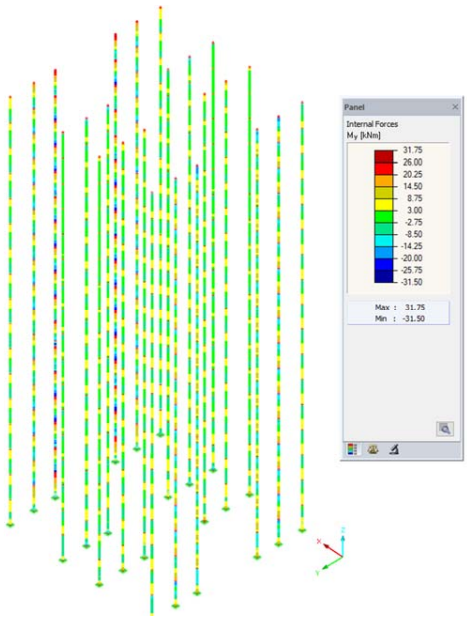

Fig. 27. Diagram of bending moments M_y of force in the columns of the building

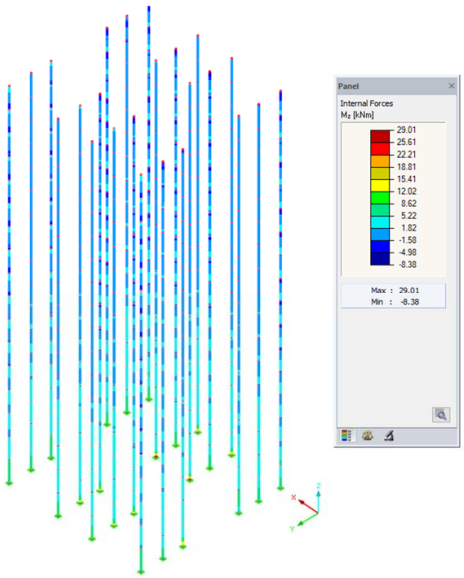

Fig. 28. Diagram of bending moments M_z of force in the columns of the building

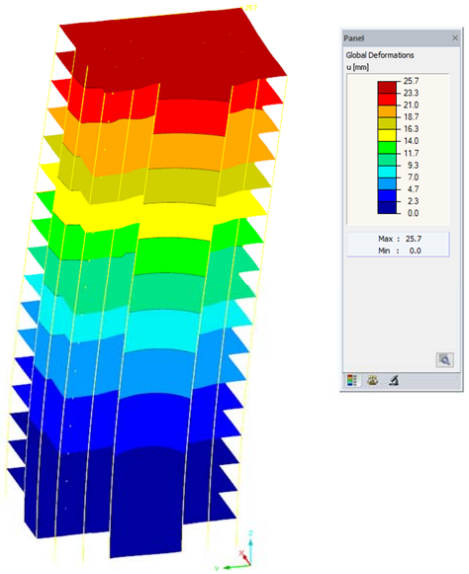

Fig. 29. Deformed scheme of the building with the reinforced concrete stiffening core

Conclusions

The studies performed confirm the possibility of using wood-composite systems for high-rise buildings without the use of concrete and reinforced concrete structures in the superstructure**.** Special attention should be paid to the selection and design of the horizontal load resistance systems, which withstand most of the seismic impact and reduce the possible oscillation amplitude.

During the comparative analysis of the two design schemes, we established the following:

- The first two modes of free oscillations are bending-translational in both cases;
- Bending-torsional modes of oscillations do not affect the stress-strain state in the elements for both the first and second design schemes, since the inclusion of masses in this mode of oscillations has a zero or near-zero value;
- The horizontal displacements of the building consisting entirely of wood composite materials amount to 28 mm, and the horizontal displacements of the building with the reinforced concrete stiffening core amount to 25.7 mm;
- The elements of the diagonal members in the first design scheme with load-bearing elements made of wood composite materials are characterized by a compressed-bent stress-strain state, while the forces of bending moments arise from loads equivalent to seismic impact.

References

Astakhova, L., Astakhov, I., Kuznetsov, A., Yukhnina, A., and Tsyganovkin, V. (2022). Research of parameters affecting the column-foundation joint ductility and the frameworks frame stress-deformed condition. In: Manakov, A. and Edigarian, A. (eds.). *International Scientific Siberian Transport Forum TransSiberia - 2021. TransSiberia 2021. Lecture Notes in Networks and Systems*, Vol. 403. Cham: Springer, pp. 1407–1416. DOI: 10.1007/978-3-030-96383-5_157.

Belash, T. A. and Ivanova, Zh. V. (2006). Review of theoretical and experimental studies in earthquake resistance of wood components. *Earthquake Engineering. Constructions Safety*, No. 4, pp. 50–54.

Belash, T. A. and Ivanova, Zh. V. (2019). Timber frame buildings with efficient junction designs for earthquake-prone areas. *Magazine of Civil Engineering*, No. 8 (92), pp. 84–95. DOI: 10.18720/MCE.92.7.

Belash, T. A., Ivanova, Zh. V., and Demishin, S. V. (2010). Experimental studies of earthquake resistance of timber buildings. *Earthquake Engineering. Constructions Safety*, No. 6, pp. 29–31.

Benin, A. V. and Ivanova, Zh. V. (2000). Experimental studies of mechanical properties of structural components in timber building under seismic impact. *Earthquake Engineering. Constructions Safety*, No. 2, pp. 19–21.

Black, G., Davidson, R. A., Pei, S., and Van de Lindt, J. (2010). Empirical loss analysis to support definition of seismic performance objectives for woodframe buildings. *Structural Safety*, Vol. 32, Issue 3, pp. 209–219. DOI: 10.1016/j.strusafe.2010.02.003.

Chernykh, A. G., Nizhegorodtsev, D. V., Kubasevich, A. E., and Tsyganovkin, V. V. (2020). Design and calculation of building structures using BIM technologies. *Bulletin of Civil Engineers*, No. 3 (80), pp. 72–78. DOI 10.23968/1999-5571-2020-17-3-72-78.

Filiatrault, A., Isoda, H., and Folz, B. (2003). Hysteretic damping of wood framed buildings. *Engineering Structures*, Vol. 25, Issue 4, pp. 461–471. DOI: 10.1016/S0141-0296(02)00187-6.

Finetti, I., Russi, M., and Slejko, D. (1979). The Friuli earthquake (1976–1977). *Tectonophysics*, Vol. 53, Issues 3–4, pp. 261–272. DOI: 10.1016/0040-1951(79)90070-2.

Goda, K., Atkinson, G. M., and Hong, H. P. (2011). Seismic loss estimation of wood-frame houses in south-western British Columbia. *Structural Safety*, Vol. 33, Issue 2, pp. 123–135. DOI: 10.1016/j.strusafe.2010.11.001.

Goda, K. and Yoshikawa, H. (2013). Incremental dynamic analysis of wood-frame houses in Canada: Effects of dominant earthquake scenarios on seismic fragility. *Soil Dynamics and Earthquake Engineering*, Vol. 48, pp. 1–14. DOI: 10.1016/j.soildyn.2013.01.011.

Ivanova, Zh. V. (2005). Non-linear dynamic analysis of seismic resistance of wooden structures. *Earthquake Engineering. Constructions Safety*, No. 1, pp. 7–8.

Kirkham, W. J., Gupta, R., and Miller, T. H. (2014). State of the art: Seismic behavior of wood-frame residential structures. *Journal of Structural Engineering*, Vol. 140, Issue 4, 04013097. DOI: 10.1061/(ASCE)ST.1943-541X.0000861.

Leimke, J., Rüther, N., Kasal, B., Polococer, T., and Guindos, P. (2017). Improved moment-resisting timber frames for earthquake-prone areas Part II : shaking table tests. In: *CLEM + CIMAD 2017: II Latin American Conference on Timber Structures & II Ibero-American Conference on Construction Timber*, May 17–19, 2017, Junín, Buenos Aires, Argentina.

Porcu, M. C., Bosu, C., and Gavrić, I. (2018). Non-linear dynamic analysis to assess the seismic performance of cross-laminated timber structures. *Journal of Building Engineering*, Vol. 19, pp. 480–493. DOI: 10.1016/j.jobe.2018.06.008.

Şahin Güçhan, N. (2007). Observations on earthquake resistance of traditional timber-framed houses in Turkey. *Building and Environment*, Vol. 42, Issue 2, pp. 840–851. DOI: 10.1016/j.buildenv.2005.09.027.

Shen, Y.-L., Schneider, J., Tesfamariam, S., Stiemer, S. F., and Mu, Z.-G. (2013). Hysteresis behavior of bracket connection in cross-laminated timber shear walls. *Construction and Building Materials*, Vol. 48, pp. 980–991. DOI: 10.1016/j.conbuildmat.2013.07.050.

О ВОЗМОЖНОСТИ ИСПОЛЬЗОВАНИЯ ДЕРЕВЯННЫХ КОНСТРУКЦИЙ В СТРОИТЕЛЬСТВЕ ЗДАНИЙ ПОВЫШЕННОЙ ЭТАЖНОСТИ В СЕЙСМИЧЕСКИХ РАЙОНАХ

Александр Григорьевич Черных, Татьяна Александровна Белаш, Виктор Цыгановкин*, Антон Владимирович Ковалевский

[1]Санкт-Петербургский государственный архитектурно-строительный университет
Санкт-Петербург, Россия

*E-mail: viktorts@bim-structure.ru

Аннотация:
Введение: Часть территории России находится в сейсмически опасной зоне. В последнее время, большую популярность в частном домостроении, а так же в других секторах строительства набирает популярность клееная древесина. Но в отечественной нормативной базе отсутствуют расчетные и конструктивные требования по проектированию зданий и сооружений из клееной древесины**. Метод:** в данной статье производится обзор зарубежного опыта строительства с применением клееной древесины, а так же приводится расчет многоэтажного здания из древесины и материалов на ее основе на сейсмостойкость. **Результаты:** был рассмотрен расчет многоэтажного здания из древесины на сейсмостойкость, рассмотрен зарубежный опыт строительства зданий из клееной древесины. Рассмотрено влияние выбора материала отдельных несущих конструкций на сейсмостойкость.

Ключевые слова: клееная древесина, сейсмостойкость, землетрясения, многоэтажные здания.

DOI: 10.23968/2500-0055-2023-8-1-71-81

FLEXURAL PERFORMANCE OF REINFORCED CONCRETE BEAMS RETROFITTED USING FERROCEMENT WIRE MESH

Md. Basir Zisan*, Biplob Kanti Biswas, Md. Abul Hasan, Mithu Chanda, Anindya Dhar

Chittagong University of Engineering & Technology, Raozan, Chittagong, Bangladesh

*Corresponding author's e-mail: basirzisan@cuet.ac.bd

Abstract

Introduction: Ferrocement is a low-cost material that can be utilized as a replacement for expensive fiber-reinforced polymer (FRP), which is generally used for retrofitting structural and non-structural reinforced concrete members. **The objective** of this paper is to investigate the effectiveness of wire mesh in the retrofitting of flexural members such as reinforced concrete beams. It also investigated the flexural capacity of the beams, which are reinforced with wire mesh as a partial or complete replacement of regular rebar. The orientations and various forms of the wire mesh within the beam section are taken into consideration. The **finite element method** is used to model and analyze the beams. The structural performance of the studied beams, including the load-deflection relationship, first cracked and ultimate cracked loads, crack patterns, and flexural stress, were evaluated using the finite element method. The finite element model of the beam which is reinforced with wire mesh has been verified with experimental results. **The results** show that beams retrofitted with ferrocement or beams in which rebar is replaced by wire mesh have superior flexural performance and low crack depth. The beams retrofitted with wire mesh have a high ultimate load-carrying capacity and ductility. The confinement of three-sided wire mesh improves the flexural performance of the beam. It is observed that flexural performance remains the same when the length of the wire mesh exceeds half of the span length.

Keywords: Reinforced concrete beam; wire mesh, retrofitting; load-deflection; stress; crack.

Introduction

A reinforced concrete structure often exhibits partial damage due to improper design, overloading, corrosion of the reinforcement, and adverse environmental conditions that reduce the serviceability of the structure. It is uneconomical to completely replace or demolish a structure that has impairments. Therefore, retrofitting or restrengthening is necessary to increase the performance at the serviceability levels of a partially damaged structure or structural components. Retrofitting using carbon fiber (CFRP) (Hasan et al., 2020; 2022) or glass fiber (GFRP) polymers (Tanaka et al., 1994), steel plate bonding (Zisan et al., 2011; Oehlers et at., 2000), and concrete jacketing (Kaish at al., 2012; 2013; 2014; Jamil et al., 2013) are generally used to regain the serviceability of deficient concrete structures. The fiber-reinforced polymer known as FRP is widely recommended due to its high strength, effectiveness, and durability (Pham and Al-Mahaidi, 2014; Adhikary and Mutsuyoshi, 2006; Obaidat et al., 2011; Kibria et al., 2020). In addition, the seismic protection efficiency of the FRP retrofitting method is superior to that of traditional retrofitting methods (Al Rjoub et al., 2019; Cao and Nguyen, 2019).

However, application of FRP material in developing countries is rare due to the cost and paucity of FRP materials. On the other hand, ferrocement composites are low-cost and relatively light and have been used in repairing concrete structures (Gaidhankar et al, 2017; Leeanansaksiri et al., 2018). Instead of steel or timber formwork, ferrocement formwork can be used as a permanent component of structural elements (Matalkah et al., 2017; Shaaban, 2002). It is claimed that ferrocement composite has high strength, homogeneous crack propagation and distribution, including a low crack depth, and high toughness, which makes ferrocement a superior building material (Fahmy et al., 2004; 2012; Husein et al., 2013; Shaheen and Eltehawy, 2017). The ferrocement has sufficient bending capacities, and its well-distributed cracks provide adequate warning before failure (El-Wafa and Fukuzawa, 2008; 2010; Kadir et al. 1997; Al-Sulaimani et al., 1991). Therefore, ferrocement composite could be an important retrofitting tool for reinforced concrete beams.

In previous research, it has been concluded that ferrocement increases the shear capacity while limiting the crack opening (Fahmy et al., 2014). It was reported that RC slabs and masonry walls retrofitted with ferrocement have superior performance under different loading conditions (Hago et al., 2005; Ashraf et al., 2012). The ferrocement composite has been widely used in column jacketing because of high confinement and ductile performance of the column under cyclic and axial loads (Kaish et al., 2012; Abdullah and Takiguchi, 2003). Some researchers claimed that ferrocement enhances the shear bond performance of RC beams (Li et al., 2018; 2013; El-Sayed and Erfan, 2018). The structural behavior of concrete beams fabricated with lightweight core material

and then furnished with various wire mesh has been examined by Shaaban et al. (2011; 2013). It is claimed that these beams are lightweight and cost-effective for the retrofitting of residential buildings. The effectiveness of ferrocement for retrofitting beam-column joints was studied by Shaaban and Seoud (2018) and Li et al. (2013). It indicated that ferrocement layers revealed high ultimate capacities, high ultimate displacements, and large ductility. It did not suffer heavy damage, as was observed for the traditionally reinforced concrete RC beam. Muhit et al. (2021) and Niloy and Islam (2017) conducted flexural tests on RC beams retrofitted with ferrocement and discovered that elastic stiffness and ultimate load carrying capacity increase in ferrocement beams while crack width decreases. The performance of a ferrocement beam due to the orientation of wire in the wire mesh and the amount of layer to be used, was studied by Fahmy et al. (2014), using a U-shaped form of the ferrocement. Shaheen and Eltehawy assessed the effectiveness of U-shaped ferrocement forms (Shaheen et al. 2017). However, these studies do not cover the flexural performance of beams with partial or complete replacement of shear and main reinforcements with ferrocement, which is considered in this study. It also studied the flexural performance of a reinforced concrete beam with a rectangular shape of ferrocement as well as ferrocement placed only at the bottom of the beam.

The use of ferrocement throughout the length of beams is costly. Therefore, the optimum length of the wire mesh is necessary to minimize the cost and labor. In the current study, RC beams retrofitted with a U-shape, closed-rectangular shape ferrocement, or ferrocement added at the bottom of the RC beam were investigated in order to identify the effectiveness of wire mesh in enhancing the flexural performance. In addition, the effectiveness of ferrocement in retrofitting of a beam with partial and complete replacement of conventional steel bars is being investigated. The finite element (FE) method is an efficient tool for analyzing nonlinear behavior such as stress-strain and crack patterns in beams. This method was used by several researchers to analyze the nonlinear flexural characteristics of RC and prestressed concrete beams (Faherty, 1972; Anthony and Wolanski, 2004; Sowmya and Venkatasubramani, 2017). Tjitradi et al. (2017) examined the collapse mechanics and observed the flexural crack generation method. In this study, analysis of beams was carried out using the ANSYS program. The critical load, deflection, and stress at the midspan of the beam, and the crack within the concrete are taken as key parameters to measure the performance of the beam with different ferrocement approaches.

Finite Element Modelling

Table 1 defines and describes the various types of beams that are modeled and examined in this study. A standard reinforced concrete beam, which is called an experimental beam, is abbreviated as CB. The length of the CB is 1000 mm, and the cross section is 225 × 150 mm. The effective span is assumed to be 900 mm. There are two 12 mm bars at the bottom and two 10 mm bars at the top of the beam. The clear cover for the main steel is assumed to be 25 mm. The diameter of the web reinforcement is 8 mm and it is placed at a rate of 8 mm center-to-center distance. A detailed description of the geometric properties, vertical load, and boundary conditions of the experimental beam is given in (Fig. 1) (Niloy and Islam, 2017; Chanda et al., 2022). The original bar in the experimental beam is substituted by an equal amount of wire mesh by mass in the type I beams (CB-1 and CB-2). In CB-1, only the web reinforcement is replaced, whereas in CB-2, both the web and the main reinforcement are replaced by wire mesh. The wire diameter and the size of the wire mesh opening are given in Table 1. In beam type II, the experimental beam is reinforced with wire mesh, as shown in (Fig. 2), which includes the possible arrangement of wire mesh from a practical point of view. The opening size of the wire mesh is 25 mm, which is used for retrofitting beams in Group II. In group II, the wire mesh is first glued around the periphery of the beam and then tightened using the royal plus and screw (Niloy and Islam, 2017). Then a 25 mm fresh cement mortar cover was used above the wire mesh. Table 2 shows the material. An isotropic and bilinear stress-strain model is assumed for the wire mesh and rebar. To determine the compressive strength of concrete, cylindrical specimens were prepared while experimental control beams were cast. The compressive strength of concrete, 22 MPa, is determined by a laboratory test (Niloy and Islam, 2017). A multilinear isotropic material model specified by Eqns. (1) and (2) as shown in (Fig. 3), is assumed for concrete materials.

$$f = \frac{E_c \varepsilon}{1 + \left(\frac{\varepsilon}{\varepsilon_0}\right)^2} \quad (1)$$

$$\varepsilon_0 = \frac{2 f_c'}{E_c} \quad (2)$$

Here, f is the concrete stress (MPa) at strain ε, ε_0 is the strain at crushing strength, f'_c. The rupture modulus of concrete is measured by Eq. (3).

$$f_r = 0.7\sqrt{f_c'} \quad (3)$$

The shear transfer coefficient determines the amount of shear transfer through a crack, and it ranges from 0 to 1.0, with 0 representing no shear transfer and 1.0 representing full shear transfer. In this study, the coefficient of open shear transfer

Table 1. **Definition of various types of beams**

Beam type	Model	Definition of the beam
I	CB	Experimental beam
	CB-1	The web reinforcement of CB is replaced by wire mesh (3.5 mm wire has 25 mm mesh opening)
	CB-2	Both web and main bars of CB are replaced by wire mesh (4.7 mm wire has 25 mm mesh opening)
II	FRB-1	Ferrocement retrofitted beam with square wire mesh along three sides
	FRB-2	Ferrocement retrofitted beam with only bottom side square wire mesh
	FRB-3	Ferrocement retrofitted beam with diagonal wire mesh along three sides
	FRB-4	Ferrocement retrofitted beam with only bottom side diagonal wire mesh
	FRB-5	Ferrocement retrofitted beam with all side square wire mesh

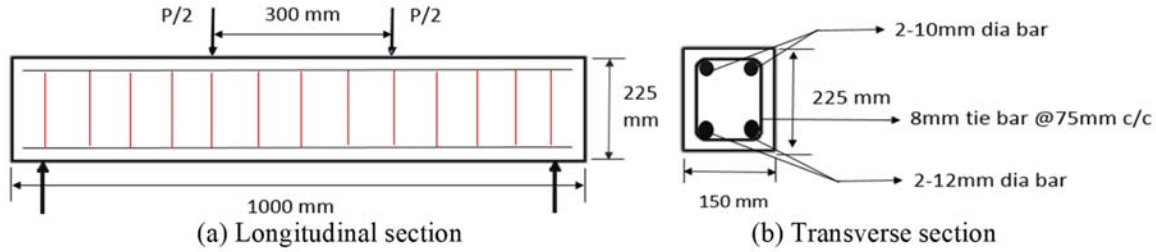

Fig. 1. Geometry and boundary conditions of experimental beam (CB)

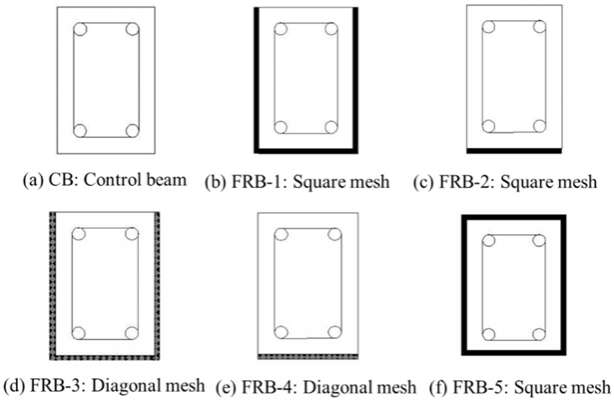

Fig. 2. Cross-section of different retrofitted beams with wire mesh

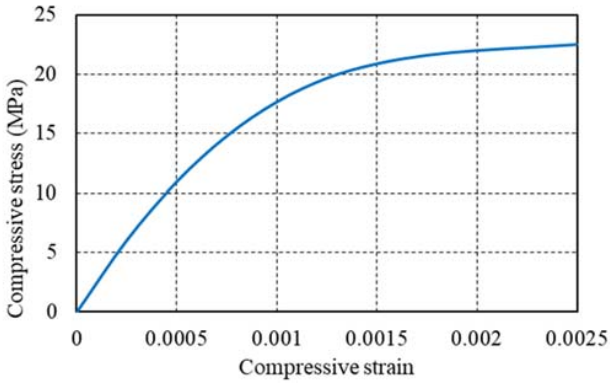

Fig. 3. Multilinear stress-strain curve of concrete

is assumed to be 0.30. It is assumed to be larger than 0.20 to avoid the difficulties related to the convergence of solutions. The close shear transfer coefficient is assumed to be 1.0 (Tjitradi et al., 2017; Si et al., 2008). In the finite element analysis, it is assumed that concrete and steel are isotropic. There is adequate bond strength at the interface of these two materials.

The Solid65 and Link180 elements that are used to discretize the reinforced concrete beam are shown in (Fig. 4) (ANSYS, 2013). Solid65 has eight nodes. It is used to model concrete parts, beam support plates, and loading plates. Link8 has two nodes that are used to model rebar and wire mesh. Each element has three translation degrees of freedom at each node. The FE models of different types of beams are shown in (Fig. 5). The support reactions

Table 2. **Material parameters**

Material	E [GPa]	v	f_c' [MPa]	σ_y [MPa]	E_t [MPa]	Open Shear Transfer Coefficient	Close Shear Transfer Coefficient
Concrete	20	0.2	22.0	—	—	0.3	1.0
Support and loading plates	200	0.3	—	—	—	—	—
Reinforcement and wire mesh	200	0.3	—	414	20	—	—
E: Elastic modulus, *v*: Poisson's ratio, f_c': Concrete strength, σ_y: Yield strength, and E_t: Tangent modulus							

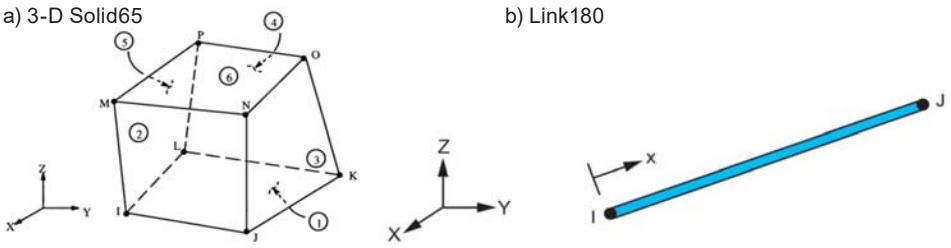

Fig. 4. Element used to discretize reinforced concrete beam

and imposed vertical load at the 1/3rd point of the beam are shown in (Fig. 5d). The beam ends are modelled as simple support conditions. Steel and concrete share a common node, and it is assumed that the strain in concrete is equal to the strain in steel. The whole vertical load is divided into two parts and placed at the 1/3rd point location of the beam, as shown in (Fig. 5d). The finite element model has about 3000 elements, around 4000 nodes, and 10,000 degrees of freedom. A convergence analysis is performed to check the competency of the finite element model. It is found that the beam deflection at the midspan is almost the same when the number exceeds 2500 as shown in (Fig. 6). The solution for the analyzed beam is obtained through an incremental nonlinear static analysis.

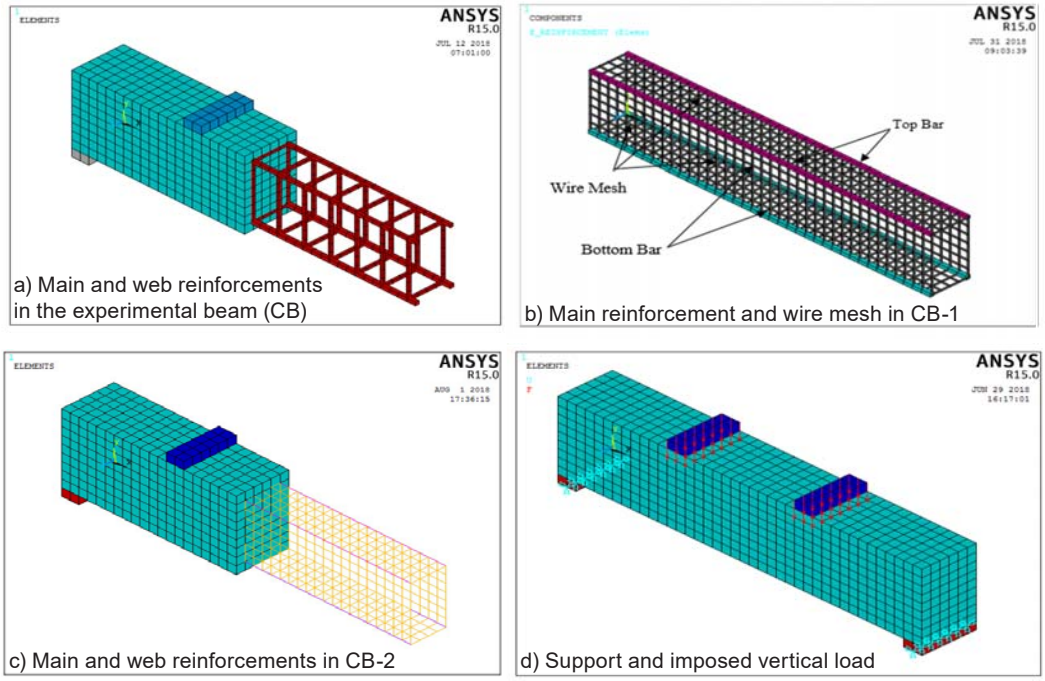

Fig. 5. FE models of beam

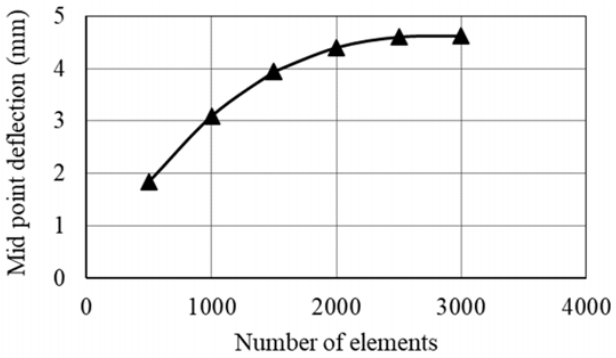

Fig. 6. Convergence test of the FE model

Model Verification

The loading test that was conducted using the UTM in the structural engineering laboratory at Chittagong University of Engineering & Technology is shown in (Fig. 7a). The contour for the deformed shape of the experimental beams found from the finite element analysis is shown in (Fig. 7b). A comparison of the displacement at different levels of the load between results of the finite element analysis and that from the loading test is shown in (Fig. 8). A detailed explanation of the model verification can be found in Chanda et al. (2022). From a comparison, it is assumed that the finite

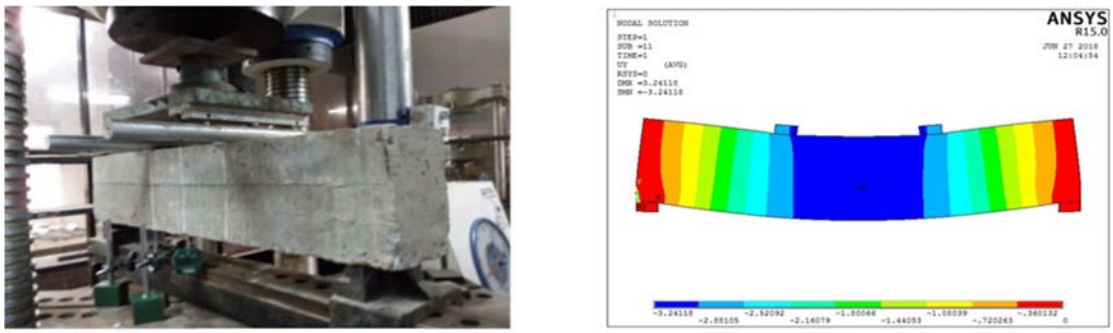

(a) Flexural test (Niloy and Islam, 2017) (b) Deflection from FE model

Fig. 7. Deflection of the beam (a) Experiment (b) Finite element analysis

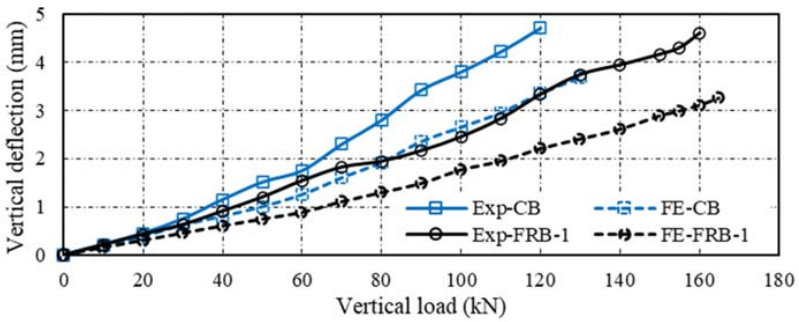

Fig. 8. Comparison of vertical displacement between experimental and finite element analysis at different levels of load

element model is quite accurate and can be used to predict the flexural behavior under vertical load.

Performance of the Beams

The load versus vertical displacement for the retrofitted beams and that for the experimental beams until the ultimate cracking point is shown in (Fig. 9a). The deflection is measured at the midspan of the beams. The deflection of beams shows a proportional relationship with the applied load. All beams remain elastic up to a displacement of 1.0 mm, and the elastic capacity lies in the range of 50~70 kN. The capacity of the retrofitted beams is higher than that of the experimental beam (CB), which is more pronounced in the large loading range. The flexural capacities of the FRB-1, FRB-3, and FRB-5 are about 32%~40% greater than those of the CB. Similarly, the capacity of FRB-2 and FRB-4 is about 15% higher than that of the CB. The superior capacity of FRB-1, FRB-3, and FRB-5 beams is expected due to the confinement effect of the U-shaped or rectangular-shaped arrangement of wire mesh. Besides, the flexural capacity of retrofitted beams made with square and diagonal openings of wire mesh does not differ significantly. The figures show that, beyond the displacement of 2.5 mm, the retrofitted beams exhibit large vertical displacement without increasing failure loads where cracks are observed before the failure. It is ensured that ferrocement enhances the ductility of beams, which is necessary for balance control design. It is found that only the replacement of shear reinforcement by wire mesh has no significance as shown (Fig. 9b). However, when both main and shear reinforcements are replaced by wire mesh, the capacity remains below CB. On the other hand, it increases the ultimate load capacity by 12% and the vertical displacement at the midspan by 25% at ultimate load. Therefore, wire mesh enhances the ductility and flexural capacity of a reinforced concrete beam.

The first and ultimate cracking loads among the retrofitted and experimental beams are shown in (Fig. 10). Imposed loads on the beams at the first and ultimate cracks in the CB and FRB-1, which are found from the experiment, are comparable with the FE computation. The maximum deviation of the FE computation is 12.5% and 7.6% for the first and ultimate cracking loads, respectively. The distribution of flexural cracks under the first and ultimate cracking loads is shown in (Fig. 11). The crack pattern in the beam found in the experiment and that from the finite element analysis are also comparable, which indicates the efficiency of the FE computation. According to (Fig. 10a), the first cracking load found from the loading test is about 80 kN for CB and 90 kN for FRB-1. The ultimate load capacity for the same beams is 120 kN and 160 kN, respectively. It indicates that capacity is increased by 13% and 33% at the first and ultimate cracking stages, respectively, due to the implementation of wire mesh along three sides of the beam. It is

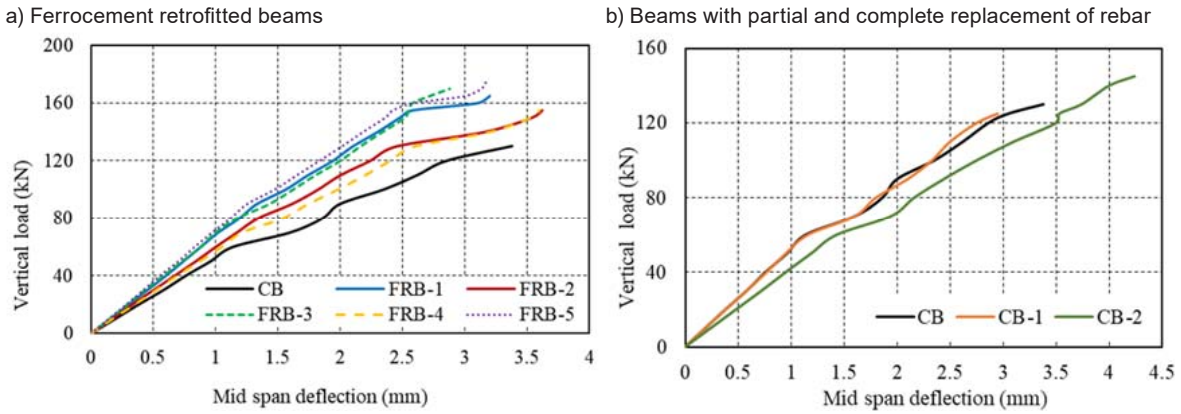

Fig. 9. Load-deflection of the analyzed beams

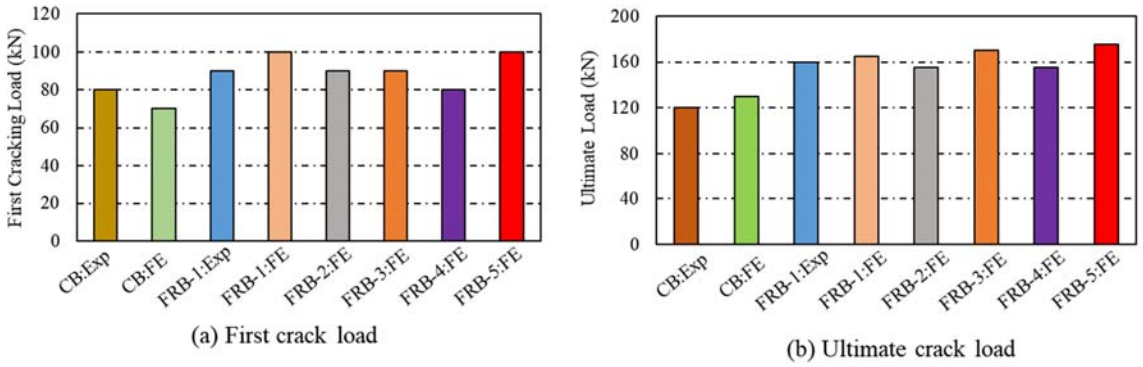

Fig. 10. First and ultimate crack loads in different retrofitted beams

also seen that the first cracking load increases by 42.85%, 28.57%, 28.57%, 14.28%, and 42.85% in the case of FRB-1, FRB-2, FRB-3, FRB-4, and FRB-5, respectively, compared to the numerical result of the CB. The ultimate load capacity of CB and FRB-1 is 130 kN and 165 kN, respectively, and the ultimate capacity increases when wire mesh is placed along three sides (FRB-1, FRB-3, and FRB-5) of the beam. The ultimate capacity of FRB-1, FRB-2, FRB-3, FRB-4, and FRB-5 is 26.93%, 19.23%, 30.76%, 19.23%, and 34.61%, respectively, higher than that of the CB. In general, it can be concluded that wire mesh increases the flexural capacity of a beam by 15%~43% at the first crack condition and 20%~35% at the ultimate load condition, and these capacities increase significantly when wire mesh is used along three sides of the beam.

The first and ultimate flexural crack and its propagation and distribution in different retrofitted beams are shown in (Fig. 12). In comparison with (Fig. 11), the flexural crack is more uniform and well distributed in the beam retrofitted with wire mesh. A similar crack pattern in the CB-1 and CB-2 in comparison with the crack pattern in the CB is observed in (Fig. 13). It indicates that when the main reinforcement is replaced by wire mesh, the length of the crack part of the concrete beam is enlarged. When both shear and flexural reinforcements are

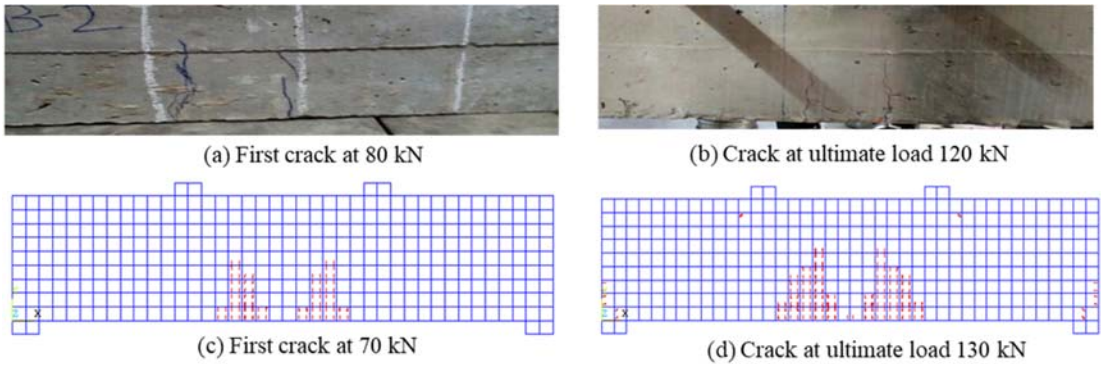

Fig. 11. First and ultimate crack distribution: Experiment beam CB: (a, b) and FE analysis (c, d)

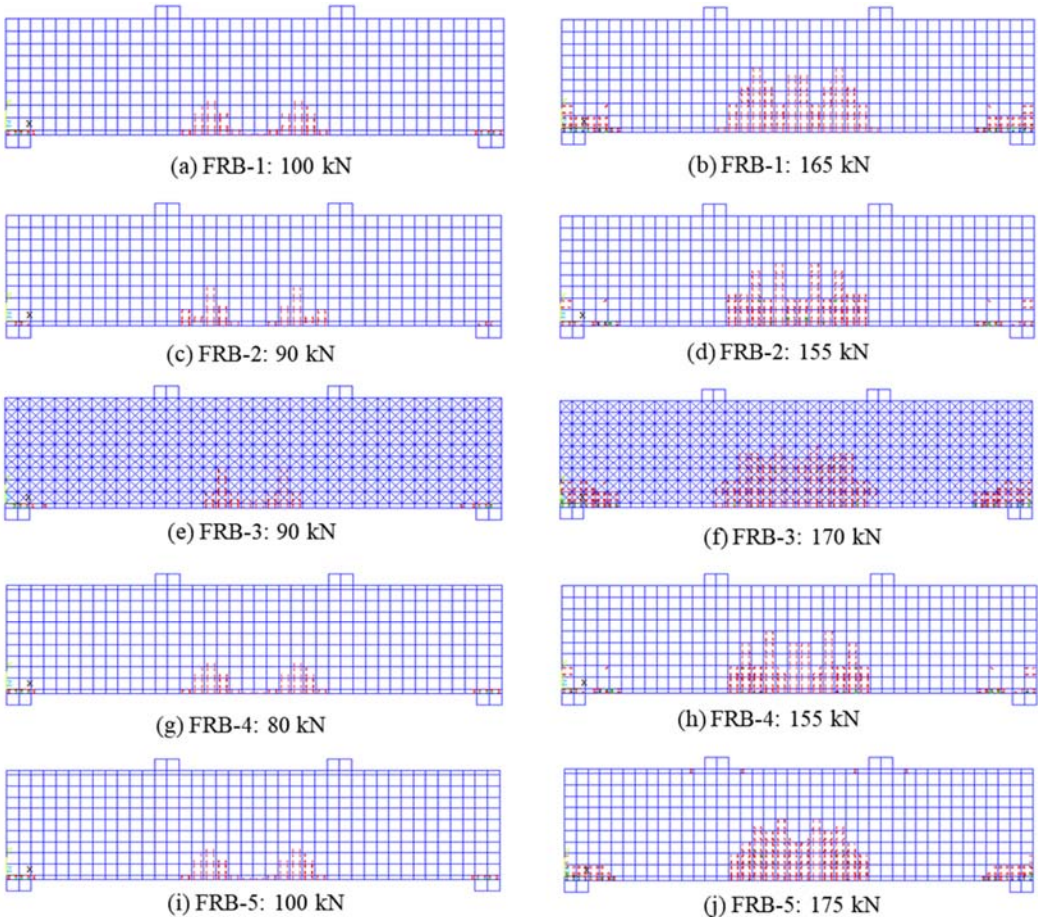

Fig. 12. Flexural crack distribution in different retrofitted beams at first crack and ultimate loads crack

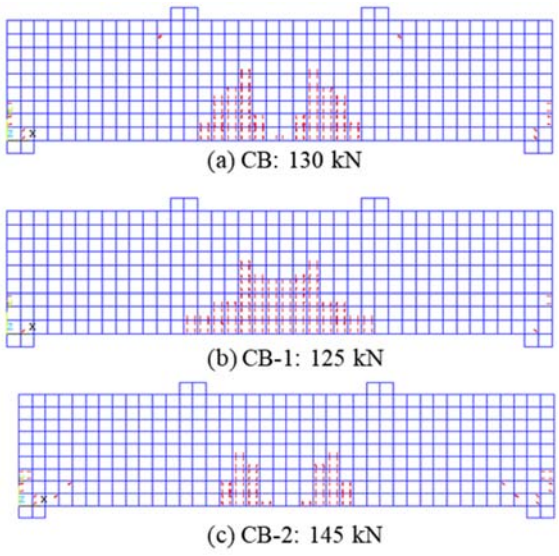

Fig. 13. Flexural crack distribution in different beams

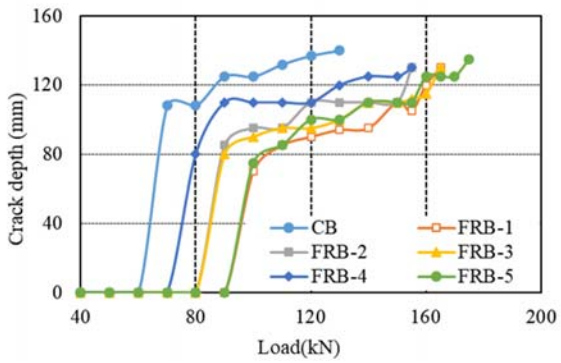

Fig. 14. crack depth in different retrofitted beams

replaced by wire mesh, the crack depth is reduced due to the confinement effect. The crack depth in different beams is shown in (Fig. 14). Under a fixed value of the imposed load, the flexural crack depth is the lowest in the FRB-1, FRB-3, and FRB-5 in comparison to the CB, FRB-2, and FRB-4. It implies that the flexural tension crack is improved when wire mesh is employed in the reinforced concrete beam.

Flexural Stress in Concrete

The flexural stress at the top and bottom surfaces is shown in (Fig. 15a). These stresses are estimated at the middle of the span of the beams. These stresses are proportional to the vertical displacement of the beam. It shows that the top fiber stress (compression) in the CB is comparable with that of the CB-1. The maximum value of compression

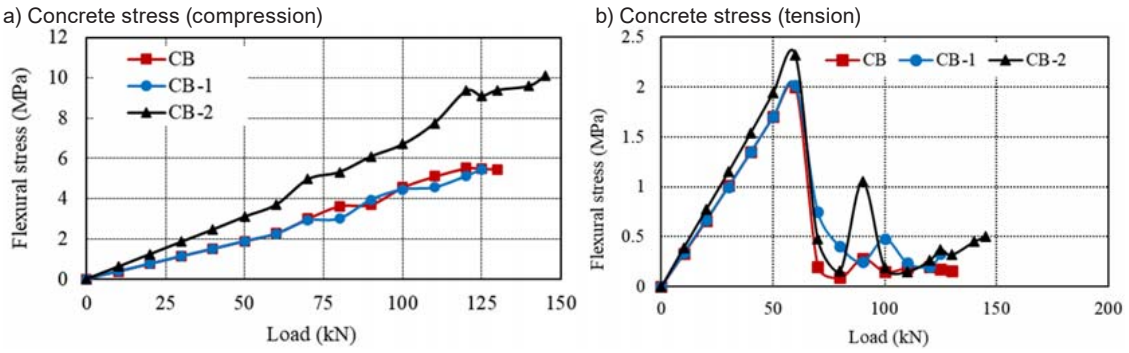

Fig. 15. Flexural stress in different experimental beams

stress in CB-1 is 5.9 MPa at a failure load of 125 kN. The compression stress in the CB-2 at the same level of vertical load is about two times that of the CB or CB-1. The flexural stress (tension) at the mid-span location is shown in (Fig. 11b). It shows that a beam reinforced with wire mesh is capable of sustaining a high bending force. The first crack within the beams is observed at 60 kN, until which the stress within the beam is proportional to the strain. Concrete stress (tension) drops significantly and moves to zero due to an increase in vertical load after the first crack appears. The concrete stress remains close to zero because the tension force is carried by the reinforcement. The flexural stress in retrofitted beams with different layouts of wire mesh in comparison with the stress in the experimental beam is given in (Fig. 16). The peak ultimate compressive and tensile stresses in the retrofitted beams are comparable to those of the CB and lie between 5.0~6.0 MPa and 2.0 MPa, respectively. It means that the stress in the retrofitted beams is not significantly changed when reinforced with wire mesh. After the first flexural crack, the tensile stress in the bottom concrete becomes unpredictable.

Optimum Length of Wiremesh

The use of wire mesh along the entire length of a partially damaged beam is uneconomical. Therefore, the optimum length of the wire mesh for satisfactory flexural performance is of concern. In the current study, the wire mesh length is defined as a percentage of the span of the beam. The optimum length is the length of the wire mesh beyond which the stress and deflection remain unchanged under a fixed flexural load. The optimum length is determined using the incremental load procedure. The maximum load is assumed to be 140 kN. The stress is measured at the tip of the major crack, while the deflection is at the middle of the span length. The midspan deflection in the retrofitted beams with different lengths of the wire mesh is shown in (Fig. 17a). The rate of displacement decreases when the length of the wire mesh is increased. For a length exceeding 50%, the displacement is almost the same. Similarly, flexural stress, as shown in (Fig. 17b) remains the same when length exceeds 40%. In general, the influence of wire mesh length is negligible when the length of wire mesh exceeds 50%. Therefore, 50% of the span length of a beam may be considered the optimum length of wire mesh.

Conclusion

The FE approach is used to evaluate the bending behavior of reinforced concrete beams strengthened with wire mesh. The possibility of a concrete beam that has been partially or completely reinforced with steel wire is also being studied. The finite element model of the experimental beam is tested against the loading test results. The bending load performance of the beams is assessed in terms of load carrying

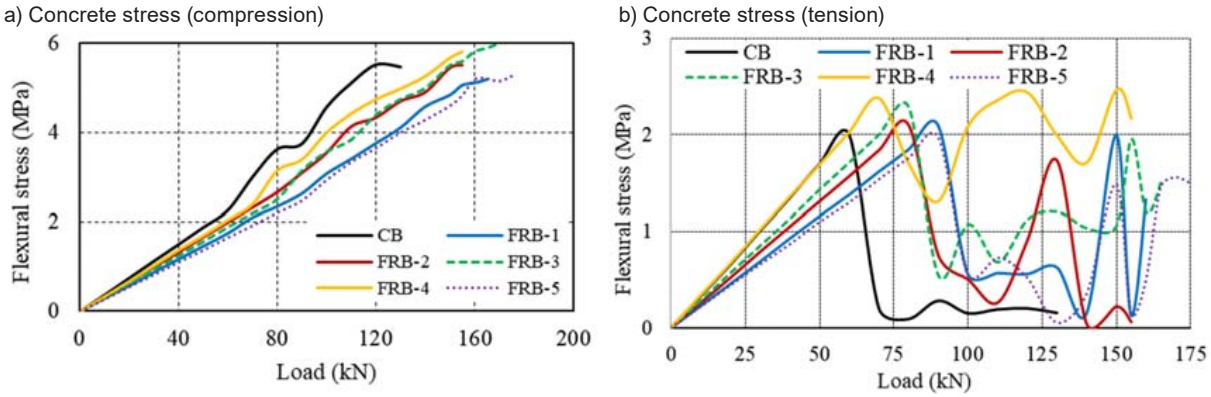

Fig. 16. Flexural stress at different retrofitted beams

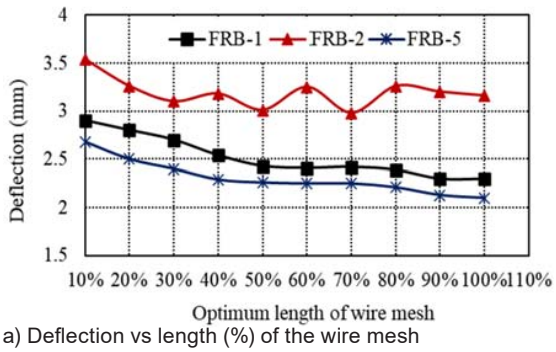

a) Deflection vs length (%) of the wire mesh

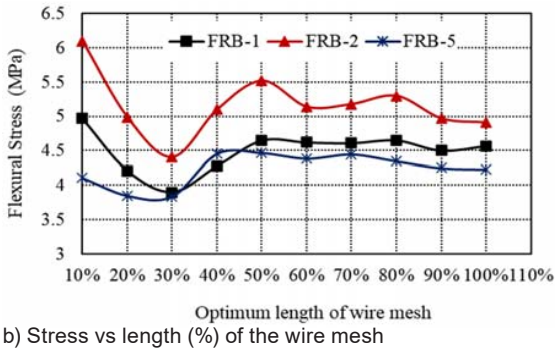

b) Stress vs length (%) of the wire mesh

Fig. 17. Deflection and flexural stress for different lengths of the weir mesh

capacity, beam deflection, working stress, crack and crack depths, and wire mesh optimal length. The main findings of this research are briefly summarized below:

– A beam in which rebars are partially or completely replaced by steel wire or a steel-reinforced concrete beam strengthened with wire mesh has greater bending capacity than a conventional steel-reinforced concrete beam. The wire mesh increases the flexural capacity by 15%~43% at the first crack and 20%~35% at the ultimate load, which is significant when wire mesh is used along three sides of a beam.

– The deflection and concrete stress at the failure load level are large when regular reinforcement is replaced with an equal quantity of wire mesh by mass. The beam retrofitted with wire mesh has higher ductility and lower flexural stress.

– Wire mesh improves the flexural crack distribution and reduces the depth of flexural cracks.

The length of wire mesh equal to 50% of the span length is sufficient to reinforce a partially damaged beam, beyond which the concrete stress and beam deflection remain unaffected.

References

Adhikary, B. B. and Mutsuyoshi, H. (2006). Shear strengthening of reinforced concrete beams using various techniques. *Construction and Building Materials, 20*, pp. 366–373. DOI: https://doi.org/10.1016/j.conbuildmat.2005.01.024

Anthony J. Wolanski, B.S. (2004). Flexural Behavior of Reinforced and Prestressed Concrete Beams Using Finite Element Analysis, *Master's Thesis*, Marquette, May, 2004.

ANSYS Inc., Release 15.0 Documentation, Theory References, 2013.

Ashraf, M., Khan, A. N., Naseer, A., Ali, Q., and Alam, B. (2012). Seismic behavior of unreinforced and confined brick masonry walls before and after ferrocement overlay retrofitting. *International Journal of Architectural Heritage*, 6(6), pp. 665–688. DOI: https://doi.org/10.1080/15583058.2011.599916.

Abdullah and Takiguchi, K. (2003). An investigation into the behavior and strength of reinforced concrete columns strengthened with ferrocement jackets, *Cement and Concrete Composites,* 25(2), pp. 233–242. DOI: https://doi.org/10.1016/S0958-9465(02)00005-7.

Chanda, M., Zisan, M.B., Dhar, A. (2022). Flexural Behaviour of Reinforced Concrete Beams Retrofitted with Ferrocement. In: Arthur, S., Saitoh, M., Pal, S.K. (eds) *Advances in Civil Engineering. Lecture Notes in Civil Engineering*, vol 184. Springer, Singapore. DOI: 10.1007/978-981-16-5547-0_24.

El-Wafa, M. A., and Fukuzawa, K. (2008). Various sizes of wire mesh reinforcement effect on tensile behavior of ferrocement composite plates. *Proceedings of the 10th International Summer Symposium Organized*, JSCE, Tokyo, Japan.

El-Wafa, M. A., and Fukuzawa, K. (2010). Characteristics of ferrocement thin composite elements using various reinforcement meshes in flexure. *Journal of Reinforced Plastic Composite*, 29(23), pp. 3530-3539. DOI: https://doi.org/10.1177/0731684410377814

El-Sayed, T. A., and Erfan, A. M. (2018). Improving shear strength of beams using ferrocement composite. *Construction and Building Materials*, 172, pp. 608–617. DOI: https://doi.org/10.1016/j.conbuildmat.2018.03.273

Faherty, K. F. (1972). An Analysis of a Reinforced and a Prestressed Concrete Beam by Finite Element Method. *Doctorate's Thesis*, University of Iowa, Iowa City.

Fahmy, E. H., Shaheen, Y., M., and Zeid, A. (2004). Development of ferrocement panels for floor and wall construction, *5th Structural Specialty Conference of the Canadian Society for Civil Engineering,* Canada.

Fahmy, E. H., Shaheen Y. B., Abou, Z.M.D., and Gaafar, A. M. (2012). Ferrocement sandwich and hollow core panels for floor construction. *Canadian Journal of Civil Engineering,* 27 (1), pp.1297–1310. DOI: https://doi.org/10.1139/cjce-2011-0016

Fahmy, E. H., Shaheen, Y. B. I., and Abdelnaby, A. M. (2014). Applying the Ferrocement Concept in Construction of Concrete Beams Incorporating Reinforced Mortar Permanent Forms. *International Journal of Concrete Struct and Materials*, 8, pp. 83–97. DOI: https://doi.org/10.1007/s40069-013-0062-z

Gaidhankar, D. G., Kulkarni, M. S., and Jaiswal, A. R. (2017). Ferrocement Composite Beams Under Flexure. *International Research Journal of Engineering and Technology*, 10, pp. 117–124.

G.J. Al-Sulaimani, I.A. Basunbul, E.A. Mousselhy (1991). Shear behavior of ferrocement box beams. *Cement and Concrete Composites*, 13(1), pp. 29–36. DOI: https://doi.org/10.1016/0958-9465(91)90044-I

Hago, A. W., Al-Jabri, K. S., and Alnuaimi, A. S. (2005). Ultimate and service behavior of ferrocement roof slab panels. *Construction and Building Materials*, 19(1), pp. 31–37. DOI: https://doi.org/10.1016/j.conbuildmat.2004.04.034

Hasan, M. A., Akiyama, M., Kashiwagi, K., Kojima, K., and Peng, L. (2020). Flexural behaviour of reinforced concrete beams repaired using hybrid scheme with stainless steel rebars and CFRP sheets. *Construction and Building Materials*, 208, pp. 228–241. DOI: https://doi.org/10.1016/j.conbuildmat.2020.120296

Hasan, M. A., Akiyama, M., Kojima, K., and Izumi, N. (2022). Shear behavior of reinforced concrete beams repaired using hybrid scheme with stainless steel rebars and CFRP sheets. *Construction and Building Materials*, 363, 12817. DOI: https://doi.org/10.1016/j.conbuildmat.2022.129817

Husein, N. R., Agarwal, V. C. and Rawat, A. (2013). An experimental study on using lightweight web sandwich panel as a floor and a wall, *International Journal of Innovative Technology and Exploring Engineering*, 3, pp. 2278–3075.

Jamil, A. K., Zisan, M. B., Alam, M. R., and Alim, H. (2013). Restrengthening of RCC Beam by Beam Jacketing, *Malaysian Journal of Civil Engineering* 25(2), pp. 119-127. DOI: https://doi.org/10.11113/mjce.v25.15847.

Kadir, M. A., Samad, A. A., Muda, Z. C. and Ali A. (1997). Flexural behavior of composite beam with ferrocement permanent formwork. *Journal of Ferrocement*, 27, pp. 209–214.

Kaish, A. B. M. A., Alam, M. R., Zain, M. F. M., and Wahed, M. A. (2012). Improved ferrocement jacketing for restrengthening of square RC short column. *Construction and Building Materials,* 36, pp. 228–237. DOI: https://doi.org/10.1016/j.conbuildmat.2012.04.083.

Kaish, A. B. M. A, Alam. M. R, Jamil. M. and Wahed. M. A. (2013). Ferrocement Jacketing for Restrengthening of Square Reinforced Concrete Column under Concentric Compressive Load, *Journal of Procedia Engineering*, 54, pp. 720 – 728. DOI: https://doi.org/10.1016/j.proeng.2013.03.066

Kaish, A. B. M. A, Jamil. M, Raman S. N., Zain M. F. M. and Alam. M. R. (2016). An approach to improve conventional square ferrocement jacket for strengthening application of short square RC column. *Journal of Material and Structure*, 49, pp. 1025–1037. DOI: https://doi.org/10.1617/s11527-015-0556-z

Kibria, B. M. G., Ahmed, F., and Ahsan, R. (2020). Experimental investigation on behavior of reinforced concrete interior beam column joints retrofitted with fiber reinforced polymers. *Asian Journal of Civil Engineering,* 21, pp. 157–171. DOI: https://doi.org/10.1007/s42107-019-00204-3

Leeanansaksiri, A., Panyakapo, P., and Ruangrassamee A. (2018). Seismic capacity of masonry infilled RC frame strengthening with expanded metal ferrocement. *Engineering Structures*, 159:, pp. 110–127. DOI: https://doi.org/10.1016/j.engstruct.2017.12.034.

Li, B., and Lam, E. S. S. (2018). Influence of interfacial characteristics on the shear bond behaviour between concrete and ferrocement. *Construction and Building Materials*, 176, pp. 462–469. DOI: https://doi.org/10.1016/j.conbuildmat.2018.05.084

Li, B., Lam, E. S. S., Wu, B., and Wang, Y. Y. (2013). Experimental investigation on reinforced concrete interior beam–column joints rehabilitated by ferrocement jackets. *Engineering Structures*, 56, pp. 897–909. DOI: https://doi.org/10.1016/j.engstruct.2013.05.038

Matalkah, F., Bharadwaj, H., and Soroushian, P. (2017). Development of sandwich composites for building construction with locally available materials. *Construction and Building Materials*, 147, pp. 380–387. DOI: https://doi.org/10.1016/j.conbuildmat.2017.04.113

Muhit, I. B., Jitu, N. E. T., and Alam, A. R, (2021). Structural shear retrofitting of reinforced concrete beam: multilayer ferrocement technique. *Asian Journal of Civil Engineering*, 22, pp. 191–203. DOI: https://doi.org/10.1007/s42107-020-00306-3

Niloy, S. H., and Islam, M. M. (2017). Flexural Behavior of Reinforced Concrete Beams Retrofitted with Ferrocement. *Bachelor's Thesis*, Chittagong University of Engineering & Technology, Chittagong, Bangladesh.Oehlers, D. J., Nguyen, N. T., and

Bradford, M. A. (2000). Retrofitting by adhesive bonding steel plates to the sides of R.C. beams. Part 1: Debonding of plates due to flexure. *Structural Engineering and Mechanics*, 9(5), pp. 491–504. DOI: https://doi.org/10.12989/SEM.2000.9.5.491

Obaidat, Y. T., Heyden, S., and Dahlblom, O. (2011). Retrofitting of reinforced concrete beams using composite laminates. *Construction and Building Materials, 25*(2), pp. 591–597. DOI: https://doi.org/10.1016/j.conbuildmat.2010.06.082

Pham, H., and Al-Mahaidi, R. (2004). Experimental investigation into flexural retrofitting of reinforced concrete bridge beams using FRP composites. *Composite Structures, 66*(1–4), pp. 617–625. DOI: https://doi.org/10.1016/j.compstruct.2004.05.010

Shaaban, I. G. (2002), Expanded Wire Fabric Permanent Formwork for Improving Flexural Behaviour of Reinforced Concrete Beams, *Proceedings of the International Congress: Challenges of Concrete Construction*, Dundee, Scotland, UK.

Shaaban, I. G., Shaheen, Y. B., and Elsayed E. L. (2018). Flexural characteristics of lightweight ferrocement beams with various types of core materials and mesh reinforcement. *Construction and Building Materials*, 171, pp. 802–816. DOI: https://doi.org/10.1016/j.conbuildmat.2018.03.167

Shaaban, I. G., Shaheen, Y. B. I., and Elsayed, E. L. (2013). Flexural behaviour and theoretical prediction of lightweight ferrocement composite beams. *Case Studies in Construction Materials*,9, pp. e00204. DOI: https://doi.org/10.1016/j.cscm.2018.e00204

Shaaban, I. G. and Seoud, O. A. (2018). Experimental behavior of full-scale exterior beam-column space joints retrofitted by ferrocement layers under cyclic loading, *Case Studies in Construction Materials*, 8, pp. 61–78. DOI: https://doi.org/10.1016/j.cscm.2017.11.002

Shaheen, Y. B. I., and Eltehawy, E. A. (2017). Structural behaviour of ferrocement channels slabs for low-cost housing. *Challenge Journal of Concrete Research Letter*, 8 (2), pp. 48–64. DOI: https://doi.org/10.20528/CJCRL.2017.02.002

Si, B.J., Sun, Z.G., Ai, Q.H., Wang, D.S., and Wang, Q.X, (2008). Experiments And Simulation Of Flexural-Shear Dominated Rc Bridge Piers Under Reversed Cyclic Loading, *The 14th World Conference on Earthquake Engineering,* Beijing, China.

Sowmya, E., and Venkatasubramani, R. (2017). Numerical Study of Wire Mesh Orientation on Retrofitted RC Beams Using Ferrocement Jacketing. *International Research Journal of Engineering & Technology*, 4(11), pp.1471-1475.

Tanaka T., Yagi K., and Kojima N. (1994). Retrofit method with carbon fiber for reinforced concrete structures, *Advanced Composite Materials*, 4(2), pp.183-195. DOI: 10.1163/156855194X00303.

Tjitradi, D, Eliatun, E, and Taufik, S. (2017). 3D ANSYS Numerical Modeling of Reinforced Concrete Beam Behavior under Different Collapsed Mechanisms. *International Journal of Mechanics and Applications*, 7(1), pp.14-23. DOI: 10.5923/j.mechanics.20170701.02

Van Cao, V., and Quoc Nguyen, T. (2019). Effects of CFRP/GFRP flexural retrofitting on reducing seismic damage of reinforced concrete frames: a comparative study. *Asian Journal of Civil Engineering,* 20, pp. 1071–1087. DOI: https://doi.org/10.1007/s42107-019-00173-7

Yousef S. Al Rjoub, Ahmed M. Ashteyat, Yasmeen T. Obaidat & Saleh Bani-Youniss (2019). Shear strengthening of RC beams using near-surface mounted carbon fibre-reinforced polymers. *Australian Journal of Structural Engineering, 20*(1), pp. 54–62. DOI: https://doi.org/10.1080/13287982.2019.156561

Zisan M. B., Haque, M. N., Chowdhury, M. S. U. (2011). A Finite Element Analysis for Optimization of Flexural Cracked Beam Strengthened using CFRP composites, Proceedings of the International Conference on Mechanical Engineering and Renewable Energy 2011 (ICMERE2011) 22-24 December 2011, Chittagong, Bangladesh.

DOI: 10.23968/2500-0055-2023-8-1-82-87

STUDYING THE OPERATION OF THE PNEUMOHYDRAULIC SHOCK ABSORBER WITH ZERO BOTTOMING IN THE SUSPENSION OF A TRANSPORT AND HANDLING MACHINE

Sergey Repin*, Ivan Vorontsov, Denis Orlov, Roman Litvin

Saint Petersburg State University of Architecture and Civil Engineering
Saint Petersburg, Russia

*Corresponding author's e-mail: repinserge@mail.ru

Abstract
Introduction: The movement smoothness of transport and handling machines (THM) (excavators, cranes, road maintenance equipment, etc.) on a vehicle chassis significantly affects their durability as a result of the large weight of equipment and uneven load distribution along the axes of the base chassis, which causes heavy dynamic loads when moving along roads with imperfect pavement. However, THM often have to move along those very roads. **Purpose of the study:** We aimed to increase the movement smoothness of THM on a vehicle chassis by using a shock absorber of new design as the main vehicle undercarriage suspension element. **Methods:** The hydropneumatic shock absorber is considered the most common. The principle of its operation is based on hydraulic resistance that occurs when the piston with the rod move in a space filled with oil, while the gas in the closed part is compacted, compensating for changes in the internal volume. Most often, the main disadvantage related to the operation of hydropneumatic shock absorbers (HPSA) is the probability of bottoming when hitting a barrier (obstacle), which results in dynamic loads reducing the service life of the vehicle and the parts of the shock absorber. **Results:** The paper describes a new shock absorber design ruling out bottoming, provides a mathematical model of its elastic response, and presents the results of modeling in Mathcad, confirming the operability of the device.

Keywords: movement smoothness, shock absorber, elastic response.

Introduction

The movement smoothness of transport and handling machines (THM) (excavators, cranes, road maintenance equipment, etc.) on a vehicle chassis significantly affects their durability as a result of the large weight of equipment and uneven load distribution along the axes of the base chassis, which causes heavy dynamic loads when moving along roads with imperfect pavement. However, THM often have to move along those very roads. Particularly heavy dynamic loads occur when they move over large irregularities causing shock absorber bottoming. Often, after relocation, it may be required to repair mechanical damage to the operating equipment.

The movement smoothness of THM is guaranteed by a system of devices ensuring elastic connection between the wheels and the body, called suspension. The suspension absorbs energy from bumps and shocks that occur while moving along the road. The suspension includes both damping and elastic components. The latter reduce the dynamic load that occurs during suspension operation when moving over rough roads. The elements of the damping components dampen the vibrations of the body. In standard suspensions, damping and elastic components are usually separated and operate in parallel (Carway.info, 2017), Dobromirov et al., 2006; Rotenberg, 1972).

The hydropneumatic shock absorber is considered the most common. The principle of its operation is based on hydraulic resistance that occurs when the piston with the rod move in a space filled with oil, while the gas in the closed part is compacted, compensating for changes in the internal volume. Most often, the main disadvantage related to the operation of hydropneumatic shock absorbers (HPSA) is the probability of bottoming when hitting a barrier (obstacle), which results in dynamic loads reducing the service life of the vehicle and the parts of the shock absorber.

Recently, an elastic component has been introduced into this type of suspension, which makes it possible to change the stiffness and clearance of the suspension. The operation of this component is based on a pneumatic cylinder (Akopyan, 1979; Chelomey, V. N.,1981; Lukin, P. P. et al., 1984; Techautoport.ru, 2022). This scheme significantly reduces the probability of shock absorber operation in bottoming when it is compressed. Besides, it has a complex design because its parts are made in the

form of individual components. These components require other attachment points for full operation, as well as space for placement and connection with the linkage system.

Widely distributed HPSA meet the requirements for the functionality of suspensions: the combination of a hydro cylinder and a pneumatic cylinder makes it possible to achieve the effect of a “gas spring” (Audi, 2001; Zaitsev, A. V.,2007; Zhileykin, M. M. et al., 2012; Repin et al., 2019; Repin et al., 2020). The specifics of their operation is in reducing the risk of HPSA bottoming during compression, but at rebound the probability of bottoming remains quite high. Thus, as a result of studies and HPSA modeling, a new scheme of HPSA operation with two hydraulic and pneumatic cylinders installed both above and below was proposed, which significantly reduced the probability of HPSA bottoming both during compression and rebound.

During the studies, we simulated the operation of the modified HPSA equipped with two gas springs placed above and below the hydraulic part of the shock absorber and ruling out its bottoming during compression and rebound.

Shock absorber operation

Fig. 1 presents a new shock absorber design (Repin, 2022).

Places of rigid connection are shown with crosses.

Chambers G1 and G3 act as an elastic element (gas springs) and rule out shock absorber bottoming during compression (G1) and rebound (G3). The clearance can be adjusted on account of the difference in the values of pumping pressure in chambers G1 and G3.

Geometric parameters of the HPSA

The geometric parameters of the HPSA are determined based on the technical characteristics of the machines and shown in Fig. 2.

$S_{e1}...S_{e5}$ — extra stroke of the shock absorber elements;

S_{d_comp}, S_{d_reb} — dynamic compression and rebound stroke, respectively;

$S_{full} = S_{d\_comp} + S_{d\_reb}$ — full stroke of the shock absorber;

S_{p2} — stroke of the pneumatic piston at full stroke of the hydraulic piston;

h_{p1} — height of the hydraulic piston;

h_{p2} — height of the pneumatic piston;

d_1, L_1 — diameter and length of the hydraulic cylinder;

d_2, L_2 — diameter and length of the pneumatic cylinder;

δ_{wall} — thickness of the cylinder walls;

δ_g — gap between the cylinders;

L_{max}, L_{min} — maximum and minimum length of the HPSA;

L_{av} — average length of the HPSA, which is comparable with the length at the resultant load P_{des};

L_{br_up}, L_{br_low} — distance from the pneumatic cylinder to the center of the upper and lower mounting bracket, respectively.

Analysis of the elastic response of the HPSA

We investigated the extreme indicators of the suspension resisting dynamic loads during vehicle

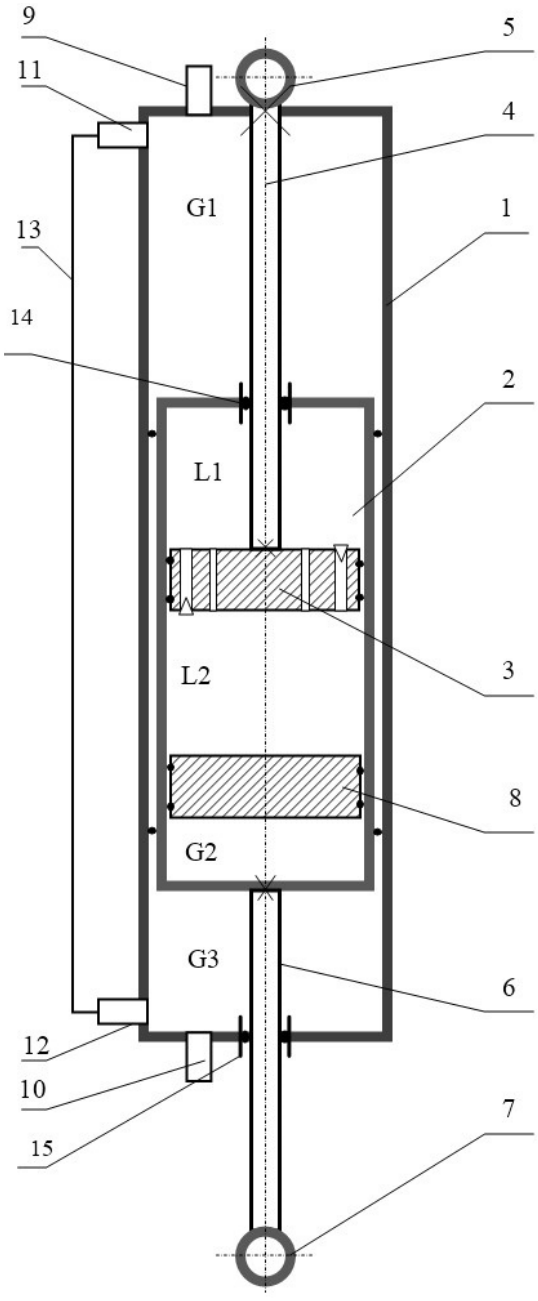

Fig. 1. Shock absorber design: 1 — a pneumohydraulic shock absorber (filled with gas under pressure — chambers G1, G2, G3); 2 — an operating cylinder (filled with liquid); 3 — a hydraulic piston; 4, 6 — a rod; 5, 7 – a rod eye; 8 — a pneumatic piston; 9, 10 — a nipple; 11, 12 — safety valves; 13 — a pipe; 14, 15 — a sealing guide bushing; G1 — an upper gas chamber; G2 — a compensation gas chamber; G3 — a lower gas chamber; L1 — an upper hydraulic chamber; L2 — a lower hydraulic chamber

movement. First of all, we analyzed its indicators determining the elastic component of the suspension and acting on the wheel during movement of the suspension elements (Fig. 3) according to a particular method (Dobromirov et al., 2006; Rotenberg, 1972):

- at curb weight — P_{curb};
- static HPSA deflection — S_{st};
- displacement during compression — S_{d_comp};
- displacement during rebound — S_{d_reb};
- forces P_{d_comp} on the HPSA at S_{d_comp};
- forces P_{d_reb} on the HPSA at S_{d_reb}.

The algorithm for the analysis of the elastic response is as follows:

1. At the selected static deflection S_{st} and load P_{curb} on the shock absorber (with curb weight), gas pressure in chambers G1, G2 and G3 is selected;

2. Calculation of pressure in chambers G1, G2 and G3 during shock absorber stroke from 0 to full stroke $S_{full} = S_{d\_comp} + S_{d\_reb}$.

3. Plotting of the elastic response.

Calculation of gas pressure in chambers G1, G2, G3 at THM curb weight

The shock absorber rod force is determined by the difference in the values of pressure in chambers G1 and G3: p_1 and p_3:

$$P = (p_1 - p_3)F_1,$$

where F_1 — the cross-sectional area of the inner surface of cylinder 1 (Fig. 1).

$$F_1 = (d_1 - d_r)^2 / 4,$$

where d_1 and d_r — the diameter of cylinder 1 and the diameter of the rod, respectively.

Then pressure p_{1curb} in chamber G1 under load at curb weight P_{curb} can be found based on the following relations:

$$\Delta p_{curb} = \frac{P_{curb}}{F_1},\ p_{1curb} = \Delta p_{curb} - p_{3curb}.$$

where p_{3curb} — the selected pressure in chamber G3 under load at curb weight P_{curb}.

Restrictive conditions when selecting pressure:

– the minimum pressure in chamber G3 shall exceed atmospheric pressure;

– the maximum pressure in the gas chambers shall not exceed 4 MPa (Dobromirov, 2006). It is expedient to adopt pressure in chamber G2 to be equal to p_{1curb}.

Changes in pressure during compression

The volume of chamber G1 during compression varies from the average value V_{1av} at the average length L_{av} of the shock absorber, corresponding to static deformation S_{st}, to the minimum value V_{1min} at the length of the shock absorber L_{min}, corresponding to dynamic compression deformation S_{d_comp}:

$$V_{1av} = F_1 \cdot (S_{d\_comp} + S_{e1}),$$

$$V_{1\min} = F_1 \cdot S_{e1}.$$

Then pressure in chamber G1 during dynamic compression will be as follows:

$$p_{1d\_comp} = p_{1curb}\left(\frac{V_{1av}}{V_{1\min}}\right)^n,$$

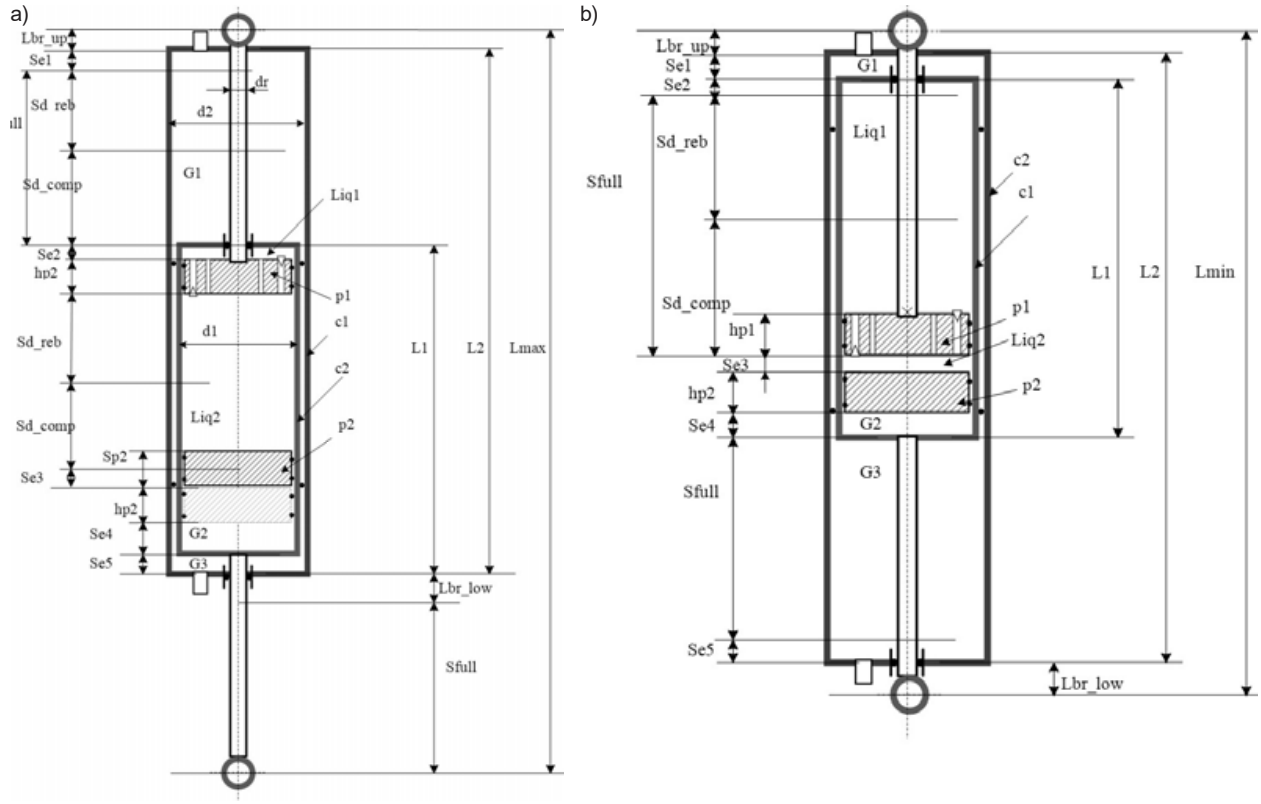

Fig. 2. Design scheme of the geometric parameters at the maximum (a) and minimum (b) length of the shock absorber

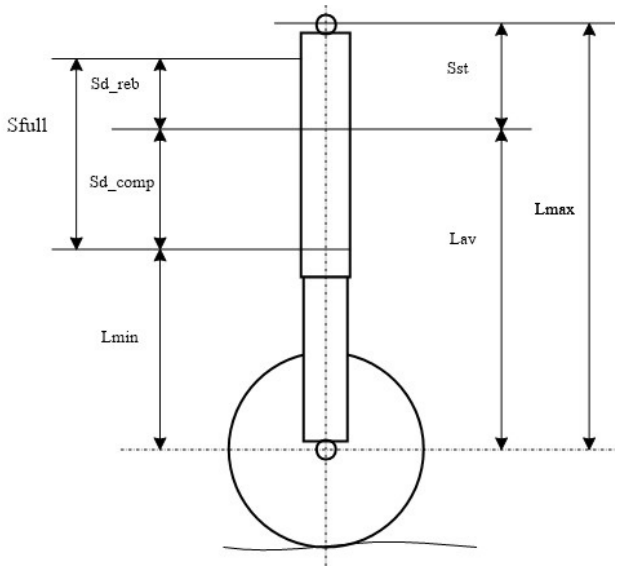

Fig. 3. Shock absorber parameters

where n is the polytropic index (n = 1.26) (Dobromirov et al., 2006; Rotenberg, 1972).

The volume of chamber G3 during compression varies from the average value V_{3av} at the average length L_{av} of the shock absorber, corresponding to static deformation S_{st}, to the maximum value V_{3max} at the length of the shock absorber L_{min}, corresponding to dynamic compression deformation S_{d_comp}:

$$V_{3av} = F_1 \cdot (S_{d\_reb} + S_{e5}),$$

$$V_{3\max} = F_1 \cdot \left(S_{full} + S_5\right).$$

Then pressure in chamber G1 during dynamic compression will be as follows:

$$p_{3d\_comp} = p_{3curb}\left(\frac{V_{3av}}{V_{3\max}}\right)^n.$$

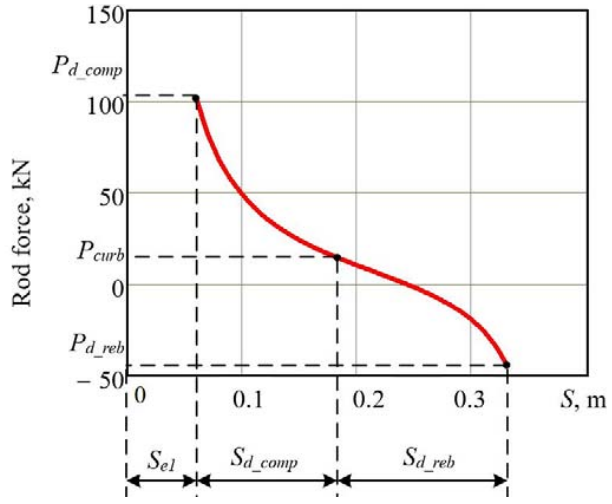

Fig. 4. Results of indicators for the elastic response of the shock absorber in Mathcad

Changes in pressure during rebound

The volume of chamber G1 during rebound varies from the average value V_{1av} at the average length L_{av} of the shock absorber, corresponding to static deformation S_{st}, to the maximum value V_{1max} at the length of the shock absorber L_{max}, corresponding to dynamic rebound deformation S_{d_reb}:

$$V_{1\max} = F_1 \cdot \left(S_{full} + S_{e1}\right).$$

Then pressure in chamber G1 during dynamic rebound will be as follows:

$$p_{1d\_reb} = p_{1curb}\left(\frac{V_{1av}}{V_{1\max}}\right)^n.$$

The volume of chamber G3 during rebound varies from the average value V_{3av} at the average length L_{av} of the shock absorber, corresponding to static deformation S_{st}, to the minimum value V_{3min} at the length of the shock absorber L_{max}, corresponding to dynamic rebound deformation S_{d_reb}:

$$V_{3\min} = F_1 \cdot S_{e5}.$$

Then pressure in chamber G3 during dynamic rebound will be as follows:

$$p_{3d\_reb} = p_{3curb}\left(\frac{V_{3av}}{V_{3\min}}\right)^n.$$

Elastic response in the HSA rod stroke function

The HPSA stroke varies from L_{min} to L_{max} (Fig. 2). In this case, the volumes V_1 and V_3 and pressures p_1 and p_3 in the stroke function S of the rod (S = 0...S_{full}) are as follows:

$$V_1(S) = F_1 \cdot \left(S_{e1} + S\right),\ V_3(S) = F_1 \cdot \left(S_{e5} + S_{full} - S\right),$$

$$p_1(S) = p_{1d\_comp} \cdot \left(\frac{V_1(S_{d\_comp})}{V_1(S)}\right)^n,$$

$$p_3(S) = p_{3d\_comp} \cdot \left(\frac{V_3(S_{d\_comp})}{V_3(S)}\right)^n.$$

Now we can determine the perpendicular load on the wheel from the HPSA deformation:

$$P(S) = F_1 \cdot \left[p_1(S) - p_3(S)\right].$$

Fig. 4 shows a potential model of the relationship under consideration for the KAMAZ-43502 chassis, developed in the Mathcad environment. It should be noted that in some cases S_{d_comp} meet the stated HPSA indicators, and then the load P_{d_reb} is different from the rest, or at least from other, HPSA. The load P_{d_reb} will be negative, which has not been previously observed in the theory of shock absorbers. As a result, a separate group of stated HPSA indicators at the S_{d_reb} graph section bends in the direction opposite to the standard one. The main result is an indication of the fact that the HPSA compression force is directly proportional to the forces acting during HPSA rebound as deformation S_{d_reb} increases. This phenomenon is due to the following: during full rebound, gas is heavily compressed in chamber

G3, and pressure in chamber G1 is minimal (see the equation above).

It is the presented relationship that provides conditions for zero HPSA bottoming during rebound.

Discussion

The modeling in Mathcad shows the probability of a wide range of changes in the characteristics by modifying the initial HPSA configuration: diameter, indicator of auxiliary displacements in chamber G3 vs. the actual forces.

Conclusions

1. The considered design scheme of the shock absorber makes it possible to increase the movement smoothness of THM due to the new scheme for the installation of gas springs, which significantly reduces the probability of HPSA bottoming in all modes of operation.

2. The efficiency of performance of the new HPSA design is confirmed by mathematical modeling in the Mathcad environment.

Acknowledgments

The authors express their gratitude to Viktor Nikolayevich Dobromirov, Professor at the Department of Land Transport and Technological Machines of the Saint Petersburg State University of Architecture and Civil Engineering, for his help and support in developing a new device and writing this paper.

References

Audi (2001). *Pneumatic suspension systems. Part 1. Clearance regulation in Audi A6. Design and operation. Self-training program 242*. [online] Available at: http://rep-air.ru/ssp242.pdf [Date accessed 20.10.2022].

Akopyan, R. A. (1979). *Pneumatic suspension of transport vehicles*. Lvov: Vishcha Shkola, 218 p.

Carway.info (2017). *ALCA®: Ridigity — an issue of measure*. [online] Available at: https://carway.info/ru/content/alcar-zhestkost-vopros-mery [Date accessed 20.10.2022].

Chelomey, V. N. (ed.) (1981). *Vibration in engineering. Reference book in 6 volumes. Vol. 1*. Moscow: Mashinostroyenie, 352 p.

Dobromirov, V. N., Gusev, Ye. N., Karunin, M. A., and Khavkhanov, V. P. (2006). *Shock absorbers. Design. Calculation. Testing.* Moscow: Moscow State Technical University "MAMI", 184 p.

Repin, S. V. (2022). *Pneumohydraulic shock absorber*. Patent RU208894U1.

Repin, S. V., Dobromirov, V. N., Orlov, D. S., and Kapustin, A. A. (2019). The study of the elastic characteristics of the new hydro-pneumatic shock absorber. *Bulletin of Civil Engineers*, No. 5 (76). pp. 260–269. DOI: 10.23968/1999-5571-2019-16-5-260-269.

Repin, S., Bukirov, R., and Vasilieva, P. (2020). Study on effects of damping characteristics of base chassis suspension on operational safety of transport and handling machinery. *Transportation Research Procedia*, Vol. 50, pp. 574–581. DOI: 10.1016/j.trpro.2020.10.069.

Rotenberg, R. V. (1972). *Motor vehicle suspension. Vibrations and running smoothness. 3rd edition*. Moscow: Mashinostroyenie, 392 p.

Techautoport.ru (2022). *Design and operation of pneumatic suspension*. [online] Available at: https://techautoport.ru/hodovaya-chast/podveska/pnevmaticheskaya-podveska.html [Date accessed 20.10.2022].

Zaitsev, A. V. (2007). *Calculation of vehicle suspension parameters*. Kurgan: Kurgan State University, 16 p.

Zhileykin, M. M., Kotiev, G. O., and Sarach, Ye. B. (2012). Method for calculating characteristics of pneumatic-hydraulic controlled suspension with two-level damping in multi-axle vehicles. *Science & Education*, No. 1, 77-30569/346660. [online] Available at: http://technomag.edu.ru/doc/346660.html. [Date accessed 20.10.2022].

Lukin, P. P., Gasparyants, G. A., and Rodionov, V. F. (1984). *Design and analysis of vehicles*. Moscow: Mashinostroyenie, 376 p.

ИССЛЕДОВАНИЕ РАБОТЫ БЕСПРОБОЙНОГО ПНЕВМОГИДРАВЛИЧЕСКОГО АМОРТИЗАТОРА В ПОДВЕСКЕ ТРАНСПОРТНО-ТЕХНОЛОГИЧЕСКОЙ МАШИНЫ

Сергей Васильевич Репин*, Иван Иванович Воронцов, Денис Сергеевич Орлов,
Роман Андреевич Литвин

Санкт-Петербургский государственный архитектурно-строительный университет
Санкт-Петербург, Россия

*E-mail: repinserge@mail.ru

Аннотация
Введение: Плавность хода транспортно-технологических машин (ТТМ) (экскаваторов, кранов, оборудования для содержания дорог и т.п.) на автомобильном шасси значительно сказывается на их долговечности в силу большой массы оборудования и неравномерности распределения нагрузок по осям базового шасси, что вызывает большие динамические нагрузки при перемещении по дорогам с несовершенным покрытием. Зачастую, именно по таким дорогам приходится перемещаться ТТМ. **Цель исследования:** повышение плавности хода ТТМ на автомобильном шасси на основе использования новой конструкции амортизатора, как главного элемента подвески ходовой части машины. **Методы:** Конструкция амортизатора с гидропневматической схемой считается более распространенной. Принцип их работы основан на гидравлическом сопротивлении, возникающем при движении поршня со штоком в объем заполненном маслом, при этом газ в закрытой части уплотняется, компенсируя изменения внутреннего объема. Главным отрицательным показателем гидропневматического амортизатора (ГПА) чаще всего бывает вероятность пробоя при эксплуатации в момент наезда на барьер (препятствие), что влечет за собой динамические нагрузки, уменьшающие ресурс машины и деталей самого амортизатора. **Результаты:** В статье описывается новая конструкция амортизатора, исключающего пробой, приводится математическая модель его упругой характеристики и результаты моделирования в Mathcad, подтверждающие работоспособность устройства.

Ключевые слова: плавность хода, амортизатор, упругая характеристика.

In Focus

BOOK REVIEW OF SUPERTALL: HOW THE WORLD'S TALLEST BUILDINGS ARE RESHAPING OUR CITIES AND OUR LIVES, BY STEFAN AL (W. W. NORTON, 2022)

Since 2007, for the first time in our human history, more than half of the world's population is now living in cities. As the world is expected to urbanize even further over the next few decades, the question is how cities can absorb urban population growth. The boundaries are exacerbated by the effect of climate change. Can skyscrapers serve as an architectural solution? How can we build them to cope with an ever-growing population and climate changes?

Supertall, a new book by Dutch architect and professor Stefan Al, offers an authoritative and insightful analysis on the future of the skyscraper, pointing to such directions as regenerative sustainability. It is a thoughtful account of the skyscraper's history and future trajectories, using some of the most famous buildings to tell the story. Al has done extensive research to help us understand how these supertall structures are made, including all the technical marvels and design innovations that allow us to make life in them possible, while relating to a complex system of external climatic factors.

The evolution of tall buildings has been remarkable. For instance, supertall buildings were first built for a single use, whether it be office or residential. But now they are increasingly becoming mixed-use, combining office, residential, hotel, commerce, and community activity areas. Concepts are becoming more mixed and flexible, extending the life cycle span of these types of structures.

His reflections of materials are very insightful. Typical construction materials used in tall buildings have changed over time, and a new environmental ethic may soon lead to further evolution. The first tall buildings were built mostly from steel frames. Today, as the compressive strength of reinforced concrete has increased, they are mostly constructed out of high-performance concrete. Al explains how the world is overly reliant on concrete, given the significant impact on global carbon emissions (about 5% of the world's total), which in turn increases climate change. Mass timber, as Al points out, offers the most promise as a more sustainable building block for skyscrapers reaching up to 30 stories.

Elevators have transformed as well. The fastest elevator is now moving passengers at a speed of 76 km/h, although the average elevator still transports people at around 22 km/h. There is research being done on the so-called "wonkavator," or the Multi, which is the world's first cableless elevator developed by ThyssenKrupp elevator company. It is a magnetically levitated elevator that could move both upwards and sideways and allow for new skyscraper design, which up until now has been constrained by vertical elevator cores.

For skyscraper architects and engineers, understanding aerodynamics is vital since wind is the most potent force affecting tall buildings. Computer simulations and more specifically computational fluid dynamics simulations help architects iterate various designs, optimizing wind reduction. In addition, since taller buildings swing more than other structures in strong gusts of wind, they can make people queasy. Such inventions as the tuned mass damper reduce the shake of a building, which acts as a giant counterweight moving in the opposite direction of the

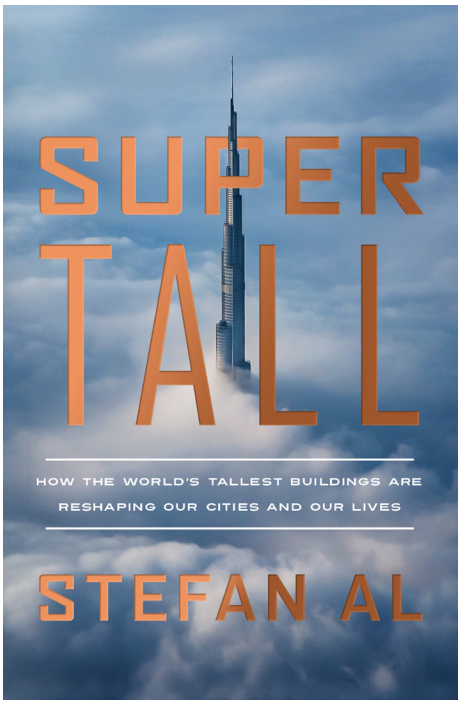

Stefan, Al (2022) **Supertall: How the World's Tallest Buildings Are Reshaping Our Cities and Our Lives.** W. W. Norton & Company (April 12, 2022), 320 p. ISBN-10 : 1324006412. ISBN-13 : 978-1324006411

wind. Better aerodynamics also means a reduction in materials needed to construct buildings.

One serious challenge in the case of tall buildings is making them climatically comfortable since in most cases they are absorbing a large amount of solar radiation. Besides, occupancy and equipment add thermal loads. As a result, HVAC (heating, ventilation, and air conditioning) equipment is substantial. Tall buildings need mechanical floors every 20 to 30 stories, which are off-limits to the general public, just to host machinery and water pumps. More sustainable skyscrapers are able to reduce cooling loads through operable windows, smaller window areas, shading devices, as well as thermal chimneys and atriums. These all could add to the "thermal aesthetic" appeal of the building. The use of sensors to monitor and improve energy efficiency is important as well, although excessive data collection could have a potential downside and be considered an invasion on people's privacy.

The reaction of the general public must also be taken into account. Skylines are often protected in historic cities, such as traditionally low-rise skylines in Europe. Restrictions are, for example, related to preservation of the right to light of shorter buildings. However, height restrictions may also come from "view protection corridors". This is the case of London where they try to preserve historical views. Not more than a century ago in these cities, buildings were typically not allowed to be taller than a safety fire ladder or a steeple of a cathedral. The current rise of tall buildings in these cities is illustrative of today's urban renaissance.

In some cities, like New York, unique conditions exist that lead to taller buildings. The purchase of air rights above New York City allows developers who "buy" the right to erect taller structures. This can result in very tall buildings, even on sites that are relatively small. The city also has a regulation in which mechanical floors do not count as buildable areas. This allows developers to build even higher when they have entire floors dedicated to mechanical equipment. But arguably New York's most innovative contribution is how the city incentivizes the creation of open space by the private sector in exchange for granting more development rights.

Hong Kong's skyscrapers are famous for their location near public transit stations. The city even features elevated footbridges that interconnect various skyscrapers and subway stops, making the city the poster child of transit-oriented development. As a result, Hong Kong has the lowest per capita energy cost for urban transportation. Singapore manages to incorporate greenery and vegetation into its skyscrapers. A new regulation forces developers to build green walls and roof gardens, contributing to Singapore's image of a Garden City. Such a biophilic approach has an important role in preserving biodiversity as well as providing temperate microclimatic conditions.

In conclusion, it appears that cities around the world will continue to build tall buildings, albeit in different ways. The book highlights the many examples of how skyscrapers can be built more regeneratively, and how the axes of ecology, decarbonization and human health are (or are not) tackled. Skyscrapers are an important typology, and their performance can be considered controversial in light of climate change: Al's book thus offers a valuable contribution to unlock a more sustainable and holistic design of tall buildings.

Emanuele Naboni
Professor, PhD

University of Parma
Royal Danish Academy, Copenhagen
University of New South Wales, Sydney
UC Berkeley
SOS Mario Cucinella Post Graduate Program, Milan

Guide for Authors
for submitting a manuscript for publication in the «Architecture and Engineering»

The journal is an electronic media and accepts the manuscripts via the online submission. Please register on the website of the journal http://aej.spbgasu.ru/, log in and press “Submit article” button or send it via email aejeditorialoffice@gmail.com.

Please ensure that the submitted work has neither been previously published nor has been currently submitted for publication in another journal.

Main topics of the journal:

1. Architecture
2. Civil Engineering
3. Geotechnical Engineering and Engineering Geology
4. Urban Planning
5. Technique and Technology of Land Transport in Construction

Title page

The title page should include:

The title of the article in bold (max. 90 characters with spaces, only conventional abbreviations should be used); The name(s) of the author(s); Author’s(s’) affiliation(s); The name of the corresponding author.

Abstract and keywords

Please provide an abstract of 100 to 250 words. The abstract should not contain any undefined abbreviations or unspecified references. Use the IMRAD structure in the abstract (introduction, methods, results, discussion).

Please provide 4 to 6 keywords which can be used for indexing purposes. The keywords should be mentioned in order of relevance.

Main text

It should have the following structure:
1) Introduction,
2) Scope, Objectives and Methodology (with subparagraphs),
3) Results and Discussion (may also include subparagraphs, but should not repeat the previous section or numerical data already presented),
4) Conclusions,
5) Acknowledgements (the section is not obligatory, but should be included in case of participation of people, grants, funds, etc. in preparation of the article. The names of funding organizations should be written in full).

General comments on formatting:

- Subtitles should be printed in Bold,
- Use MathType for equations,
- Tables should be inserted in separate paragraphs. The consecutive number and title of the table should be placed before it in separate paragraphs. The references to the tables should be placed in parentheses (Table 1),
- Use “Top and Bottom” wrapping for figures. Figure captions should be placed in the main text after the image. Figures should be referred to as (Fig. 1) in the text.

References

The journal uses Harvard (author, date) style for references:
- The recent research (Kent and Park, 1990)...
- V. Zhukov (1999) stated that…

Reference list

The list of references should only include works that are cited in the text and that have been published or accepted for publication. Personal communications and unpublished works should only be mentioned in the text. Do not use footnotes or endnotes as a substitute for a proper reference list. All references must be listed in full at the end of the paper in alphabetical order, irrespective of where they are cited in the text. Reference made to sources published in languages other than English or Russian should contain English translation of the original title together with a note of the used language.

Peer Review Process

Articles submitted to the journal undergo a double blind peer-review procedure, which means that the reviewer is not informed about the identity of the author of the article, and the author is not given information about the reviewer.
On average, the review process takes from one to five months.